

Catalytic degradation of microplastics

Elena N. Efremenko,[✉] Ilya V. Lyagin,[✉] Olga V. Maslova,[✉] Olga V. Senko,[✉] Nikolay A. Stepanov,[✉]
Aysel G. Aslanli[✉]

*Faculty of Chemistry, Lomonosov Moscow State University,
Leninskie Gory 1, stroenie 3, 119234 Moscow, Russian Federation*

The spread of microplastics is a serious environmental problem, which attracts increasing attention. The achievements of analytical chemistry made it possible to accumulate and systematize an extensive array of data on the contents of microplastics in environmental objects and living (micro)organisms. The current situation brings about the challenge to, at least, isolate microplastics from the environmental objects and, at most, efficiently decompose them. This review systematizes data on the existing (bio)catalytic methods and approaches that can be used for the decomposition of various microplastics. The benefits and drawbacks of the methods are demonstrated. Possible solutions to the existing problems related to the microplastic pollution of the environment are critically discussed, and areas for further development are outlined.

The bibliography includes 273 references.

Contents

1. Introduction	1
2. Catalytic processes for degradation of microplastics	2
2.1. Thermal conversion	2
2.2. Hydrogenolysis	18
2.3. Silylation	19
2.4. Electro- and photocatalytic decomposition and oxidation	19
2.5. Solvolysis	19
3. Biocatalytic degradation of microplastics	20
4. Immobilized biocatalysts for decomposition of microplastics	37
5. Conclusion	39
6. List of abbreviations and symbols	40
7. References	41

1. Introduction

The environmental problem associated with the spread of microplastics took shape only in the last five years, as a result of numerous thorough studies on the determination

of these micro- and nanoparticles in various environmental objects.¹ This became possible owing to advancement of the methods for chemical analysis of micro- and even nanoparticles,² which revealed the presence of these pollutants in various environments, including soils³ and atmosphere.⁴ In any case, the provided data require careful interpretation in order to avoid false-positive results of chemical analysis.⁵

There is still no generally accepted term defining what is meant by microplastic: most often, this term refers to any plastic particles of < 5 mm size, *i.e.*, particles that are not retained on a metal grid with a step size of 4.76 mm (mesh 4) and a single cell diagonal of 6.7 mm. A more detailed and, hence, less contradictory classification of microplastics was proposed in the ISO/TR 21960:2020 standard and in the currently developed ISO/DIS 24187 standard, distinguishing nanoplastics (< 1 μm), microplastics (1–1000 μm) and large microplastics (1–5 mm). In this review, plastic particles of up to 6 mm in size capable of passing through a metal grid with the above-indicated size are considered to be microplastics.

The formation of microplastic pollutants from items used in the household and in the everyday life has been noted throughout the world.⁶ The chemical analysis of samples taken from different water bodies demonstrated a broad variability of structural characteristics and chemical composition of microplastic particles.⁷ In addition, it is evident that the composition of pollutants can rapidly change under environmental conditions;⁸ therefore, it is reasonable to consider polymer products in the overall microplastic pollution. It is obvious that the component composition of microplastics generally coincides with the composition of abundant polymer sources, that is, natural, semisynthetic and synthetic polymers. The main domestic sources of microplastics are various fabrics, which may release particles during washing with detergents at elevated temperatures.⁹ Most part of fabric fibres are cellulose- (cotton, linen, rayon) and protein-containing (silk, wool) natural materials with some fraction of synthetic materials (elastane, polyamides, polyethylene terephthalates), which are not fully decomposed by waste water treatment.¹⁰

E.N.Efremenko. Doctor of Biological Sciences, Professor, Head of the Laboratory of Ecobiocatalysis, Faculty of Chemistry of MSU.
E-mail: elena_efremenko@list.ru

I.V.Lyagin. Ph.D, Senior Researcher at the Laboratory of Ecobiocatalysis, Faculty of Chemistry of MSU.

E-mail: lyagin@enzyme.chem.msu.ru

O.V.Maslova. Ph.D, Researcher at the same Laboratory.

E-mail: olga.maslova.rabota@gmail.com

O.V.Senko. Ph.D, Researcher at the same Laboratory.

E-mail: senkoov@gmail.com

N.A.Stepanov. Ph.D, Researcher at the same Laboratory.

E-mail: na.stepanov@gmail.com

A.G.Aslanli. Ph.D, Researcher at the same Laboratory.

E-mail: ayselaslanli@mail.ru

Current research interests of the authors: biocatalysis, kinetics and catalysis, hybrid processes, biocatalytic processes of waste destruction, microorganisms in the destruction of xenobiotics, enzymes in the destruction of toxins.

Translation: Z.P.Svitanko

The main hazard of microplastics (unlike, for example, solid municipal waste) is that they are able to form relatively stable disperse systems in water. As a result, microplastic particles get into rivers and then to seas and oceans together with waste water; they are carried by air mass over large distances, fall on the ground with rain drops and are involved in trophic chains at different levels.^{11–13} As a result, microplastics are gradually accumulated in living organisms.¹⁴ Currently, microplastics have been found in many food products and in potable water. It was found that, on average, people throughout the world can intake up to 0.1–5 g of microplastics per week.¹⁵

The ecotoxicological effects of microplastic particles are mainly manifested as damage to internal organs and tissues (liver, intestines), adverse effects on fetal development and reproductive function, disorders of intestinal microbiome and metabolism, immune dysfunction and oxidative stress.^{16,17} Unfortunately, modern methods for waste water treatment (and even potable water treatment) are not meant for the removal of this type of pollutants; hence, the development of such approaches is highly relevant. Furthermore, chemisorption of other organic and inorganic pollutants on these microparticles¹⁸ leads to an adverse cumulative effect. Meanwhile, the extraction of microplastics from, for example, waste water, would mean solution to only a smaller part of the existing problem. After that, it would be necessary to process the microplastics. Combustion or landfilling of microplastics seems to be the simplest solution. However, after conventional combustion, most of microplastics are either discharged to the atmosphere together with effluent gases or retained in the residue, while in the case of landfilling, they may remain non-degraded in soil for long periods of time, despite the presence of various microbial associations.¹⁹ Moreover, there are studies in which the agricultural lands were irrigated with water containing particles of microplastics, hoping that they will be subsequently biodegraded, but this resulted only in soil accumulation of the microplastics,^{20,21} the particles of which were taken up by plants through the roots.²² Wild type (wt) microorganisms did not decompose these particles, but actually, like plants, accumulated them in their cells and on the surface in the attached state. It was noted that the accumulated particles have an adverse effect on the microorganisms (bacteria and fungi);²³ the toxic effect on the biota is enhanced with decreasing particle size.

It was found that microplastics can change the biophysical properties and the bulk density of soil and the water retention behaviour of soils and can affect the formation of soil aggregates. It was shown²⁴ that plastic particles of 1 to 5 mm in size brought into soil in an amount of 0.5 mass % create channels for water flow, resulting in enhanced water evaporation and thus lead to soil drying; this is unfavourable for crop yield.²⁵ Changes in the soil structure have also other side effects, including modification of the composition of the microbial community (mycorrhiza and nitrogen fixers), which further affect plant growth and development. In addition, microplastics may contain substances toxic to plants. Studies of the mechanisms that underlie the plant uptake of microplastic particles using various analytical methods showed that these particles can penetrate into plant roots by changing (disturbing) the cell membrane structure, damaging the intracellular molecules and generating oxidative stress because of involvement of transport membrane proteins.^{22,23} For example microplastic particles considerably decreased the sprout (by 16–40%) and root

(by 20–50%) biomass for corn, wheat, rice, onions, beans and many other plants.^{22,26}

In this connection, it appears rational to perform the catalytic conversion of microplastics into products that would be, at least, not hazardous and, at best, useful, because microplastics are rather abundant organic resource, in some cases containing also nitrogen (polyurethanes).^{27–30}

The catalytic conversion of macroplastics is addressed in numerous reviews (see, for example, Refs 31, 32); however, analysis of the influence of the micro- and nano-size of polymer particles on the efficiency of their catalytic degradation also seems to be relevant. To date, data representing state-of-the-art research in the (bio)catalytic transformation of microplastics have been analyzed in a number of publications,^{27–30} which, however, almost neglect the chemical aspects of the microplastic degradation. In order to fill this gap, here we analyze publications of the period from 2012 to 2022 considering polymer particles of up to 6 mm size converted to various products using (bio)catalysts; the attention is focused on the chemical aspects of the reactions. For a correct practical comparison of different catalysts in the presence of a sufficient amount of data, a common characteristic was calculated, that is, the performance (*P*) for each process in mg of products (or litres of gases) formed in 1 h under the action of 1 mg of the catalyst.

2. Catalytic processes for degradation of microplastics

Microplastics are chemically indistinguishable from macroplastics; therefore, they can be degraded using catalysts with various chemical structure, cost, performance and stability, including catalysts developed for the destruction of plastics and waste from their production and use. In this review, the data on the catalysts are classified, according to the type of catalyzed reactions (Fig. 1, Tables 1–6), into thermal conversion, hydrolysis, silylation, electro-oxidation, photolysis and solvolysis (including alcoholysis, aminolysis, and hydrolysis).

2.1. Thermal conversion

Pyrolytic processes are carried out in the presence of various zeolites — the most accessible and abundant catalysts used, in particular, to upgrade oil residues.¹⁵⁰ The conversion can be carried out not only for single polymers, but also for polymer blends with accompanying biomass, which, in principle, can be isolated, for example, from wastewater, together with microplastics. The combined pyrolysis of polymers and biomass results, as expected, in a high content of organic acids in the products,^{34,35} which is undesirable if they are meant for the use as fuels. However, the relative content of oxygenates and nitrogen-containing compounds in the products of the catalytic co-pyrolysis can be significantly reduced compared to those in the product of the non-catalyzed process.³⁵ The halogenated polymers present in the blend would be converted into halo derivatives, which may, in turn, partly bind to bases that are additionally introduced into the catalyst [30% binding for Ca(OH)₂ (Ref. 36) and 20–25% for Al₂O₃ (Ref. 40)].

Regarding the composition of the product, important characteristics are the Si:Al ratio,³⁹ zeolite content in the catalyst,⁴⁷ zeolite type^{40,41} and porosity⁴¹ and doping with metals.^{37,45} It is to note important that repeated thermal conversion using metal-doped catalysts may lead to addi-

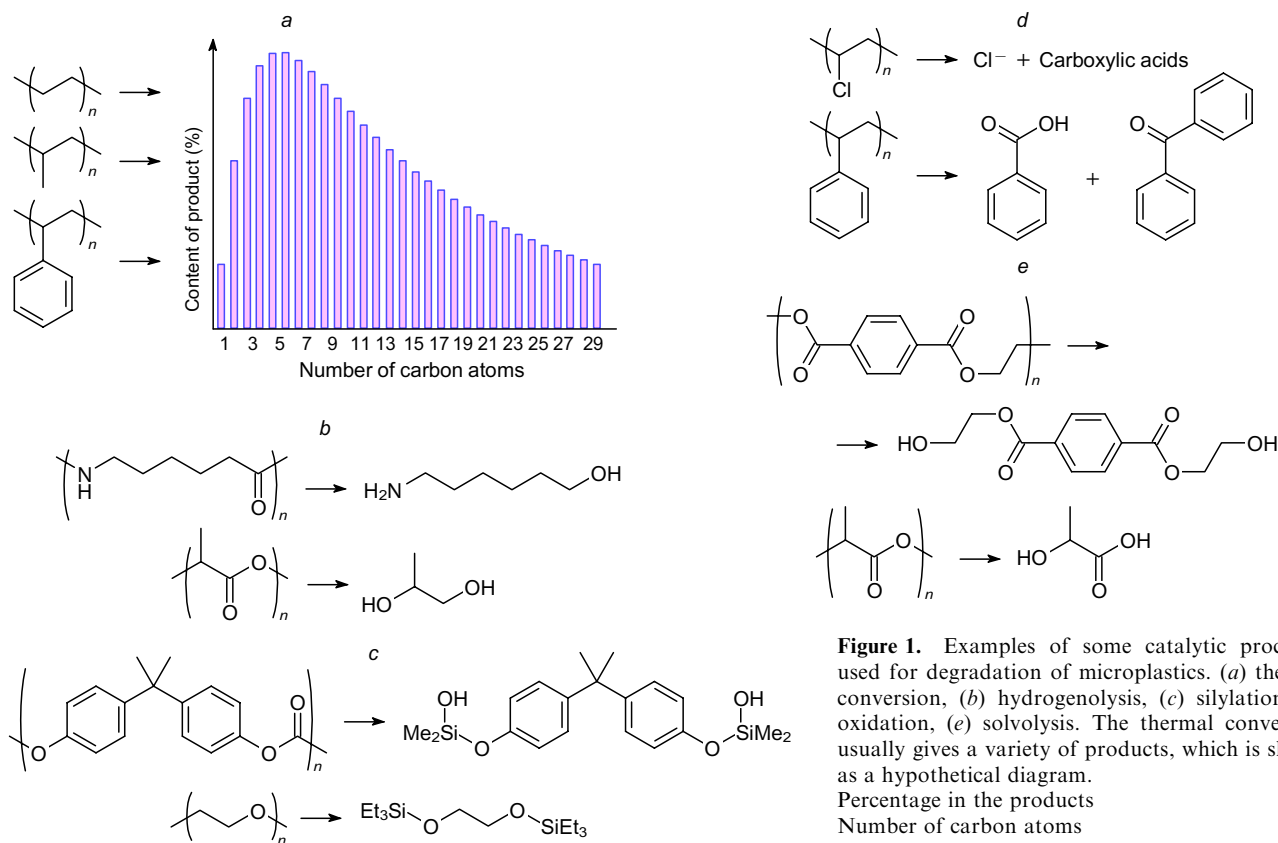


Figure 1. Examples of some catalytic processes used for degradation of microplastics. (a) thermal conversion, (b) hydrogenolysis, (c) silylation, (d) oxidation, (e) solvolysis. The thermal conversion usually gives a variety of products, which is shown as a hypothetical diagram. Percentage in the products
 Number of carbon atoms

Table 1. Chemical catalysts for the thermocatalytic reactions of microplastics. All abbreviations and symbols are indicated in the Notes to the Table.

Catalyst	Optimal reaction conditions				Catalytic characteristics		Comments	Ref.	
	$T, ^\circ\text{C}$	p, kPa	medium gas	q (mass %) $v, \text{L h}^{-1}$	$P,$ $\text{mg h}^{-1} \text{mg}^{-1}$	Q (%)			
<i>Microplastic: HDPE (d = 0.3 mm) mixed with torrefied yellow poplar sawdust (d = 0.3 mm); products: a mixture of liquid and gaseous hydrocarbons</i>									
HZSM-5 zeolite or Al-MCM-41, Si: Al = 30	600	—	N ₂	—	1000	1.9	64.6	The content of aromatics was higher for HZSM-5	
<i>Microplastic: PS (d = 1 mm) mixed with 33 mass % corn stalk (d = 0.8–1.2 mm); products: a mixture of liquid and gaseous hydrocarbons and oxygenates</i>									
HZSM-5 zeolite, SiO ₂ : Al ₂ O ₃ = 38	500	—	N ₂	3	10	—	89	Pure PS was completely converted to hydrocarbons. The addition of stalk resulted in the appearance of a solid residue. The difference of the yields from those in the non-catalyzed process was minor (at 450 °C); the composition of products changed	34
<i>Microplastic: HDPE (d = 0.5 mm) and its mixture with the Enteromorpha prolifera biomass (d = 0.18–0.45 mm); products: a mixture of liquid and gaseous hydrocarbons and oxygenates</i>									
HZSM-5 zeolite (d = 0.185–0.25 mm)	550	101.3	N ₂	9	100	1.8	90	The yield increased by 6–7% in the case of catalytic pyrolysis; the temperature increased by 50 °C	35

Table 1 (continued).

Catalyst	Optimal reaction conditions					Catalytic characteristics		Comments	Ref.
	T, °C	p, kPa	medium		Q (%)	P, mg h ⁻¹	Q (%)		
			gas	v, L h ⁻¹					
<i>Microplastic: a mixture* of 35% LDPE, 32% HDPE, 24% PP, 4% PVC, 3% C₂H₄ dimer with C₃H₆, 2% PS; products: a mixture of liquid and gaseous hydrocarbons</i>									
A mixture of Ni-doped ZSM-5 zeolite with Ca(OH) ₂ and bauxite mud in 1 : 2 : 1 ratio	510–520	101.3	N ₂	5	5	60	90	The yield decreased in comparison with the non-catalyzed process. The yield was lower with SAPO-11 than with ZSM-5	36
<i>Microplastic: PP (d < 0.5 mm); products: a mixture of liquid and gaseous hydrocarbons</i>									
Ga-doped HZSM-5 zeolite, Si : Al = 30	600	—	N ₂	—	500	—	—	Doping slightly decreased the degradation temperature; a much greater temperature change was induced by the zeolite replacement with HY (the largest surface area)	37
<i>Microplastic: PE, PP (d = 1.8–4.5 mm); products: a mixture of liquid and gaseous hydrocarbons</i>									
USY zeolite, Si : Al = 7.5 (d = 0.2–0.8 mm)	450	101.3	N ₂	—	10	12–13	98–99		38
<i>Microplastic: HDPE (d = 7.0 mm); products: a mixture of liquid and gaseous hydrocarbons</i>									
HZSM-12 zeolite (d = 7.0–14.5 μm)	360	—	N ₂	1.5	50	21	90	Low-molecular-mass hydrocarbons with the narrowest weight distribution were obtained	39
<i>Microplastic: HDPE (d = 0.6 mm); products: a mixture of liquid and gaseous hydrocarbons</i>									
MCM-41 zeolite (d < 5 μm) or Al ₂ O ₃ (d < 0.15 mm)	410	—	N ₂	1.8	10	4.8–5.1	72–77	Reactions catalyzed by MCM-41 and Al ₂ O ₃ differed only slightly from non-catalyzed reactions	40
<i>Microplastic: a mixture* of PP and PE (d = 3 mm); products: a mixture of liquid and gaseous hydrocarbons and H₂</i>									
Zeolites: Al-SBA-15(wo), HUN-ZSM-5, Al-MCM-41(hhs), KFS-16B, C-ZSM-5 or B-zeolite, Si : Al = 30	500	—	N ₂	12	3	66	99	Different product composition depending on the catalyst	41
<i>Microplastic: HDPE, LDPE, PP, PLA (d = 0.5 mm); products: a mixture of liquid and gaseous hydrocarbons</i>									
Spent FCC, Si : Al = 0.94; LTA zeolite or MgO as the catalyst	600	—	N ₂	24	20	4.9–5.0	97–99	The product yield was the same for FCC and LTA, while for MgO the yield decreased by 5–22% (for different plastics)	42
<i>Microplastic: PP or PS (d = 4 mm) mixed with groundnut shells (d = 1 mm); products: a mixture of liquid hydrocarbons</i>									
Spent FCC, Si : Al = 1.29	510	—	N ₂	—	10	4.3–6.5	43 ^a 65 ^b		43
<i>Microplastic: HDPE (d = 5 mm); products: a mixture of liquid hydrocarbons</i>									
Y zeolite or MgCO ₃	430–460	—	N ₂	—	10–20	0.7–1.5	75–84	In the presence of the catalysts, the yield decreased, and longer exposure (at lower temperature) was required in comparison with the non-catalyzed reaction	44
<i>Microplastic: PP (d = 2–8 mm); products: a mixture of liquid and gaseous hydrocarbons</i>									
ECAT containing a zeolite, silica and clay (d = 50 μm)	420	110	N ₂	3	50	2.6	98	The product yield was higher with ECAT (the highest mesoporosity) than with FCC or FCC without the zeolite	45

Table 1 (continued).

Catalyst	Optimal reaction conditions					Catalytic characteristics		Comments	Ref.
	$T, ^\circ\text{C}$	p, kPa	medium gas	q $v, \text{L h}^{-1}$ (mass %)	$P,$ $\text{mg h}^{-1} \text{mg}^{-1}$	Q (%)			
<i>Microplastic: HDPE ($d = 1-2 \text{ mm}$) mixed with a 10-fold amount of heavy gas oil; products: a mixture of liquid and gaseous hydrocarbons</i>									
A mixture of clay and Al_2O_3 or Fe_2O_3	450	101.3	N_2	0.6	100	2.8–3.1	70–77	The presence of heavy gas oil significantly increased the yields. To attain the same yield for pure PE, it was necessary to raise the temperature to 500°C . In the case of zeolite with $\text{SiO}_2 : \text{Al}_2\text{O}_3 = 0.74$, the yield was higher both for pure PE and for the mixture (at 450°C)	46
<i>Microplastic: a mixture* of HDPE, LDPE, PP, PS, PET ($d = 2-4 \text{ mm}$); products: a mixture of liquid hydrocarbons</i>									
A mixture of Y zeolite, kaolinite clay, Al_2O_3 and Na_2SiO_3 in 1 : 3 : 3 : 3 ratio	350	101.3	—	—	10	3.1	47	The product yield upon the non-catalyzed pyrolysis was 67%, but at 450°C and with the time being increased by 33%	47
<i>Microplastic: LDPE ($d = 0.2 \text{ mm}$); products: a mixture of liquid and gaseous hydrocarbons</i>									
Kaolinite clay composite with $\text{K}_6[\text{H}_2\text{AlBW}_{11}\text{O}_{40}](\text{H}_2\text{O})_9$	295	—	N_2	—	5	—	99	The lower the content of kaolinite, the higher the activity	48
<i>Microplastics: LDPE, HDPE, PP or their mixture in equal proportions ($d = 2.5 \text{ mm}$); products: a mixture of liquid and gaseous hydrocarbons</i>									
ZrO_2	500	101.3	—	—	10	8–11	99	The reaction duration increased in the series $\text{PP} < \text{LDPE} < \text{mixture} < \text{HDPE}$	49
<i>Microplastic: HDPE ($d = 0.05-2.5 \text{ mm}$); products: a mixture of liquid and gaseous hydrocarbons</i>									
Zr/Ca catalyst of uncertain composition	410	101.3	N_2	—	100	2	100		50
<i>Microplastic: PE ($d = 3-5 \text{ mm}$); products: a mixture of liquid and gaseous hydrocarbons</i>									
$\text{AlCl}_3-\text{NaCl}$	400	—	N_2	—	43	1.4	96		51
<i>Microplastic: PS foam; products: a mixture of liquid and gaseous hydrocarbons</i>									
Al_2O_3 doped with 20 mass % Cu ($d = 0.4 \text{ mm}$)	450	101.3	N_2	—	30	6.6	99	When either activated carbon or montmorillonite were used as supports, the product yields were comparable	52
<i>Microplastic: LDPE; products: a mixture of liquid and gaseous hydrocarbons</i>									
n-HZSM-5	380	—	N_2	—	1	49	98	The yields were lower with conventional zeolites	53
<i>Microplastics: PE and PS; products: a mixture of liquid and gaseous hydrocarbons</i>									
Fe_3O_4 (NPs, $d = 50-100 \text{ nm}$) with Ni-ZSM-5 or Pt-K-ZSM-5 zeolites	420	—	N_2	—	10	3.9–4.1	77–82	Microwave heating (64 mT), 10 mass % Fe_3O_4 (NPs); 97% of the products were gases	54
<i>Microplastics: HDPE, LDPE; products: a mixture of liquid and gaseous hydrocarbons</i>									
Pt (NPs, $d = 1-2 \text{ nm}$)/ $\gamma\text{-Al}_2\text{O}_3$ containing 1.5 mass % Pt	280	101.3	Ar	—	169	0.015 ^c 0.018 ^d	61 ^c 75 ^d	The yield decreased by 15% after three reaction cycles 6 h each	55

Table 1 (continued).

Catalyst	Optimal reaction conditions					Catalytic characteristics		Comments	Ref.
	$T, ^\circ\text{C}$	p, kPa	medium gas	q (mass %) $v, \text{L h}^{-1}$	$P, \text{mg h}^{-1} \text{mg}^{-1}$	Q (%)			
<i>Microplastic: PET (d = 5 mm); products: a mixture of liquid and gaseous hydrocarbons</i>									
Pd (NPs)/C containing 5 mass Pd	800	101.3	N ₂	3	1	63	82		56
<i>Microplastic: LDPE, HDPE (d = 1–10 mm, the real samples isolated from soil); products: a mixture of liquid and gaseous hydrocarbons and H₂</i>									
Ni/SiO ₂	700	—	CO ₂ :N ₂ = = 1:3	12	100	0.39 mL h ⁻¹ mg ⁻¹ (H ₂) 0.54 mL h ⁻¹ mg ⁻¹ (CO)	—	An increase in the CO ₂ content resulted in higher CO amount	57
<i>Microplastic: a mixture of PP (d = 2–3 mm) with 9.1% PE; products: H₂ and CNTs</i>									
Ni/Al–SBA-15 (d = 0.46 mm) together with Ni–Cu/CaO–SiO ₂ (d = 0.55 mm)	600 800	—	N ₂	—	5 + 5	28 (CNTs) 9.6 mL h ⁻¹ mg ⁻¹ (H ₂)	48 (CNTs) 22.5 (H ₂)	A two-stage process: T = 600 °C in the first stage and T = 800 °C in the second stage; the amount of each component of the combined catalyst is indicated as 5 + 5	58
<i>Microplastics HDPE, PP, PS (d < 2–3 mm) and their mixtures; products: H₂ and CNTs</i>									
Fe _{1.28} AlO ₄ C _{1.05}	250– 350	101.3	Ar	—	100	14.9 L h ⁻¹ mg ⁻¹ (see ^c) 13.8 L h ⁻¹ mg ⁻¹ (see ^a) 7.2 L h ⁻¹ mg ⁻¹ (see ^b)	78 (H ₂) ^c 35 (CNTs) ^c 72 (H ₂) ^a 36 (CNTs) ^a 60 (H ₂) ^b 76 (CNTs) ^b	Microwave heating (1000 W). After five catalyst cycles, the yield of H ₂ changed (49, 56 and 70% for HDPE, PP and PS, respectively) to become higher than the yield of CNTs, which were adsorbed on the catalyst; in the 10th cycle, the yield of H ₂ from HDPE was 12.5%	59
<i>Microplastic: PE or PP mixed with palm oil; products: a mixture of gaseous hydrocarbons</i>									
CAF	700– 1000	—	—	—	60	0.9	86–94.5	Microwave heating (900 W); continuous feeding of the substrate (60 mass % h ⁻¹)	60
<i>Microplastic: PBAC (d = 3 mm); products: bisphenol A, Me₂CO₃</i>									
4-Me ₂ N(C ₃ H ₄ N)	180	2500	—	—	2.4	248 (bis-phenol A) 220 (Me ₂ CO ₃)	99 (bis-phenol A) 88 (Me ₂ CO ₃)	Solvent MeOH: THF = 3:10; microwave heating (up to 850 W). The reaction was 20 times faster than that induced by conventional heating and required less catalyst. The replacement of methanol by phenol resulted in the formation of phenyl carbonate (56% yield)	61
<i>Microplastic: PP (d = 0.1–0.5 mm); products: oxygen reduction catalyst FeNi–Al₂O₃–CNT</i>									
FeNi–Al ₂ O ₃ (d = 0.01 mm)	500	—	N ₂	6	50	—	—	Oxygen reduction catalyst FeNi–Al ₂ O ₃ –CNT	62

Table 1 (continued).

Catalyst	Optimal reaction conditions					Catalytic characteristics		Comments	Ref.
	$T, ^\circ\text{C}$	p, kPa	medium		q (mass %)	$P,$ $\text{mg h}^{-1} \text{mg}^{-1}$	Q (%)		
			gas	$v, \text{L h}^{-1}$					
<i>Microplastic: PBAC ($d = 0.5 \text{ mm}$); products: bisphenol A, PhOH, etc.</i>									
MgO ($d = 0.3\text{--}0.5 \text{ mm}$)	400	108.2	N ₂	30	135	0.4	45 (bis-phenol A)	Simultaneously with the inert gas, H ₂ O (gas) was supplied at a 360 kg h ⁻¹ loading rate. The yield was lower for SiO ₂ , and a temperature of 500 °C was required to attain a comparable yield	63
<i>Microplastic: PBAC ($d = 3 \text{ mm}$); products: bisphenol A</i>									
[Bmim][OAc]	140	260	H ₂ O (gas)	—	150	0.19	96	The reaction required 35 mass % H ₂ O (second substrate). Six cycles of reuse	64
<i>Microplastic: a mixture* of plastics ($d < 5 \text{ mm}$); products: H₂ and other gases</i>									
Ni/Pd/TiO ₂ (NPs, $d = 80\text{--}300 \text{ nm}$)	700	—	N ₂	1.8	1.4	—	77	Feed flow rates: 24 mL h ⁻¹ (H ₂ O vapour) and 2.7 mL h ⁻¹ (PhOH). After 72 h of continuous process, the yield of H ₂ decreased by 12%	65
Ni/Pt/TiO ₂ –Al ₂ O ₃ (NPs, $d = 0.1\text{--}0.6 \mu\text{m}$)	700	—	N ₂	1.8	1.8	—	93	Feed flow rates: 24 mL h ⁻¹ (H ₂ O vapour) and 2.7 mL h ⁻¹ (PhOH). After 40 h of continuous process, the yield of H ₂ decreased by 12%	66

Notes. Here and in other Tables, the asterisk marks natural polymer mixtures, *i.e.*, those existing as mixtures in polymer products or wastes. In the case where the optimal conditions were not defined, the conditions for the catalytic reaction are indicated. The following symbols of physical quantities are used: d is characteristic particle size, T is temperature, p is pressure, v is gas flow rate, q is the mass ratio of the catalyst to the initial microplastic in percent, P is the process performance, Q is the yield of the product in % relative to the theoretically possible one. Designations of the catalysts and microplastics: Bmim is 1-butyl-3-methylimidazolium; CAF is a carbon-coated plate containing aluminium oxide fibres; ECAT is a commercial catalyst for the fluid catalytic cracking of crude oil; FCC is fluid cracking catalyst; HDPE is high-density polyethylene; PS is polystyrene; LDPE is low-density polyethylene; PP is polypropylene; PVC is poly(vinyl chloride); PE is polyethylene; HDPS is high density polystyrene; PLA is polylactic acid; PBAC is poly(bisphenol-A-carbonate); PET is poly(ethylene terephthalate); NP is nanoparticle; THF is tetrahydrofuran; CNT is carbon nanotube; SAPO-1 is the trade mark of a zeolite catalyst. ^a For PP; ^b for PS; ^c for HDPE; ^d for LDPE.

tional deposition of some metals on the catalyst,⁴⁵ resulting in variation of the product composition from one cycle to another.

Comparison of the catalyzed and non-catalyzed pyrolysis of microplastics gives ambiguous results. A number of publications attest to a decrease in the pyrolysis duration or temperature and/or a change in the product composition upon addition of a catalyst.^{36–38, 41–43, 45, 47–51, 53, 54, 56, 59} The authors of other studies either did not observe such differences or noted some deterioration of the process characteristics.^{40, 44}

It is of interest that upon zeolite conversion into a nano-sized form, which is accompanied by a pronounced increase in the contact surface area, the product yield increases 3.2-fold and the required process temperature decreases by 40 °C (*i.e.*, by ~10%).⁵³

An alternative way for supplying the thermal energy to a microplastic subjected to pyrolysis, that is, microwave (MW) heating of the reaction medium should be mentioned.^{54, 59–61} Apart from pyrolytic processes, this design was implemented in other catalytic processes (see below).

The composition of not only zeolites, but also other mixed (composite) catalysts markedly affects the process performance and the yield of the final products: even a minor deviation leads to a decrease in both parameters.⁵⁹ Moreover, impurities of other polymers in the major polymer (*e.g.*, PS impurity in PE or PP)⁵⁹ can also have adverse effect on these characteristics of the process.

In most studies, the stages of polymer pyrolysis and subsequent catalytic conversion of the formed intermediate products are separated in time and space. Such studies are not addressed in this review, although they have their own benefits, but also drawbacks. A comparison of the two-stage process with one-stage catalytic pyrolysis showed an advantage of the latter.³⁴ In the development of the concept of two-stage process, it was proposed to use functionally different catalysts in the two stages: Ni/Al–SBA-15 for the primary gasification and generation of carbon nanotubes (CNTs) and Ni-Cu/CaO–SiO₂ for the conversion of effluent gases to H₂.⁵⁸

A study by Jung *et al.*,⁵⁷ in which microplastic samples were isolated directly from soil, deserves special attention. For this purpose, polymer particles were salted-out with a

Table 2. Chemical catalysts for the hydrogenolysis of microplastics.

Catalyst	Optimal reaction conditions				Catalytic characteristics		Comments	Ref.
	$T, ^\circ\text{C}$	p, MPa	medium	q (mass %)	$P,$ $\text{mg h}^{-1} \text{mg}^{-1}$	Q (%)		
<i>Microplastic: HDPE ($d = 0.125 \text{ mm}$) mixed with sawdust ($d = 0.45 \text{ mm}$); products: a mixture of liquid and gaseous hydrocarbons</i>								
HZSM-5, Si : Al = 30	400	1.5	H ₂	0.2	91.5	87	The yield of aromatic products was 18.2%	67
<i>Microplastic: LDPE ($d < 0.4 \text{ mm}$); products: a mixture of liquid and gaseous hydrocarbons</i>								
H-USY or H-Beta ($d = 0.2\text{--}0.5 \text{ mm}$) zeolite doped with Pt (NPs, $d = 2\text{--}4 \text{ nm}$)	330	2	H ₂	10	9.5	> 95	The product yield was higher with H-Beta characterized by Si : Al = 1 : 2.5 than with H-Beta characterized by Si : Al = 300 or with H-USY	68
<i>Microplastics: LDPE, PP, PS; product: CH₄</i>								
FAU zeolite doped with Ru (NPs, $d = 0.2\text{--}1.5 \mu\text{m}$)	300– 350	5	H ₂	6–7	4.2–4.6	92–97	Higher temperatures were required to degrade PS	69
<i>Microplastic: PE; products: a mixture of liquid and gaseous hydrocarbons</i>								
Pt/SrTiO ₃ nanocuboids ($d = 65 \text{ nm}$)	300	1.2	H ₂	20	0.02–0.05	42–99	The higher the molecular weight of PE, the higher the yield	70
<i>Microplastic: LDPE ($d = 3 \text{ mm}$); products: a mixture of liquid and gaseous hydrocarbons</i>								
Ru (NPs, $d = 3 \text{ nm}$)/C	225	2.2	H ₂	12.5	3.8	95	A 1 : 1 anisole : THF solvent mixture was used. Long-term exposure (16 h instead of 2 h) resulted in complete conversion to CH ₄	71
<i>Microplastic: HDPE ($d = 5 \text{ mm}$); products: a mixture of liquid and gaseous hydrocarbons</i>								
Ru (NPs, $d = 3 \text{ nm}$)/C	220	3	H ₂	50	1.8	90	The solvent was n-C ₆ H ₁₄ . After five cycles of reuse, the yield of liquid hydrocarbons decreased by 10%, while the amount of volatile hydrocarbons increased	72
<i>Microplastic: PP ($d = 3 \text{ mm}$); products: a mixture of liquid and gaseous hydrocarbons</i>								
Ru (NPs, $d = 1\text{--}2 \text{ nm}$)/C	225	5	H ₂	7.1	0.32	54	The catalyst could be reused (the yield increased by 22%)	73
<i>Microplastics: LDPE, HDPE, PP, a mixture of PE ($d = 2 \text{ mm}$) with low-molecular-weight LDPE; products: a mixture of liquid and gaseous hydrocarbons</i>								
Ru (NPs, $d = 6 \text{ nm}$)/CeO ₂	240	6	H ₂	3–15	0.14	89–99	After five cycles of reuse, the yield decreased by 5%; the loss of the catalyst was 15 mass % per cycle	74
<i>Microplastic: PU; products: aniline derivatives and other products</i>								
[IrClH ₂]R ¹ , where R ¹ = [Pr ¹ ₂ P(CH ₂) ₂]NH	150– 180	3	H ₂	2	0.6–2.2	24–91	The solvent was Pr ¹ OH, 0.1–0.25 mass % K ₃ PO ₄ . Various polyurethanes were used	75
<i>Microplastics: PET ($d = 5 \text{ mm}$), PLA ($d = 5 \text{ mm}$), P3HB, P3HP, PEC, PPC; products: alcohols or acids (in the case of P3HB and P3HP)</i>								
[Ru(CO)H]R ¹ , where R ¹ = 2-(Bu ¹ ₂ PCH)-6-[2-(C ₅ H ₄ N)](C ₅ H ₃ N) or 2-(Bu ¹ ₂ PCH)-6-(Et ₂ NCH ₂)(C ₅ H ₃ N)	160	4.13	H ₂	4–12	0.2–0.5	88–99	The solvent was a 1 : 1 anisole : THF mixture. The Q and P values varied in the series PET = PLA = PPC > PEC > P3HP > P3HB	76

Table 2 (continued)

Catalyst	Optimal reaction conditions				Catalytic characteristics		Comments	Ref.
	<i>T</i> , °C	<i>p</i> , MPa	medium	<i>q</i> (mass %)	<i>P</i> , mg h ⁻¹ mg ⁻¹	<i>Q</i> (%)		
<i>Microplastics: PA6 (d = 2–3 mm), PA6.6, PA12, PBBT, PDHT, PBBC, PBBO, PMBS;</i> <i>products: amino alcohols (in the case of PA6, PA6.6 and PA12), diols and diamines (in all other cases)</i>								
[Ru(CO)H]R ¹ , where R ¹ = 2-(Bu ¹ PCH)-6- (Bu ¹ NHCH ₂)(C ₅ H ₃ N) or 2-(Bu ¹ PCH)-6- (BnNHCH ₂)(C ₅ H ₃ N), etc.	150	7	H ₂	3–9	0.06 ^a 0.08 ^b 0.05 ^c 0.06 ^c 0.13 ^d 0.23 ^e 0.24 ^e 0.12 ^f 0.11 ^f 0.18 ^g 0.21 ^g 0.1 ^h 0.23 ^h 0.13 ⁱ 0.29 ⁱ	24 ^a 32 ^b 20 (diol) ^c 25 (diamine) ^c 30 ^d 80 (diol) ^e 85 (diamine) ^e 42 (diol) ^f 45 (diamine) ^f 75 (diol) ^g 74 (diamine) ^g 77 (diol) ^h 82 (diamine) ^h 70 (diol) ⁱ 66 (diamine) ⁱ	DMSO used as the solvent played a crucial role in the process by breaking hydrogen bonds of polyamide	77
<i>Microplastics: PLA, PCL, PET, PBT, PBAC; products: diols</i>								
[RuR ¹]R ² as an equimolar mixture with [(CF ₃ SO ₂) ₂ N]H, where R ¹ = MeC(CH ₂ Ph ₂ P) ₃ or MeC(CH ₂ (3,5-Me ₂ C ₆ H ₃) ₂ P) ₃ , R ² = C(CH ₂) ₃	140	10	H ₂	3.1–10	0.65 ^j 0.94 ^k 0.58 ^l 0.90 ^m 1.8 ⁿ	99 ^j 99 ^k 64 ^l 99 ^m 99 ⁿ	1,4- Dioxane was used as the solvent; 1.1–3.6 mass % [(CF ₃ SO ₂) ₂ N]H; HDPE, PP, PS, PVC and PA6 present in equimolar amounts did not impair the efficiency of catalysis. In the absence of a solvent, the yield decreased	78
<i>Microplastics: PET (d = 0.25 mm), PBT, PHMA; products: EG and other products (Me₂TPA, p-xylene, MeOH)</i>								
Cu ₄ Fe ₁ Cr ₁	240	3	CO ₂ : H ₂ : Ar = = 12: 12: 1	100	0.02	75.5 ¹ 34 ^m 26 ^o	After three cycles, the activity decreased by 10%	79
<i>Microplastic: PET (d = 0.3 mm); products: TPA, C₂H₄</i>								
MoO ₂ /C containing 3.23 mass % Mo	260	0.1013	H ₂	76	0.04	87	Four cycles of reuse	80
<i>Microplastic: PET; products: TPA, MeTPA</i>								
MOF UiO-66	260	0.1013	H ₂	43	0.08	98	The TPA : MeTPA ratio was 2.8; in Ar atmosphere, it decreased to 2, while the yield decreased by 17%; the yield varied in the following series UiO-66 > MIL-140A >> Zr6 cluster or ZrO ₂ ≈ no catalyst; after four cycles the yield decreased by ~25%	81

Notes. The following designations are used: MeTPA is monomethyl terephthalate; MOF is metal-organic framework; PU is polyurethane; P3HB is poly(3-hydroxybutyrate); P3HP is poly(3-hydroxypropionate); PEC is poly(ethylene carbonate); PA6, PA6.6, PA12 are polyamide brands; PPC is poly(propylene carbonate); PDHT is poly(1,6-diaminohexaneterephthalamide); PBBC is poly(1,3-bis(aminomethyl)benzenecapramide); PBBO is poly(1,3-bis(aminomethyl)benzylloxalamide); PMBS is poly(4,4'-methylene-bis(cyclohexanamide)succinamide); PLA is polylactic acid; PCL is poly(ϵ -caprolactone); PBT is poly(1,4-butylene terephthalate); TPA is terephthalic acid; PHMA is poly(hexamethylene adipate); EG is ethylene glycol. ^a For PA6 (*d* = 3 mm); ^b for PA6; ^c for PA6.6; ^d for PA12; ^e for PBBT; ^f for PDHT; ^g for PBBC; ^h for PBBO; ⁱ for PMBS; ^j for PLA; ^k for PCL; ^l for PET; ^m for PBT; ⁿ for PBAC; ^o for PHMA.

Table 3. Chemical catalysts for the silylation of microplastics.

Catalyst	Optimal reaction conditions				Catalytic characteristics		Comments	Ref.	
	<i>T</i> , °C	<i>p</i> , kPa	silylating agent (mass %)	solvent	<i>q</i> (mass %)	<i>P</i> , mg h ⁻¹ mg ⁻¹			<i>Q</i> (%)
<i>Microplastics: PCL (d = 4 mm), PPC, PBAC, PEG, PEB, PDO, PLA (d < 4 mm), PET, PVC;</i> <i>products: silylated alcohols</i>									
[IrR ¹ (L)H][B(C ₆ F ₅) ₄], where L = THF, R ¹ = 1,3-(Bu ¹ ₂ P) ₂ C ₆ H ₃ ,	25–	—	Et ₃ SiH (164–492)	C ₆ H ₅ Cl	2.1–	3.9 ^a	9.9 ^a	C ₆ H ₅ Cl was used as the solvent. Polyglycolic acid and P3HB were not silylated. PVC was dechlorinated. PLA was not silylated in the presence of PVC (nor in the presence of PPC, while PPC decomposed); conversely, with another catalyst, [B(C ₆ F ₅) ₃], only PLA was silylated in a mixture	82
	65				9.2	30 ^b	99 ^b		
						12.4 ^c	98 ^c		
						4.9 ^d	46 ^d		
						2 ^e	99 ^e		
						1 ^f	82 ^f		
						0.6 ^g	95 ^g		
						0.3 ^h	83 ^h		
<i>Microplastics: PCL, PLA, PET, PBT;</i> <i>products: diols (or THF in the case of PBT), p-xylene (in the case of PET and PBT)</i>									
Zn(OAc) ₂	110	101.3	PhSiH ₃ (193–451)	PhMe PhCl (see ⁱ)	8–25	0.5 ^a	98 ^a	Successive introduction of a 3.5-fold molar amount of PET in 7 cycles resulted in 15% decrease in the yield. Selective silylation of PCL in the presence of PET or PBT with a minor (3–5%) decrease in the yield. Desilylation required treatment with 20% KOH in MeOH	83
	160 ⁱ					0.06 ^g	71 ^g		
						0.04 ^h	65 ^h		
						0.4 ⁱ	67 ^j		
<i>Microplastics: PEG, PLA, PET, PBAC and mixtures of PET with PLA, PS and/or PVC;</i> <i>product: C₂H₆ (in the case of PEG and PET), C₃H₈ (in the case of PLA), p-xylene (in the case of PET), CH₄ and silylated adduct of bisphenol A (in the case of PBAC)</i>									
B(C ₆ F ₅) ₃	20	101.3	(Me ₂ SiH) ₂ O (116–419)	CH ₂ Cl ₂	4–17	2.2 ^d	99 ^d	Argon atmosphere was used. In the case of [Ph ₃ C ⁺ , B(C ₆ F ₅) ₄ ⁻], the product yield was lower and a longer time was required. PS and PVC were not silylated. Biopolymers (tannin, suberin) were poorly silylated	84
						2.2 ^g	99 ^g		
						0.21 mL h ⁻¹ mg ⁻¹ (see ^h)	82 ^h		
						27.4 mL h ⁻¹ mg ⁻¹ (see ^c)	98 ^c		

Notes. The following designations are used: PEG is poly(ethylene glycol); PEB is poly(ethylene butanedioate); PDO is polydioxanone. ^a For PCL; ^b for PPC; ^c for PBAC; ^d for PEG; ^e for PEB; ^f for PDO; ^g for PLA; ^h for PET; ⁱ for PET or PBT; ^j for PBT.

Table 4. Chemical catalysts for electro- and photocatalytic reactions of microplastics.

Catalyst	Optimal reaction conditions				Catalytic characteristics		Comments	Ref.
	<i>T</i> , °C	<i>p</i> , kPa	medium	<i>q</i> (mass %)	<i>P</i> , mg h ⁻¹ mg ⁻¹	<i>Q</i> (%)		
<i>Microplastic: PVC (d = 0.1–0.5 mm); products: Cl⁻ ions, carboxylic acids</i>								
TiO ₂ /C-based cathode (3 × 3 × 0.2 cm)	100 ^a	—	H ₂ O, Na ₂ SO ₄ (50 mmol L ⁻¹), O ₂ (2.4 L h ⁻¹)	180	0.07 (Cl ⁻) 0.01 (carboxylic acids)	75 (Cl ⁻)	The potential was 0.7 V, pH 3. The yield of Cl ⁻ ions on an electrode without TiO ₂ /C was 29%, while that with the common Fenton reagent was < 5% (at 25 °C)	85

Table 4 (continued).

Catalyst	Optimal reaction conditions				Catalytic characteristics		Comments	Ref.
	$T, ^\circ\text{C}$	p, kPa	medium	q (mass %)	$P, \text{mg h}^{-1} \text{mg}^{-1}$	Q (%)		
<i>Microplastic: PET (d = 1 mm); product: H₂</i>								
Mo _{4.3} Cd _{0.5} Zn _{0.5} S nanosheets	—	—	H ₂ O	0.7	0	0	Exposure to light (300 W); vacuum (in the gas phase). The alkaline hydrolysis of PET was required to convert the hydrolysis intermediates (EG, TPA) to H ₂	86
<i>Microplastics PE, PP, PET (d < 0.5 mm); products: H₂, CO₂ CO</i>								
Cobalt-doped Ga ₂ O ₃ nanosheets (d = 200 nm)	25	101.3	H ₂ O	50	60 mL h ⁻¹ mg ⁻¹	22 ^a	Exposure to light (0.1 W cm ⁻²). Hydrogen (and oxygen) was generated upon photolysis of water rather than from the polymer. The yield decreased in the order PE > PP > PET. When O ₂ was supplied, the yield increased, while in the case of N ₂ it decreased	87
<i>Microplastic: PE, PP, PVC; product: CO₂</i>								
Nb ₂ O ₅ -doped PVP	25 ^b	101.3	H ₂ O	33–67	2.3 × 10 ⁻² (see ^a) 1.5 × 10 ⁻² (see ^b) 1.0 × 10 ⁻² (see ^c)	9.9 ^a 9.5 ^b 10.7 ^c	Exposure to light (0.1 W cm ⁻²). Oxidative conditions were required. When real samples were used, the yield further decreased by one third	88
<i>Microplastic: PS (d = 315 nm); products: CO₂, CO</i>								
Anodized TiO ₂ surface	30 ^c	101.3	H ₂ O	31	1.2 × 10 ⁻² mL h ⁻¹ mg ⁻¹	11	UV irradiation (21 μW cm ⁻²). The yield was calculated on the basis of TOC (total organic carbon). In the presence of other structures (such as nanotubes), the yield was lower	89
<i>Microplastics: PS (d = 140 or 510 nm), PMMA (d = 110 nm); products: CO₂, CO</i>								
β-SiC foam modified with TiO ₂ -P25 microparticles (d = 1 μm)	101.3	H ₂ O (2.4 L h ⁻¹)	16667	5.8 × 10 ⁻⁴ mL h ⁻¹ mg ⁻¹ (see ^d) 3.4 × 10 ⁻⁴ mL h ⁻¹ mg ⁻¹ (see ^e)	50 ^d 23 ^e	UV irradiation (11.2 mW cm ⁻²), pH 6.3. The yield was calculated on the basis of TOC; PS with d = 510 nm degraded more slowly	90	
<i>Microplastics: PS and its derivatives; products: PhCOOH, HCOOH, Ph₂CO</i>								
(4-Bn)SO ₃ H or other acids	100	O ₂	11	3.5–4.6	38–50 (C ₆ H ₅ COOH) 57–67 (HCOOH)	Exposure to light (λ = 405 nm, 9 W); C ₆ H ₆ : MeCN = 1:1 as the solvent. It was possible to directly obtain formilides or carry out the reaction in a continuous flow system. The presence of oxygen was obligatory	91	

Notes. The following designations are used: PVP is polyvinylpyrrolidone, PMMA is poly(methyl methacrylate). ^a For PE; ^b for PP; ^c for PVC; ^d for PMMA; ^e for PS (d = 14 μm).

Table 5. Chemical catalysts for the oxidative reactions of microplastics.

Catalyst	Optimal reaction conditions				Catalytic characteristics		Comments	Ref.
	<i>T</i> , °C	<i>p</i> , kPa	medium ^a	<i>q</i> (mass %)	<i>P</i> , mg h ⁻¹ mg ⁻¹	<i>Q</i> (%)		
<i>Microplastic: PE (0.125–0.2 mm)</i>								
Fenton reagent	80	—	FeCl ₃ (<1), H ₂ O ₂ (1)	—	0	0	pH 2.6; the polymer should be first modified by ClSO ₃ H	92
<i>Microplastics PE, PP, PVC (d = 0.125–0.2 mm)</i>								
Fenton reagent	—	—	H ₂ O ₂ (0.33)	—	0	0	Exposure to light (500 W); pH 2.5; the polymer should be first modified by ClSO ₃ H	93
<i>Microplastics: PS, PET, HDPE, LDPE and PP (d = 0.1 mm), PVC</i>								
Fenton reagent	140	—	FeSO ₄ (4), H ₂ O ₂ (0.2), HCl (0.2)	—	0	0	The polymer should be first modified by ClSO ₃ H	94
<i>Microplastics: PS (0.48, 1.2, 2.1, 8.8 μm), PE (d = 0.6–4.3 μm), PMMA (d = 0.42 μm), PVC (d = 0.2–2.1, 46–163 μm), PP (d = 1–19 μm), PET (d = 9–51 μm)</i>								
Fenton reagent	80	—	FeCl (3.75), H ₂ O ₂ (1)	—	0	0	The polymer should be first modified by ClSO ₃ H	95
<i>Microplastic: PVC (d = 0.15 mm); products: dechlorinated compounds</i>								
K ₂ S ₂ O ₈	—	101.3	H ₂ O	810	1.1 × 10 ⁻⁴ (Cl ⁻)	—	UV irradiation; pH 7. PVC particles were reduced in size during the process	96
<i>Microplastic: LDPE (d = 0.2–0.3 mm); product: a mixture of carboxylic acids</i>								
HNO ₃ or H ₂ SO ₄	180	400	H ₂ O	0.4	127	71	Microwave heating (1200 W). A comparable yield was attained with a smaller amount of H ₂ SO ₄	97

^aThe values in parentheses are the concentrations in water expressed in mmol L⁻¹ for iron salts and in mol L⁻¹ for other compounds.

Table 6. Chemical catalysts for the solvolysis of microplastics.

Catalyst	Optimal reaction conditions				Catalytic characteristics		Comments	Ref.
	<i>T</i> , °C	<i>p</i> , kPa	medium	<i>q</i> (mass %)	<i>P</i> , mg h ⁻¹ mg ⁻¹	<i>Q</i> (%)		
<i>Microplastics: a mixture of PBAC and PET; products: TMADC, bisphenol A</i>								
TBD:MSA	130	101.3	N ₂ TMAD (410)	9.5	0.23	98	Selective modification of PBAC	98
<i>Microplastics: low-molecular weight PEF and its mixtures with PA-6, PPS, PEG, PS, PVC, PLA, PCL, PET; products: Me₂FDA, MeCH(OH)COOMe (in the case of PLA) or HO(CH₂)₅COOMe (in the case of PCL)</i>								
Zn(OAc) ₂	120	101.3	— MeOH (730–1190)	3–5	32 ^a 18 ^b 4.5 ^c	86 ^a 83 ^b 15 ^c	Microwave heating; PA-6, PPS, PEG, PS, PVC and PET were not converted and did not affect the yield (except for low-molecular-weight PEG, which did not degrade, but increased the yield); PLA and PCL decreased the yield of products from PEF by 5%	99

Table 6 (continued).

Catalyst	Optimal reaction conditions					Catalytic characteristics		Comments	Ref.
	T, °C	p, kPa	medium		q (mass %)	P, mg h ⁻¹ mg ⁻¹	Q (%)		
			gas	solvent (mass %)					
<i>Microplastics: PEF, PET (d = 0.15–0.18 mm); products: Me₂FDA (in the case of PEF), Me₂TPA (in the case of PET)</i>									
[Bmim][OAc]	130 ^a 150 ^d	101.3	—	MeOH (400)	3.7	42 ^a 2.8 ^d	78 ^a 42 ^d	The yield decreased by 3% after the sixth cycle	100
<i>Microplastic: PET (d = 5 mm); product: Me₂TPA</i>									
PEVIA doped with Zn ²⁺ ions	170	—	—	MeOH (400)	2	46	90	The metal content decreased by 19% after six cycles, while the yield decreased by 10%. The decrease in the yield was insignificant in the case of methanolysis of fibres; in the case of other contaminants (especially acrylates), the yield decreased by 24%	101
<i>Microplastic: PLA (d = 3 or 5 mm); product: MeCH(OH)COOMe</i>									
ZnR ₂ ¹ , where R ¹ = 2,4-Bu ₂ -6-(MeNH(CH ₂) ₂ N=CH)C ₆ H ₂ O	40	—	N ₂	MeOH: THF = = 1:4 (435)	12	0.16	92 ^e		102
<i>Microplastics: PLA, PET (d = 5 mm); products: MeCH(OH)COOMe (in the case of PLA), Bn₂TPA (in the case of PET)</i>									
ZnR ₂ ¹ , where R ¹ = 2,4-Bu ₂ -6-(MeNH(CH ₂) ₃ N=CH)C ₆ H ₂ O	130– 150	101.3	Ar	MeOH (634) or BnOH (832)	1–5	142 ^f — (see ^d)	98 ^f — (see ^d)		103
<i>Microplastics: PLA (d = 3 mm), PET (d = 3 mm), PCL (d = 3 mm) and their mixtures; products: methyl esters of organic acids</i>									
[TMGasme]ZnCl ₂	150	—	N ₂	MeOH (311)	6	26 ^f	98 ^f	k ₁ = 2.9 × 10 ⁻⁴ mol h ⁻¹ mol ⁻¹ (60 °C). The catalyst can be reused. The catalyst activity changed in the order PLA > PCL > PET	104
<i>Microplastic: PET (d = 3 mm); product: Et₂TPA</i>									
Co ₃ O ₄ (NPs, d = 5–10 nm) or NiO (NPs, d = 20–50 nm)	255	11600	—	EtOH (3156)	0.67	97	84		105
<i>Microplastic: PET (d = 4 mm); product: BHET</i>									
TBD:MSA	180	101.3	N ₂	EG (500)	24.5	2.3	91	The catalyst was stable up to 300 °C	106
<i>Microplastic: PET (d = 74 μm); product: BHET</i>									
DBN:[4-MePh]	190	101.3	N ₂	EG (600)	6	35	87.3		107
<i>Microplastic: PET (d = 0.25–0.42 mm); product: BHET</i>									
[Me ₃ N(CH ₂) ₂ OH]CO ₂ H	180	101.3	N ₂	EG (400)	5	2.3	84.5		108
<i>Microplastic: PDCT (d < 1 mm); product: BHDET</i>									
Zn(OMe) ₂	190	101.3	—	DEG (1520)	35	0.64	90		109
<i>Microplastic: PET (d = 0.25–0.4 mm); product: BHET</i>									
Zn(OAc) ₂	190	101.3	—	EG (200), DMSO	5	267	84		110
<i>Microplastic: PET (d = 0.5, 1.5, 3 mm); product: BHET</i>									
Zn(OAc) ₂	196	101.3	N ₂	EG (500)	2	88	78 ^g	Microwave heating (500 W). The greater the PET size, the lower the yield	111

Table 6 (continued).

Catalyst	Optimal reaction conditions				Catalytic characteristics			Comments	Ref.
	T, °C	p, kPa	medium		q (mass %)	P, mg h ⁻¹	Q (%)		
			gas	solvent (mass %)					
	<i>Microplastic: PET (d = 6 mm); product: BHET</i>								
Zn(OAc) ₂	190	101.3	—	EG (600)	0.5	233	44	Microwave heating (460 W)	112
	<i>Microplastic: PET (d = 1 or 5 mm); product: BHET</i>								
3-Tropanol complex with Zn(OAc) ₂ in 1 : 4 molar ratio	190	101.3	—	EG (500)	5	11	82 ^h	A decrease in the particle size resulted in a decrease in the yield (by 3%). The yield decreased by 10% after five catalytic cycles	113
	<i>Microplastic: PET (d = 0.35, 0.85, 1.2, 2.0–2.7 mm); product: BHET</i>								
NH ₄ HSO ₄ /ZnO-TiO ₂	180	101.3	—	EG (557)	3	10.7	73	Four cycles of catalyst reuse without change in the yield. A decrease in the PET particle size resulted in a minor decrease in the yield	114
	<i>Microplastic: PET (d = 1 mm); product: BHET</i>								
[Bmim][ZnCl ₃]	190	101.3	—	EG (1100)	1.25	45	85	Five cycles of catalyst reuse without change in the yield	115
	<i>Microplastic: PET (d = 2.7 mm); product: BHET</i>								
[Amim][ZnCl ₃]	175	101.3	N ₂	EG (400)	10	7.8	80		116
	<i>Microplastic: PET (d = 2–2.7, 1.4–1.7, 0.8–1.4, 0.6–0.8, 0.25–0.42 mm); product: BHET</i>								
[Bmim] ₂ [CoCl ₄]	170	101.3	N ₂	EG (400)	10	2.6	78	Six cycles of catalyst reuse. A decrease in the PET particle size resulted in 5% decrease in the yield	117
	<i>Microplastic: PET (d = 4 mm); product: BHET</i>								
A mixture of [Hmim][ZnCl ₃] and [Hmim][CoCl ₃]	190	101.3	N ₂	EG (1100)	1	58	87	The maximum yield was attained with an equimolar mixture of catalysts	118
Cu(OAc) ₂ –[Bmim][OAc] or Zn(OAc) ₂ –[Bmim][OAc]	190	101.3	N ₂	EG (1000)	50	0.3–0.4	53.2 (Cu) 42.7 (Zn)	Six cycles of catalyst reuse	119
[Mmim] ⁺ -2-COO ⁻	185	101.3	N ₂	EG (1000)	15	5.4	61		120
[Bmim][OAc]	190	101.3	—	EG (667)	33	0.8	58		121
	<i>Microplastic: PET (d = 0.3 mm); product: BHET</i>								
PBVI containing ZnCl ₂	195	101.3	—	EG (400)	20	2.6	78	Five cycles of catalyst reuse. When the metals were used without the polymer, the product yields were higher and the temperature was lower by 5 °C	122
	<i>Microplastic: PET (d = 0.2 mm); product: BHET</i>								
ZnMn ₂ O ₂₋₄ (spinel structure, d = 20 nm)	260	506.6	Ar	EG (555)	1	122	92	This catalyst had the highest acidity	123
	<i>Microplastic: PET (d = 4 mm); product: BHET</i>								
(Mg _x , Zn _y , Al _z)O _{x+y+1.5z} , brucite structure	196	101.3	N ₂	EG (1000)	1	30	75	Four cycles of catalyst reuse	124
	<i>Microplastic: PET (d = 5 mm); product: BHET</i>								
Mg _x Al _y O _z doped with TiO ₂ (NPs)	180	101.3	N ₂	EG (97)	20	2.6	40	Six cycles of catalyst reuse (decrease in the yield by 4%)	125

Table 6 (continued).

Catalyst	Optimal reaction conditions				Catalytic characteristics			Comments	Ref.
	T, °C	p, kPa	medium		q (mass %)	P, mg h ⁻¹	Q (%)		
			gas	solvent (mass %)					
	<i>Microplastic: PET (d = 2 mm); product: BHET</i>								
MgO/Al ₂ O ₃ , hydrotalcite structure, Mg: Al = 2.83	196	101.3	N ₂	EG (500)	1	129	81	Three cycles of catalyst reuse (the yield decreased by 18.6%; recalcination was required)	126
	<i>Microplastic: PET (d = 2.7 mm); product: BHET</i>								
K ₆ SiW ₁₁ ZnO ₃₉ (H ₂ O)	185	101.3	—	EG (400)	2	111	84	Eight cycles of catalyst reuse	127
	<i>Microplastic: PET (d = 125 μm); product: BHET</i>								
CeO ₂ (NPs, d = 2.7 nm)	196	101.3	N ₂	EG (700)	1	478	90	The yield decreased by 40% in the fourth cycle	128
	<i>Microplastic: PET (d = 0.15 mm); product: BHET</i>								
γ-Fe ₂ O ₃ (NPs, d = 10.5 nm)	300	1100	—	EG (370)	2	60	90	The catalyst could be separated by magnetic decantation (87–94% recovery). The yield decreased by 3% in the ninth cycle	129
	<i>Microplastic: PET (d = 4 mm); product: BHET</i>								
Multiwalled CNTs doped with Fe ₃ O ₄ (NPs, d = 3 nm)	190	101.3	—	EG (1000)	5	13	100	Eight cycles of catalyst reuse	130
	<i>Microplastic: PET (d = 1–2.4 mm); product: BHET</i>								
TiO ₂ nanotubes (d = 9 nm) with sorbed Zn ²⁺ ions	196	101.3	—	EG (400)	0.3	115	87		131
	<i>Microplastic: PET (d = 1 mm); product: BHET</i>								
Co _x O _y (NPs, d = 3 nm) on carbon supported	180	101.3	—	EG (2775)	1.5	23	77	Five cycles of catalyst reuse; the carbon support was a product of tannic acid reduction of uncertain composition and structure	132
	<i>Microplastic: PET (d = 0.2 mm); product: BHET</i>								
Mn ₃ O ₄ nanocomposite with graphene oxide in 2:3 ratio	300	110	Ar	EG (367)	1	96	96		133
	<i>Microplastic: PET (d = 3–5 mm); product: BHET</i>								
Fe ₃ O ₄ (NPs, d = 11 nm) coated by SiO ₂ and modified with N-MeIm and FeCl ₃	180–190	101.3	—	EG (1130)	15	0.36	99	The yield decreased to 84% in the twelfth cycle	134
	<i>Microplastics: PET, PBT (d = 0.3 mm) and their mixture; product: BHET</i>								
ZIF-8/ZIF-67 MOF composite modified with CoFe ₂ O ₄ (NPs)	195–200	101.3	—	EG (500)	1	117 ⁱ 90 ^j 104 ^k	89 ⁱ 78 ^j 84 ^k	After five cycles, 8.7% of Zn and 6.1% of Co were lost, but the yield did not change	135
	<i>Microplastic: PET (d = 3 mm); product: BHET</i>								
MOF ZIF-8	197	101.3	—	EG (500)	1	68	77	The yield decreased by 7% in the third cycle	136
	<i>Microplastic: PET (d = 2.5 or 5 mm); product: BHET</i>								
MOF MAF-6 (d = 0.3 μm)	180	101.3	—	EG (600)	1	27 ^l 20 ^h	82 ^l 62 ^h	The yield decreased by 10% in the second cycle and then it remained constant for five cycles	137

Table 6 (continued).

Catalyst	Optimal reaction conditions				Catalytic characteristics		Comments	Ref.	
	$T, ^\circ\text{C}$	p, kPa	medium		$P, \text{mg h}^{-1} \text{mg}^{-1}$	$Q (\%)$			
			gas	solvent (mass %)					q (mass %)
<i>Microplastic: PET (d = 5 mm); product: BHET</i>									
[Me ₃ N(CH ₂) ₂ OH] ₃ PO ₄ together with poly-dopamine-modified CNTs	180	101.3	—	EG (400), [Ch] ₃ PO ₄ (20)	2	1.4	82	Exposure to light (0.6 W cm ⁻²); the addition of PE had no effect on the outcome	138
<i>Microplastic: PET (d = 5 mm); product: TPA dihydrazide</i>									
Na ₂ CO ₃	65	101.3	—	N ₂ H ₄ ·H ₂ O	1	28	84		139
<i>Microplastic: PET (d = 3 mm); products: BHET amide and other TPA amides</i>									
TBD	120	101.3	N ₂	AE (210)	3.6	25	93	$k_1 = 2 \times 10^{-4} \text{ mol}^{-1} \text{ s}^{-1}$. The product yield was lower when other amines were used	140
<i>Microplastic: PET (d = 3–5 mm); product: 1,4-bis(benzimidazolyl)benzene or 1,4-bis(benzoxazolyl)benzene</i>									
TBD	190	101.3	N ₂	1,2-(NH ₂) ₂ C ₆ H ₄ (425) or 2-NH ₂ C ₆ H ₄ OH (456)	3.6	0.35 (imad-azolyl) 0.2 (ox-azolyl)	62 (imad-azolyl) 62 (ox-azolyl)	Remaining TPA reacted. For the preparation of 1,4-bis(benzoxazolyl)benzene, the addition of <i>N</i> -cyclohexyl-2-pyrrolidone was required	141
<i>Microplastic: PET; product: BHET amide</i>									
ZnO (Sn ^{II} -doped NPs, $d = 40–70 \text{ nm}$)	160	101.3	—	AE (4000)	10	1.9	95	Seven cycles of catalyst reuse	142
<i>Microplastic: PET (d < 0.5, 0.5–0.2, > 0.2 mm); product: TPA</i>									
NaOH together with [Bu ₄ N] ⁺ I ⁻	90	—	—	NaOH (2.5) ^m	3	26–33	98 ⁿ 86 ^o 78 ^p	Microwave heating (200 W). The smaller the particle size, the lower the yield of the product	143
<i>Microplastic: PET (d = 0.2–0.5 mm); products: TPA and EG</i>									
NaOH together with [Bu ₄ N] ⁺ I ⁻	90	101.3	—	H ₂ O, NaOH (167)	3	38	99	Ultrasonic treatment (20 kHz, 190 W power of the unit) accelerated the process by 36%	144
<i>Microplastic: PET (d < 50 mm); products: TPA and EG</i>									
KOH	60	—	—	H ₂ O	178	0.03 mL h ⁻¹ mg ⁻¹	96.7	In the second stage, EG was electro-catalytically converted to diformate	145
<i>Microplastic: PET (particles, d = 0.3 mm, or microfibrils), PLA (d < 3 mm); products: TPA and EG (in the case of PET), MeCH(OH)COOH (in the case of PLA)</i>									
KOH	40	101.3	—	H ₂ O	224	8.2 × 10 ⁻³ (see ^q) 4.2 × 10 ⁻³ (see ^r) 1.7 × 10 ⁻³ (see ^f)	51 ^q 26 ^r 72 ^f	In the second stage, the products were converted to H ₂ and various organic compounds (e.g., acetate and formate)	146
<i>Microplastic: PET (d = 1 or 4 mm); products: TPA and EG</i>									
TiO ₂ ($d = 0.1 \text{ mm}$) doped with 4 mass % H ₂ SO ₄ in supercritical CO ₂	160	15000	CO ₂	H ₂ O (1000)	10	0.7 (TPA) 0.2 (EG)	99 (TPA) 91 (EG)	The size of PET particles does not affect the yield (1%)	147

Table 6 (continued).

Catalyst	Optimal reaction conditions				Catalytic characteristics		Comments	Ref.
	T, °C	p, kPa	medium	q (mass %)	P, mg h ⁻¹	Q (%)		
			gas solvent (mass %)					
<i>Microplastic: PET (d = 0.5–1.18 mm); products: TPA, HET (HET: TPA = 0.02)</i>								
Zn(OAc) ₂ /(NH ₂) ₂ CO in 1 : 4 molar ratio in the first stage and CaLipB lipase (39 kg mol ⁻¹) from <i>Moesziomyces</i> <i>antarcticus</i> (formerly <i>Candida antarctica</i>) in the second stage	<i>First stage</i>							
	197	101.3	—	EG (400)	6	15	68 (BHET)	In the second stage, BHET was enzymatically hydrolyzed with CaLipB
<i>Second stage</i>								
	50	—	—	Phosphate buffer (0.2 mol L ⁻¹)	0.6	5	98 (TPA)	
<i>Microplastic: PET (d = 3 mm); products: TPA, HET (HET: TPA = 0.02)</i>								
K ₂ CO ₃ in the first stage and BsEst- ^{N,C} His ₆ esterase (55.6 kg mol ⁻¹) from <i>Bacillus subtilis</i> in the second stage	<i>First stage</i>							
	200	101.3	—	EG (400)	2	16.2	73.5 (BHET)	In the second stage pH 7.5; BHET was hydrolyzed with BsEst- ^{N,C} His ₆ (the activity of other esterases was lower)
<i>Second stage</i>								
	30	—	—	Phosphate buffer (0.1 mol L ⁻¹)	0.8	9.3	125 (TPA)	to give TPA, which was then converted to catechol using genetically modified bacteria

concentrated NaCl brine, which was followed by mineralization of labile (bio)organic compounds using 30% H₂O₂. According to an original publication,¹⁵¹ the recovery of microplastics was, on average, 30–60% and was most efficient for HDPE, LDPE, PP and PS (without changes in the chemical composition). Despite the fact that the performance of the used catalyst was rather low, transition from the model microplastics to real samples should be highly encouraged and implemented in other works.

Upon pyrolysis, polymers such as PE, PP, PS, PVC, PET, PLA are converted to hydrocarbons and CO₂/CO or, more rarely, to H₂ and CNTs. Cai *et al.*⁶² combined the PP decomposition with the simultaneous preparation of the catalyst for the subsequent electrolysis of water.

The steam hydrolysis of PBAC to give bisphenol A and other phenolic compounds can be considered separately.^{63,64} The use of ionic liquid⁶⁴ made it possible, on the one hand, to considerably decrease the reaction temperature and, on the other hand, to increase the product yield as a result of dissolution of the polymer and, as a consequence, homogeneous catalysis. High temperatures⁶³ caused partial decomposition of bisphenol A to phenol and *p*-isopropenylphenol. During pyrolysis of PBAC,

destruction gave only phenol and polyphenol compounds, which formed a solid residue.

Nabgan *et al.*^{65,66} carried out steam reforming of microplastics together with phenol. With this experimental design, it was impossible to calculate the yields of H₂ separately from phenol and from microplastics.

To summarize the discussion of thermocatalytic reactions for the degradation of microplastics, it should be noted that this process consumes a lot of energy and requires heating, on average, up to 500 °C and higher (Fig. 2). Most often, researchers try to minimize the energy consumption by reducing the process time and/or temperature. With few exceptions, for example, when specific polymers are used,⁶⁴ the temperature cannot be markedly reduced, because this would decrease the performance and the yield of the reaction products.⁵⁵ This results in the loss of the main benefit of the pyrolytic conversion, that is, versatile degradability irrespective of the composition of applicable microplastics. A possible solution to reduce the energy consumption is to combine catalysts with different types of action, *e.g.*, ionic liquids and nano-sized zeolites, in the same catalytic system.

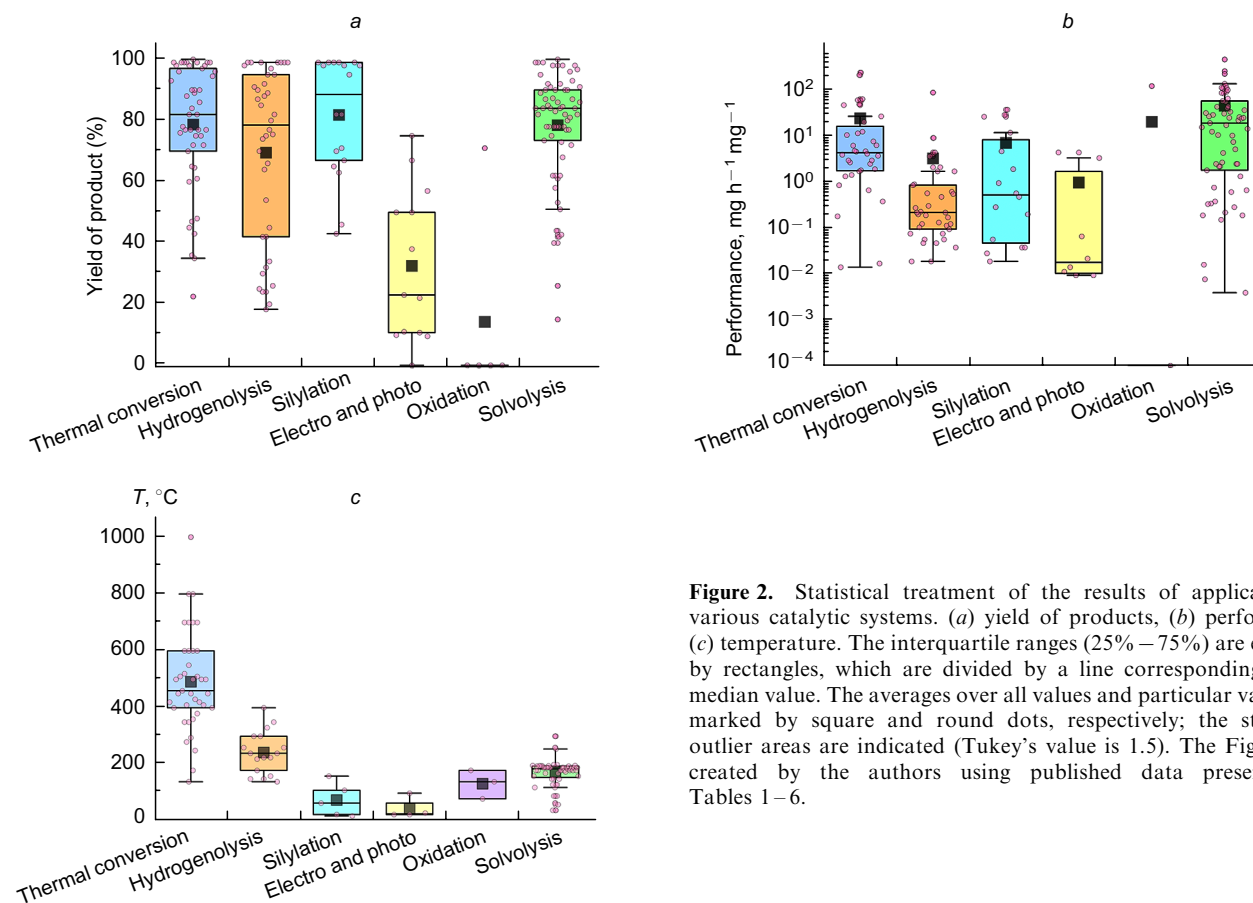


Figure 2. Statistical treatment of the results of application of various catalytic systems. (a) yield of products, (b) performance, (c) temperature. The interquartile ranges (25%–75%) are enclosed by rectangles, which are divided by a line corresponding to the median value. The averages over all values and particular values are marked by square and round dots, respectively; the statistical outlier areas are indicated (Tukey's value is 1.5). The Figure was created by the authors using published data presented in Tables 1–6.

2.2. Hydrogenolysis

Unlike pyrolysis, hydrogenolysis of microplastics is more often catalyzed by organic metal complexes structurally similar to the complexes used in the polymerization¹⁵² and by platinum group metals. Zeolites, including those doped with noble metals (Pt, Pd, Ru), can also be successfully used, but at higher temperatures (they demonstrate higher performance than other types of catalysts, see Table 2).

In the case of nano-sized catalysts, the metal nature is of primary importance; most often, the Ru-based catalysts are more active than samples based on Ni, Co, Pt,⁷¹ Cu, Fe, Ni, Pt, Pd, Rh,⁷² Ir, Rh, Pt, Pd, Cu, Co and Ni.⁷⁴ One more important aspect in the hydrogenolysis of microplastics is the type of the support; the lowest activity was observed for Al₂O₃, TiO₂, MgO, ZrO₂ and SiO₂.^{71,74} It is of interest that in the reaction medium without a solvent, a CeO₂-supported catalyst was more active than a carbon-supported one.⁷⁴

In the studies of organic metal complexes as catalysts, Ru complexes were used most often,^{76–78} and the results were comparable with those obtained for Ir and Mn complexes.⁷⁵ However, the use of ruthenium compounds required lower temperatures (140–180 °C) for reactions to proceed. The structure of the organic ligand, the presence of dopants and the solvent are important not only for maximizing the activity, but also for the mere possibility of the catalyzed reaction.⁷⁷

The yield of the target products and the performance of processes substantially depended on the polymer type,^{69,74,76–79} molecular weight (MW),^{70,74} the presence of additional cross-links⁷⁵ and impurities of other polymers.^{73,81} The adverse effect of some factors can be partially counterbalanced by increasing the reaction time and/or

temperature (for example, the effect of polymer impurities have been avoided^{78,80}).

Interestingly, the Cu₄Fe₁Cr₁ catalyst can successfully perform methanolysis when the gas mixture (CO₂–H₂–Ar) is replaced by methanol.⁷⁹ This catalyst can be considered as versatile, although its performance is still lower compared to more specific catalysts.

Wu *et al.*⁸¹ are among the few researchers who developed a catalyst based on the UiO-66 metal-organic framework (MOF) containing zirconium. Currently, these materials attract increasing attention for a number of reasons.¹⁵³ Anticipating a little bit, we would like to note that this catalyst is not the only one MOF used for the degradation of microplastics; some other compounds of this type are considered below. During the microplastic degradation, UiO-66 undergoes an intriguing transformation into MIL-140A, which is also a Zr-containing MOF with a somewhat lower activity compared to that of UiO-66. Furthermore, repeated use of the same catalyst resulted in lower yields of the products. It is noteworthy that Zr or ZrO₂ are not catalytically active, and the reaction in the presence of these compounds does not differ from the reaction in the absence of a catalyst. The catalytic activity is determined particularly by the supramolecular structure of MOF, which facilitates β-scission of the C–C bond in the ethylenediol substituent.⁸¹ The MOF potential for the degradation of microplastics is very high, since MOFs can be designed using computer modelling methods before their actual synthesis.

Unlike thermal conversion catalysts, computer modelling was applied to some catalysts for hydrogenolysis. Most often, quantum chemical calculations of the surface poten-

tials for an infinite plane have been carried out.^{69,70} More rarely, the molecular dynamics was studied, in particular the conformational changes in the C₂₀ polymer chain in various solvents.⁷² Density functional theory (DFT) calculations for the interaction of the catalyst with the low-molecular-weight analogues of substrates⁸⁰ or with solvents⁷⁷ provide much more information, although they are less relevant to degradation of polymer substrates.

2.3. Silylation

Usually silylation of various organic and inorganic compounds is reduced to modification of some chemical groups with silicon-containing substituents. However, appropriate choice of catalysts and reaction conditions may result in the destruction of polymers that form macro- and microplastics (see Table 3). Strong Lewis acids serve as catalysts; as the acidity increases, the reaction temperature decreases (down to room temperature, see Fig. 2). It was shown that the silylating agent affects the nature of the final product: reactions with Et₃SiH, (Me₂SiH)₂NH and PhSiH₃ give silylation adducts,^{82–84} which can be converted to alcohols by alkaline hydrolysis^{82,83} or even to hydrocarbons (by increasing the reaction time and/or temperature).⁸² When (Me₂SiH)₂O is used, such hydrocarbons can be obtained in one step.⁸⁴

It is important to note that neither the catalyst nor the silylating agent alone is able to degrade a polymer under conditions of this type.⁸³ Currently, this accounts for some difficulties in the selection of components for this catalytic system.

Perhaps the only disadvantage of silylation-induced degradation of microplastics is the limited range of polymers that can be successfully degraded in this way; moreover, many of such polymers are polyesters, which are often considered to be biodegradable. Much more common aliphatic polymers such as PE, PP, PVC and, for example, PS cannot be degraded by this method.

2.4. Electro- and photocatalytic decomposition and oxidation

All catalysts of the destruction of microplastics exploit a common mechanism consisting in the artificial ageing of polymers induced by reactive oxygen species. These species can originate either from O₂ or water subjected to electrolysis or photolysis, or from chemically decomposed H₂O₂, or from various combinations of the above sources.

The degradation of microplastics is often impossible without preliminary modification (*e.g.*, by hydrolysis or sulfonation) of the polymer.^{86,92–95} In most of other cases, the yield of products and the process performances are very low, being markedly inferior to analogous parameters of the processes discussed above. The best characteristics, comparable with the average characteristics obtained using thermal conversion, hydrogenolysis and silylation, were attained^{91,97} using strong acid catalysts. In both of these studies, various acids were tested and, along with the reaction conditions, the nature of the acid affected the composition of the reaction products.

Studies of so-called nanoplastics, that is, submicrometre-size microplastics, should also be noted.^{89,90} Despite some drawbacks (in particular, the sorption of nanoplastics on porous photocatalysts was not studied), these works deserve attention because they clearly demonstrate that turbidimetry is inapplicable for determining the catalyst activity, unlike, for example, the reliable method based on determination of the content of elemental carbon. More-

over, chromatography, NMR and other quantitative techniques are even more trustworthy for identification of the products of degradation of microplastics. Therefore, in this review, the priority is given to the studies that use particularly these methods for analysis of the results; otherwise, the method of determination of the products is specially noted. Meanwhile, the frequently used determination of the loss of mass of the initial polymer should be mentioned: according to Ouyang *et al.*⁹⁶ and some other authors, treatment of microplastics may lead to reduction of the particle size without the formation of degradation products. Therefore, the results of determining the process efficiency obtained by this method were not considered in this review.

In some studies dealing with photocatalysts, quantum chemical calculations are performed to examine the interaction of the hypothesized intermediates ([COOH], [CO], [H]) with the catalyst surface during the electroreduction of CO₂.^{87,88} However, the authors did not calculate any physicochemical parameters that could be compared with the characteristics of other catalysts.

Huang *et al.*⁹¹ carried out DFT calculations for 1,3-Ph₂Bu used as a model of PS. The energy barriers for pathways of the reactions of 1,3-Ph₂Bu with various reactive oxygen species were determined, but in the absence of catalysts; therefore, the results obtained in this work are of limited utility for our subject matter.

2.5. Solvolysis

Solvolysis results in decomposition of mainly polyesters and, much more rarely, polycarbonates. However, the number of catalysts developed for this process markedly exceeds the number of thermal conversion catalysts (see Tables 1 and 6). The types of this method can be classified into methanolysis, ethanolysis, glycolysis (*i.e.*, reactions with ethylene glycol and other diols), aminolysis, and hydrolysis.

A comparison of catalysts containing different metals showed the highest efficiency for Zn²⁺-containing catalysts (see^{101,110,113,115,118,122,127}). In rare cases, the activity of Co²⁺ catalysts was comparable with that of Zn²⁺-based samples.¹¹⁷ When Mn²⁺, Cu²⁺, Ni²⁺, Fe³⁺ or Cr³⁺ was used, either the yields of products considerably decreased or no catalytic activity was detected. The anion present in the catalyst also played a role; for example, AcO⁻-containing catalysts were more active than the catalysts containing Cl⁻, Br⁻, CF₃SO₃⁻, CH₂=C(Me)COO⁻ or NO₃⁻ anions.^{99,110,148} Similarly, in the case of ionic liquids, the catalysts containing acetate anions showed the highest activity^{100,121} {in combination with the [1-Bu-3-MeIm]⁺ cation, they provided yields comparable with those obtained with Zn(OAc)₂}.¹⁰⁰ Some authors made attempts to combine different catalysts, *e.g.*, ionic liquids with ZnCl₂. However, it must be admitted that the performance of such processes remained moderate or even decreased.¹²² A better performance can be attained by alternative methods, particularly, by increasing the polymer solubility by adding one more solvent^{103,110} or other additives,¹⁴⁴ by increasing the temperature,^{102,104} by conducting the reaction in a supercritical fluid¹⁴⁷ and using ultrasonic treatment.¹⁴⁴

It is noteworthy that various types of reactions can be carried out with the same catalyst, *e.g.*, methanolysis,¹⁰⁰ glycolysis¹¹⁰ and hydrolysis.¹⁴⁸ Of course, the reaction conditions should be optimized for each particular case to maximize the product yields. However, the reactivity of

glycols significantly decreases with increasing molecular weight,¹¹² while some alcohols, in particular Bu¹OH, cannot react;¹⁰⁴ therefore, the set of solvents that are able to provide satisfactory yields of products upon solvolysis is limited.

Organic zinc complexes can be used to carry out destruction of microplastics at the lowest temperatures (40–50 °C) with retention of high yields and a satisfactory performance of the process;^{102, 103} however, the presence of an additional solvent is necessary.

In the case of nanocatalysts, the highest activity is observed for other metals, for example, Co or Fe.^{105, 129} The catalyst activity increased by a large factor¹⁰⁵ or even appeared particularly owing to the use of nano-sized catalyst forms.¹²⁸ A decrease in the nanoparticle size¹²⁸ or doping with reactive metals^{131, 134} resulted in higher product yields. In view of the above, primary attention should be paid to trace impurities present in the catalyst, *e.g.*, noble metals, the presence of which was neglected in some studies^{131, 132} addressing the degradation of PET.

Combination of various nanocatalysts is a more efficient approach for improving the performance of the overall process than the use of composites with ionic liquids.^{125, 130, 133} Special mention should be made of the composite catalyst containing Zn-based MOF,¹³⁵ which markedly improved the characteristics of catalysis. Among the studied MOFs, the highest surface area was inherent in ZIF-8; the same sample was most efficient in comparison with ZIF-67 and MOF-5.¹³⁶ A similar beneficial effect of increasing surface area was also found for other catalysts.^{125, 126} Yang *et al.*¹³⁷ found a higher activity for MAF-6 over MAF-5 or MAF-32 and also over Zn(OAc)₂ in the glycolysis of PET.

It is of interest that the particle size of microplastic may have some influence on the product yields. According to various studies, as the size increases, the yield increases,^{113, 114, 117, 143} decreases^{111, 137} or remains virtually unchanged.¹⁴⁷ A decrease in the yield with increasing microplastic particle size was also detected in the electrophotocatalytic process.⁹⁰

A combination of solvolysis with photothermolysis¹³⁸ in which CNTs present in the composite catalyst converted the incident light energy into heat is worth noting; hence, no additional heating of the reaction mixture is required. When the reaction was conducted in this regime, the product yield increased 1.5-fold in comparison with the conventional solvolysis.

Density functional theory calculations for the interaction of 3-tropanol (one of the catalyst components) with ethylene glycol were carried out;¹¹³ however, these results do not describe the catalytic glycolysis of PET as a whole. According to DFT calculations for the interactions of the product with various solvents,¹¹⁰ the complex with DMSO had the highest energy, which was partially correlated with experimental data for PET solubility. The DFT calculations for the complex of the ionic liquid cation with the product¹⁰⁰ are also of limited interest.

The energy barrier (the activation energy E_a) for dissociation of the components of the TBD:MSA composite catalyst was calculated by quantum chemistry methods; the result of 156.5 kJ mol⁻¹ served as the basis for theoretical substantiation of the catalyst thermal stability.¹⁰⁶ More recently,⁹⁸ the dissociation energy of this complex in EG was determined in the same way; it was found to be 3.3 times lower than that calculated earlier.¹⁰⁶ The ionization

energy in the gas phase (413 kJ mol⁻¹) was several-fold higher than the initially calculated value. Thus, the original hypothesis about the cause for the catalyst thermal stability was, if not completely rejected, then at least, found to be of low significance for real conditions. Unfortunately, the subsequent calculations of the energy barriers along the reaction pathway were performed for low-molecular-weight models of substrates: BzMe for PET and (PhO)₂CO for PBAC. As applied to microplastics, these results provide only a qualitative estimate (2 and 4 barriers for PET and PBAC, respectively, without considering the initial ionization and the interaction of the anion with EG). A similar situation exists for Me₂TPA¹⁴⁰ and BzMe.¹⁴¹

According to DFT calculations,¹⁰⁸ the formation energy of [Me₃N(CH₂)₂OH]⁺ complexes with two EG–TPA monomer units varied in the 400–450 kJ mol⁻¹ range depending on the used anion. However, the yield of the reaction products did not correlate with the calculated values for various anions. Nevertheless, all of the models were found to have a hydrogen bond between the OH group of the cation and the oxygen atom of the TPA carboxyl group.

Relying on DFT calculations for the complex of a variable phenol-containing moiety of the DBN:[4-MePh] catalyst with EG, Wang *et al.*¹⁰⁷ noted that the calculated energy of the O–H bond within EG was somewhat correlated with the product yield (the lower the energy, the higher the yield). However, these results should be considered to be tentative, since they are clearly incomplete, as there are also other energy barriers along the reaction pathway.

Looking again at the issue of combining different methods for the degradation of microplastics, it should be emphasized that the process can be conducted in two stages, *e.g.*, using solvolysis and the subsequent electrochemical conversion of the obtained products.^{145, 146}

The results of two successful studies,^{148, 149} in which solvolysis (in the first stage) was combined with enzymatic hydrolysis (in the second stage) are also noteworthy. Since the BsEst-N₆CHis₆ enzyme is able to directly hydrolyze PET and HET, the yield of TPA exceeded 100% (based on BHET determined after the first stage) as a result of hydrolysis of the residual amount of the initial polymer, oligomers and HET. In addition, the enzyme was not inhibited by the final product (up to 20 mmol L⁻¹) but was inhibited by intermediates (HET and BHET), especially when the enzymatic reaction was carried out in the TRIS buffer at the same pH.

3. Biocatalytic degradation of microplastics

The possibility of using biocatalysts (Fig. 3) in the biodegradation processes of macro-^{154, 155} and microplastics has long been discussed, and considerable advances have been made in this area. Meanwhile, biocatalysts are still much inferior in the performance to high-temperature chemical catalysts, but they are comparable or even superior to the low-temperature catalysts (Table 7). It is noteworthy that not all polymers that are claimed to be biodegradable are susceptible to microbial degradation under environmental conditions.²⁴¹ This may be caused by a variety of factors starting with the reduced bioavailability of the substrate for degradation and ending with the presence of various chemical agents (modifiers, dyes) that are additionally introduced into the polymer and are toxic particularly to biological objects.²⁴²

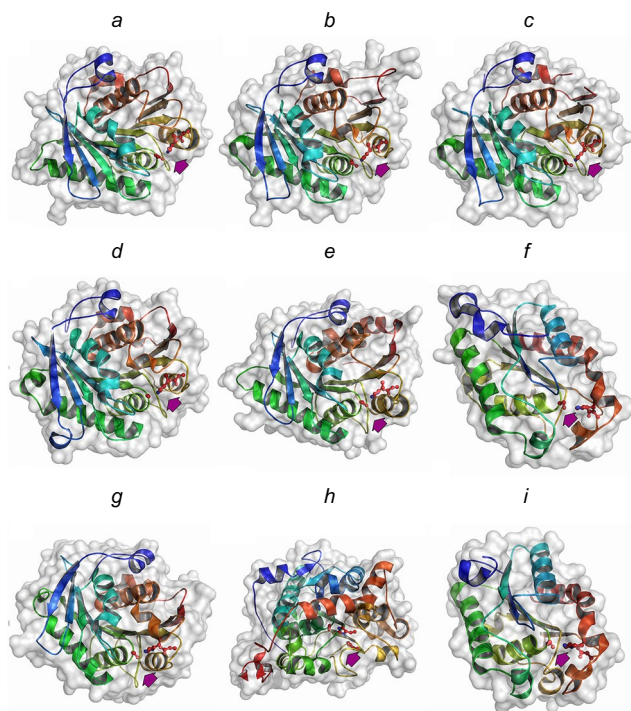


Figure 3. Structures of enzymes: IsPETase (a), TfCut (b), ThcCut2 (c), LCC-ICCG (d), RgPETase (e), HiCut (f), PHL7 (g), CaLipB (h) and AoCut (i); the crystallographic data were taken from the RSCB PDB: 6EQD, 5ZOA, 5LUJ, 6THT, 7DZT, 4OYY, 7NEI, 6TP8 and 3GBS, respectively, and illustrated using PyMOL (version 1.7.6, Schrödinger, LLC). The catalytic triads in the active sites are highlighted with a colour and marked by an arrow.

The same inactivation problems may arise in the enzymatic catalysis; therefore, a number of methodological solutions that can somewhat level off the possible deterioration of the process efficiency have been proposed.

First, the bioavailability of the polymer substrate for the biocatalytic transformation can be improved by adding organic solvents,^{156, 162, 166, 173, 226, 230} detergent emulsifiers^{158, 183, 187, 194, 195, 221, 234, 238} or hydrophobic binding proteins (*i.e.*, proteins that have high affinity to hydrophobic surfaces)^{178–180} into the reaction medium or by incorporating the enzyme into the polymer matrix directly during its formation.²¹⁸ As a result, the reaction rate may increase up to 129-fold¹⁵⁸ (however, in practice, the typical improvement of biocatalysis is much more modest). Also, the additional component introduced into the reaction medium can, in some cases, lead to inactivation of the enzyme;^{83, 187, 234} therefore, a trade-off adjustment of suitable conditions is necessary.

Second, the biocatalytic reaction can be combined, for example, with ultrasonic treatment,²⁰⁴ or the starting polymer substrate can be additionally pretreated before reaction with microwave¹⁶³ or conventional heating.²¹⁵ However, the enzyme efficiency is not always improved upon this type of pretreatment.¹⁷² For example, Kaabel *et al.*²⁰⁸ combined enzymatic hydrolysis with simultaneous mechanochemical treatment of microplastics in a ball mill. However, to attain 49% yield of products, repeated addition of fresh portions of the enzyme was required, since the enzyme was inactivated in the reaction medium.

Third, it is possible to improve binding of the biocatalyst to the polymer substrate by modification of the enzyme itself, *e.g.*, by conjugation¹⁷⁶ or insertion of an additional high-affinity amino acid sequence,^{175, 177, 193, 203} which promotes better enzyme–substrate binding.

Enzyme binding to the substrate requires special attention. Unlike the chemical catalysts considered above, a soluble biocatalyst should first interact with the insoluble substrate for the subsequent efficient biocatalysis. Therefore, it is impossible to transfer the biocatalytic process into a single phase, thus switching to homogeneous catalysis. The adsorption of various enzymes on diverse polymer substrates follows different kinetics; for example, the adsorption of IsPETase enzyme on PET takes 2 h.¹⁵⁸ In some studies, adsorption isotherms for various enzymes on PET were measured: the maximum PET capacity for HiCut enzyme, which has the minimum size (1.5–1.6 times smaller than IsPETase or TfCut), was 1.7 times higher, but the calculated dissociation constant (K_d) was worst (3–5 times higher).¹⁶⁸ The PET binding capacity for TfCut and LCC enzymes with approximately equal weights differed by a factor of two (0.5 and > 1 mg g⁻¹, respectively) at 40 °C, and TfCut was adsorbed on PET faster than LCC.¹⁸⁷ ThcCut1 and ThcCut2 enzymes, which are even more similar in the structure and properties, differed fundamentally in K_d (by a factor of 4 at 60 °C), and differed in the binding capacity to PET (0.25 and 0.28 µg g⁻¹, respectively), but the differences were not statistically significant.²⁰⁰ The increase in both characteristics with decreasing temperature^{193, 200} attests to a complex character of the enzyme interaction with the solid surface of a substrate, comprising contributions of both electrostatic (including hydrogen bonding) and hydrophobic interactions.

Of certain interest are studies of the adsorption of biocatalysts with fluorescence-labelled enzymes on a polymer substrate^{219, 228} and their direct determination using a quartz microbalance.^{202, 203} By introducing point mutations,²¹⁹ it was possible to attain faster binding of lipase to PET surface and slower dissociation of the enzyme–substrate complex. The bimodal dissociation attested to the following processes taking place simultaneously:

- true dissociation followed by the enzyme migration to the bulk of the solvent;
- change in the position and/or conformation of the enzyme on the surface of substrate particles.

From this standpoint, the insertion of a high-affinity sequence into the protein molecule not only accelerates the formation of the enzyme–substrate complex, but also decreases the enzyme desorption from the substrate surface, which was established by studying competitive binding of native and modified cutinase ThcCut1.²⁰³ Upon enzyme modification by adding polyhydroxybutyrate-binding module (PBM) as a fusion partner, the adsorption capacity of the polymer increased by only 15%;²⁰³ however, this value can be increased by changing the high-affinity module, which is genetically introduced into the enzyme molecule; for example, the use of the amino acid sequence of the chitin binding domain (ChBD) led to a threefold increase in the adsorption capacity.¹⁹³ It should be noted that the effect of introducing a particular high-affinity sequence into the molecules of protein catalysts that degrade microplastics is difficult to predict. The introduction of hydrophobin HFB4 or PBM not only did not give useful result, but, conversely, it rather impaired the parameter in question, especially at

Table 7. Enzyme biocatalysts for the degradation of microplastics.

Enzyme designation (MW, kg mol ⁻¹)	source	Optimal reaction conditions					P , mg h ⁻¹ mg ⁻¹	Comments	Ref.
		T , °C	pH	medium		q (mass %)			
				buffer (mmol L ⁻¹)	other components				
<i>Microplastic: PET, PBT, PHT; products: HET: BHET: TPA = 2.4 : 0.06 : 1 (for PET)</i>									
IsPETase- ^{N,C} His ₆ (30.5)	<i>Ideonella sakaiensis</i>	37	7.2	Phosphate (50)	DMSO (10 vol.%)	0.4	0.8	For PBT and PHT, the activity was 160 (or more) times lower	156
<i>Microplastic: PET (d = 6 mm); products: HET: TPA = 2.1</i>									
IsPETase- ^C His ₆ (28.8)	<i>I. sakaiensis</i>	30	7	Phosphate (50)	—	0.01	0.35		157
<i>Microplastic: PET (d = 6 mm); products: HET: TPA ≈ 6</i>									
IsPETase- ^N His ₆ (31.5)	<i>I. sakaiensis</i>	30	7	Bicine (50)	Me(CH ₂) ₁₃ OSO ₃ (50 mg L ⁻¹)	0.2	7.4	Other detergents had a lower stimulating effect or were to be used in higher amounts	158
<i>Microplastic: PET (d = 6 mm); products: HET: TPA = 3.3</i>									
IsPETase- ^C His ₆ (28.8)	<i>I. sakaiensis</i>	30	7	Phosphate (50)	—	0.004	2.1		159
<i>Microplastic: PET; products: HET: TPA = 0.37 (after 48 h)</i>									
IsPETase- ^C His ₆ with pelB_A20T signal peptide at the N-terminus (31)	<i>I. sakaiensis</i>	30	9	Carbonate (50)	—	1960 vol.%	0.06 mg h ⁻¹ mL ⁻¹	Crude enzyme	160
<i>Microplastic: PET (d = 6 mm); products: HET: BHET: TPA (the ratio was not indicated)</i>									
IsPETase- ^C His ₆ with LamB signal peptide (31.2)	<i>I. sakaiensis</i>	30	9	Glycine (50)	—	0.02	0.008		161
<i>Microplastic: PET; products: HET: TPA = 0.5</i>									
IsPETase- ^C His ₆ (31.3)	<i>I. sakaiensis</i>	30	7.5	Phosphate (45)	NaCl (90 mmol L ⁻¹), DMSO (10 vol.%)	0.2	2.5 mg h ⁻¹ L ⁻¹		162
<i>Microplastic: PET; product: TPA</i>									
IsPETase- ^C His ₆ (31.3) together with IsMHETase- ^C His ₆ (64.2)	<i>I. sakaiensis</i>	30	7.5	Phosphate (45)	NaCl (90 mmol L ⁻¹), DMSO (10 vol.%), IsPETase (0.2 mass %)	0.1	5 mg h ⁻¹ L ⁻¹		162
IsMHETase-IsPETase- ^C His ₆ (96.1)	<i>I. sakaiensis</i>	30	7.5	Phosphate (45)	NaCl (90 mmol L ⁻¹), DMSO (10 vol.%)	0.1	2.6 mg h ⁻¹ L ⁻¹		162

Table 7 (continued).

Enzyme designation (MW, kg mol ⁻¹)	source	Optimal reaction conditions				<i>P</i> , mg h ⁻¹ mg ⁻¹	Comments	Ref.	
		<i>T</i> , °C	pH	medium					<i>q</i> (mass %)
				buffer (mmol L ⁻¹)	other components				
<i>Microplastic: PET (d = 0.45 mm), microwave-pretreated PET (d = 0.2 mm); product: HET</i>									
IsPETase- ^C His ₆ with S238A mutation (31.8)	<i>I. sakaiensis</i>	30	7.2	Phosphate (50)	–	0.02	See ^a	After 2-hour pretreatment, conversion to TPA	163
<i>Microplastic: PET (d = 6 mm); products: HET : TPA = 2.6 (wt), 1.62 (Y58A)</i>									
IsPETase- ^C His ₆ with Y58A mutation (29.1 kg mol ⁻¹)	<i>I. sakaiensis</i>	30	9	Glycine (50)	NaCl (50 mmol L ⁻¹)	0.01	2.4 × 10 ⁻³ (wt) 7.3 × 10 ⁻³		164
<i>Microplastic: PET (d = 6 mm); products: HET : BHET : TPA (the ratio was not indicated)</i>									
IsPETase- ^N His ₆ with R280A mutation (31.5)	<i>I. sakaiensis</i>	30	9	Glycine	–	0.02	2.6 × 10 ⁻² (wt) 3.2 × 10 ⁻²		165
<i>Microplastic: PET; products: HET : BHET : TPA (the ratio was not indicated)</i>									
IsPETase- ^C His ₆ with W159H/S238F mutations (31.3)	<i>I. sakaiensis</i>	40	7.5	Phosphate (50)	NaCl (0.1 mol L ⁻¹), DMSO (10 vol.%)	0.3	0.5 (wt) 0.7	wt: <i>K</i> _M = 26 g L ⁻¹ , <i>k</i> _{cat} = 102 min ⁻¹ , W159H/S238F: <i>K</i> _M = 95 g L ⁻¹ , <i>k</i> _{cat} = 72 min ⁻¹	166
<i>Microplastic: PET (d = 6 mm); products: HET : BHET : TPA (the ratio was not indicated)</i>									
IsPETase- ^N His ₆ with S121E/D168H/N246D mutations (31.5)	<i>I. sakaiensis</i>	37	9	Glycine	–	0.05	4.5 × 10 ⁻³ (wt) 2.2 × 10 ⁻²		167
<i>Microplastic: PET (d = 0.1 or 0.2 mm); products: HET : BHET : TPA (the ratio was not indicated)</i>									
IsPETase- ^C His ₆ with S238F/W159H mutations (31.3)	<i>I. sakaiensis</i>	40	8	Phosphate (50)	–	0.1	2.4	The smaller the particle size, the higher their enzyme binding capacity	168
<i>Microplastic: PET (d = 6 mm); products: HET : TPA = 2.2</i>									
IsPETase- ^N His ₆ with S121E/D186H/R280A mutations (29.1)	<i>I. sakaiensis</i>	40	9	Glycine (50)	–	0.04	0.02		169
<i>Microplastic: PET (d = 6 mm); product: TPA</i>									
IsPETase- ^C His ₆ with S121E/D186H/R280A mutations (30.6) follow by IsMHETase- ^C His ₆ (62.7)	<i>I. sakaiensis</i>	37	9	Glycine (50)	–	0.07	–	Successive treatment with IsPETase- ^C His ₆ and then with IsMHETase- ^C His ₆	170
		30	8	Phosphate (50)	–	0.6			

Table 7 (continued).

Enzyme designation (MW, kg mol ⁻¹)	source	Optimal reaction conditions				<i>P</i> , mg h ⁻¹ mg ⁻¹	Comments	Ref.	
		<i>T</i> , °C	pH	medium					<i>q</i> (mass %)
				buffer (mmol L ⁻¹)	other components				
<i>Microplastic: PET; products: HET : BHET : TPA (the ratio was not indicated)</i>									
Dura-PETase (31.8)	<i>I. sakaiensis</i>	60	9	Glycine (50)	—	0.3	1.2 (wt) 3.5 ^b	171	
<i>Microplastic: PET (d = 6 mm); product: TPA</i>									
FAST-PETase (30.8)	<i>I. sakaiensis</i>	50	8	Phosphate (100)	—	0.01	2.7	172	
<i>Microplastic: PET (d = 6 mm); products: HET : TPA = 3 (wt) and 4 (mutant)</i>									
TS-PETase (28.7)	<i>I. sakaiensis</i>	30	9	Glycine (50)	NaCl (50 mmol L ⁻¹), DMSO (10 vol.%)	0.01	1.7 (wt) 2.2 (mutant)	173	
<i>Microplastic: PET (d = 85 nm); products: HET : BHET : TPA = 5.3 : 0.6 : 1 (after 24 h)</i>									
TS-PETase (28.7)	<i>I. sakaiensis</i>	50	7.5	Phosphate (50)	—	0.4	28	174	
<i>Microplastics: PET, PBT, PHT; products: HET : BHET : TPA = 1.7 : 0.04 : 1 (in the case of PET)</i>									
IsPETase-Trx-N ^C His ₆ (42.9)	<i>I. sakaiensis</i>	37	7.2	Phosphate (50)	DMSO (10 vol.%)	0.5	0.9 (PET)	156	
<i>Microplastic: PET; product: HET : TPA = 1.9</i>									
IsPETase-CBM-C ^C His ₆ (37.8)	<i>I. sakaiensis</i> and <i>Trichoderma reesei</i> (CBM)	40	9	Glycine (50)	—	0.3	0.27	The activity increased compared to wt by 71.5 and 41.5% at 30 and 40 °C, respectively	175
<i>Microplastic: PET (d = 6 mm); products: HET : BHET : TPA (the ratio was not indicated)</i>									
IsPETase-C ^C His ₆ conjugate (29) with MAA, MAA-Bu ^t , MAA-(CH ₂) ₂ OH or MAA-(CH ₂) ₂ NMe ₂ (3–6 mol per mol of the enzyme)	<i>I. sakaiensis</i>	40	9	Glycine (50)	—	0.004	0.46	The activity varied in the series Bu ^t > (CH ₂) ₂ NMe ₂ > (CH ₂) ₂ OH ≈ MAA > wt	176
IsPETase-C ^C (Glu-Lys) ₃₀ His ₆ (59)	<i>I. sakaiensis</i>	40	9	Glycine (50)	—	0.04	0.05		177
<i>Microplastic: PET; products: HET : TPA = 1.76 and 1.93 (in the presence of hydrophobins)</i>									
IsPETase-C ^C His ₆ (31.1) together with hydrophobin RolA (16.1) or HGFI (11.4)	<i>I. sakaiensis</i> and <i>Aspergillus oryzae</i> (RolA) or <i>Grifola frondosa</i> (HGFI)	30	8	Phosphate (50)	RolA (2.1 mass %) or HGFI (1.5 mass %)	0.13	1.2 1.7–1.8 (with hydrophobin)	178	

Table 7 (continued).

Enzyme designation (MW, kg mol ⁻¹)	source	Optimal reaction conditions					<i>P</i> , mg h ⁻¹ mg ⁻¹	Comments	Ref.
		<i>T</i> , °C	pH	medium		<i>q</i> (mass %)			
				buffer (mmol L ⁻¹)	other components				
<i>Microplastic: PET (d = 6 mm); products: HET: TPA = 1.9 (EAS) and 2.3 (HFBII)</i>									
IsPETase- ^C His ₆ with MERACVAV-pelB signal peptide at the N-terminus (31.9), together with hydrophobin EAS (10.9) or HFBII (8.8)	<i>I. sakaiensis</i> and <i>Neurospora crassa</i> (EAS) or <i>T. reesei</i> (HFBII)	30	9	Glycine (50)	EAS (0.16 mass %) or HFBII (0.07 mass %)	0.02	0.31 (EAS) 0.35 (HFBII)		179
<i>Microplastic: PET; products: HET: TPA = 1.4</i>									
IsPETase- ^C His ₆ with S121E/D186H/R280A mutations (30.6) together with PcAA14A- ^C His ₆ (32.8)	<i>I. sakaiensis</i> and <i>Pycnoporus</i> <i>coccineus</i> (PcAA14A)	40	9	Glycine (50)	PcAA14A- ^C His ₆ (0.07 mass %)	0.17	0.15 (without PcAA14A- ^C His ₆) 0.25		180
<i>Microplastic: PET (d = 0.1–0.16 μm); products: HET: TPA = 0.3 (after 1 h, HET peak); almost complete conversion to TPA after 24 h</i>									
TfCut2- ^C His ₆ (31.2)	<i>Thermobifida</i> <i>fusca</i>	60	8.5	TRIS (500)	—	4	1.7	Competitive inhibition of the enzyme by HET and BHET products (<i>K_i</i> ≈ 1.8 mmol L ⁻¹)	181
<i>Microplastic: PET (fibres); products: complete conversion to TPA (wt), HET: TPA = 0.1 (G62A)</i>									
TfCut2- ^C His ₆ with G62A mutation (31.5)	<i>T. fusca</i>	65	8	TRIS (1000)	CaCl ₂ (10 mmol L ⁻¹)	0.25	0.004 (wt) 0.011	The enzyme was inhibited by a product (HET)	182
<i>Microplastic: PET (d = 6 mm); products: HET: TPA = 0.6 (after 24 h, without DTMAC)</i>									
TfCut2- ^C His ₆ with G62A/F209A mutations (30.7)	<i>T. fusca</i>	65	9	Bicine (50)	CaCl ₂ (10 mmol L ⁻¹), DTMAC (30 mg L ⁻¹)	0.2	6.4 13.3 (with DTMAC)		183
<i>Microplastic: PET (d = 0.25–0.5 mm); products: HET: BHET: TPA (the ratio was not indicated)</i>									
TfCut2- ^C His ₆ with D204C/E253C mutations (31.5)	<i>T. fusca</i>	60	8	Phosphate (100)	—	5	0.006 0.19 ^c		184
<i>Microplastic: PET (d = 0.5 mm); products: complete conversion to TPA (wt), HET: TPA = 0.5 (S121P/D174S/D204P)</i>									
TfCut2- ^N His ₆ with S121P/ D174S/D204P mutations (31.5)	<i>T. fusca</i>	70	8	Phosphate (100)	NaCl (0.1 mol L ⁻¹)	0.5 0.87	0.02 (wt)		185
<i>Microplastic: PET; products: HET: BHET: TPA (the ratio was not indicated)</i>									
DS-TfCut2 (31.9)	<i>T. fusca</i> and <i>Pithecopus oreades</i> (DS)	70	8	Phosphate (100)	—	2.2	0.27		186

Table 7 (continued).

Enzyme		Optimal reaction conditions				P , mg h ⁻¹ mg ⁻¹	Comments	Ref.	
designation (MW, kg mol ⁻¹)	source	T , °C	pH	medium					q (mass %)
				buffer (mmol L ⁻¹)	other components				
<i>Microplastic: PET (d = 0.1 mm); products: HET : BHET : TPA (the ratio was not indicated)</i>									
TfCut-C ₆ His ₆ with AmyL signal peptide (32.5)	<i>T. fusca</i>	50	8	Phosphate (50)	n-C ₁₆ H ₃₃ -N(Me) ₃ Br (20 μmol L ⁻¹)	0.02	5.3	Determined from the absorbance	187
LCC-C ₆ His ₆ with AmyL signal peptide (32.1)	Non-culturable bacterium from leaf compost	50	8	Phosphate (50)	n-C ₁₆ H ₃₃ -N(Me) ₃ Br (6 μmol L ⁻¹)	0.02	10.4	Determined from the absorbance	187
<i>Microplastic: PET (d = 5 mm); products: HET : BHET : TPA (the ratio was not indicated)</i>									
Glycosylated LCC-N ₆ C ₆ His ₆ (~35)	Non-culturable bacterium from leaf compost	70	8	TRIS (500)	—	0.05	9.3	Determined by titration	188
<i>Microplastic: PET (d = 10–150, 100–400, 200–500 μm); products: HET : TPA = 0.04 (after 72 h) up to 0.3 (after 24 h, for d = 10–150 μm)</i>									
LCC-ICCG (28.3)	Non-culturable bacterium from leaf compost	65	8	Phosphate (100)	—	0.3	18.5 (d = 100–400 μm)		189
<i>Microplastic: PET (d = 0.6 and 3 mm); product: TPA</i>									
LCC-ICCG (28.3)	Non-culturable bacterium from leaf compost	65	8	Phosphate (100)	—	0.4	See ^d		190
<i>Microplastic: PET (d < 0.5 mm); products: HET : BHET : TPA (the ratio was not indicated)</i>									
LCC-ICCG (28.3)	Non-culturable bacterium from leaf compost	72	8	Phosphate (100)	—	0.1	2.8 (wt) 4.3 (ICCG)	The yield of the products was 55% (wt) and 86% (ICCG)	191
<i>Microplastic: PET (d = 1–2 mm); products: HET : BHET : TPA (the ratio was not indicated)</i>									
LCC-WCCG (28.3)	Non-culturable bacterium from leaf compost	72	10	Phosphate (100)	—	0.8	9	Crude enzyme. The products were transformed to vanillin by engineered bacterium	192
<i>Microplastic: PET; products: HET : BHET : TPA = 1.63 : 0.35 : 1</i>									
LCC-ICCG-ChBD (51.3)	Non-culturable bacterium from leaf compost and <i>Chitinolyticbacter meiyuanensis</i> (ChBD)	65	8	Phosphate (100)	—	21	0.36	The activity was 27% higher than that of LCC-ICCG	193

Table 7 (continued).

Enzyme		Optimal reaction conditions					P , $\text{mg h}^{-1} \text{mg}^{-1}$	Comments	Ref.
designation (MW, kg mol^{-1})	source	T , °C	pH	medium		q (mass %)			
				buffer (mmol L^{-1})	other components				
<i>Microplastic: PET; products: HET : BHET : TPA (the ratio was not indicated)</i>									
SvCut190- ^N His ₆ with S226P/R228S mutations (30.3)	<i>Saccharomonospora viridis</i>	63	8.2	TRIS (100)	CaCl ₂ (50 mmol L^{-1}), glycerol (24 vol.%)	0.3	0.4–1	No enzyme inhibition by EDTA (10 mmol L^{-1}) and by the products of hydrolysis (up to 6 mmol L^{-1}) was observed	194
<i>Microplastic: PET (d = 6 mm); products: HET : BHET : TPA (the ratio was not indicated)</i>									
SvCut190- ^N His ₆ with Q138A/Q123H/N202H/D250C/E296C mutations (30.2)	<i>S. viridis</i>	70	8.5	TRIS (100)	CaCl ₂ (2.5 mmol L^{-1}), glycerol (24 vol.%)	0.6	1.5×10^{-4}	Determined from the absorbance	195
<i>Microplastic: PEF (d < 0.18 and 0.18–0.43 mm); products: HEF : BHEF : FDA (the ratio was not indicated)</i>									
TheCut1- ^C His ₆ (29.1)	<i>T. cellulositytica</i>	65	8	Phosphate (1000)	—	3	0.04 (d = 0.18–0.43 mm)	The activity was reduced in the TRIS buffer	196
<i>Microplastic: PEF; products: HEF : BHEF : FDA (the ratio was not indicated)</i>									
TheCut1- ^C His ₆ (29.1)	<i>T. cellulositytica</i>	50	7	Phosphate (100)	—	1.5	0.2		197
<i>Microplastic: PEF analogues with various diols; products: HEF : BHEF : FDA (the ratio was not indicated)</i>									
TheCut1- ^C His ₆ (29.1)	<i>T. cellulositytica</i>	50	7	Phosphate (100)	—	2	See ^e		198
<i>Microplastic: PBHT (d = 0.1–0.3 mm) with different AA : TPA ratios; products: HBT : BHBT : TPA and AA (the ratio was not indicated)</i>									
TheCut1- ^C His ₆ (29.4)	<i>T. cellulositytica</i>	50	7	Phosphate (100)	—	0.4	1.6 (AA : TPA = 70 : 30)	TPA in trace amounts	199
<i>Microplastic: PET (d = 0.01–0.3 mm); products: HET : BHET : TPA = 6.4 : 1 : 1</i>									
TheCut1- ^C His ₆ (29.4)	<i>T. cellulositytica</i>	60	7	Phosphate (50)	—	0.015	3.6		200
<i>Microplastic: PET (d = 0.05–0.1, 0.1–0.25 or 0.25–0.5 mm) and its mixtures* with 8% PA or PE (d = 0.25–0.5 mm), PTMT (d = 0.25–0.5 mm); products: HET : TPA = 0.07</i>									
TheCut1- ^C His ₆ with S31A/T51A/S163A mutations (29.1)	<i>T. cellulositytica</i>	50	7	Phosphate (100)	—	0.3	See ^f		201
<i>Microplastics: PET, PBB, PHBHP; products: HET : TPA = 0.04 (in the case of PET)</i>									
TheCut1- ^C His ₆ with S31A/T51A/S163A mutations (29.1)	<i>T. cellulositytica</i>	65	8	Phosphate (1000)	—	0.3 (PET) or 2.9 (PBB, PHBHP)	See ^g		202

Table 7 (continued).

Enzyme		Optimal reaction conditions					P , $\text{mg h}^{-1} \text{mg}^{-1}$	Comments	Ref.
designation (MW, kg mol^{-1})	source	T , °C	pH	medium		q (mass %)			
				buffer (mmol L^{-1})	other components				
<i>Microplastic: PBH ($d = 0.1-0.3$ mm); products: HBA: BHBA : AA (the ratio was not indicated)</i>									
ThcCut1-PBM- ^C His ₆ (38.3)	<i>T. cellulosilytica</i> and <i>Alcaligenes faecalis</i> (PBM)	20	7	Phosphate (100)	—	0.05	32 25 (without PBM)		203
<i>Microplastic: PET; products: HET: TPA = 0.38 and 0.57 (ultrasonic treatment)</i>									
ThcCut1- ^C His ₆ (29.4), together with ultrasonic treatment	<i>T. cellulosilytica</i>	60	7	Phosphate (100)	—	0.3	0.06 0.18 (ultrasonic treatment)	Ultrasonic treatment (42 kHz, 150 W)	204
<i>Microplastic: PET ($d = 0.1-0.3$ mm); products: HET: BHET: TPA = 5.1 : 1.3 : 1</i>									
ThcCut2- ^C His ₆ (29.7)	<i>T. cellulosilytica</i>	60	7	Phosphate (50)	—	0.015	3.5		200
<i>Microplastic: PLA ($d = 1$ mm); product: MeCH(OH)COOH</i>									
ThcCut2- ^C His ₆ with R29N/A30V mutations (29.7)	<i>T. cellulosilytica</i>	60	7	Phosphate (100)	—	—	0.008		205
<i>Microplastic: PBHT ($d = 0.1-0.3$ mm) with different AA : TPA ratios; products: HBT: TPA \approx 0.6</i>									
Novozym® 51032 (24)	<i>Humicola insolens</i>	50	7	Phosphate (100)	—	0.3	3.7 (AA : TPA = 70 : 30)		199
<i>Microplastic: PET; products: HET: BHET: TPA = 0.005 : 0.001 : 1</i>									
Novozym® 51032 (24)	<i>H. insolens</i>	63	9	TRIS (400)	—	3.3	0.02	The activity was reduced in the TRIS buffer. The product yield was 23%	206
<i>Microplastic: PET (fibres $d = 3$ or 10 mm); products: HET: TPA = 0.03 (after 14 days)</i>									
Novozym® 51032 (24)	<i>H. insolens</i>	70	8	Phosphate (500)	—	11	1.1×10^{-4} ($d = 3$ mm) 2.8×10^{-4} ($d = 10$ mm)		207
<i>Microplastics: PET ($d = 3$ mm), PBT, PBAC; products: TPA (in the case of PET), bisphenol A (in the case of PBAC)</i>									
Novozym® 51032 (24)	<i>H. insolens</i>	55	7.3	Phosphate (100)	—	0.6	See ^h	Mechanocatalytic hydrolysis; PBT was not hydrolyzed; 200 mass % PS or MCC decreased the yield of products from PET by 3–6%	208

Table 7 (continued).

Enzyme		Optimal reaction conditions					P , $\text{mg h}^{-1} \text{mg}^{-1}$	Comments	Ref.
designation (MW, kg mol^{-1})	source	T , °C	pH	medium		q (mass %)			
				buffer (mmol L^{-1})	other components				
<i>Microplastic: PET ($d = 0.075-0.25, 0.25-0.6, 0.6-0.85 \text{ mm}$); products: HET: BHET: TPA = 0.24 : 0.01 : 1</i>									
Novozym® 51032 (24)	<i>H. insolens</i>	70	7	Phosphate (200)	—	2	0.07 ($d = 0.075-0.25 \text{ mm}$)		209
<i>Microplastic: PET ($d < 0.21, 0.21-0.42, 0.42-0.85, 0.85-1, 1-1.18$ or $> 1.4 \text{ mm}$); products: HET: TPA = 0.02 (0.07 for $d = 0.85-1 \text{ mm}$)</i>									
Novozym® 51032 (24)	<i>H. insolens</i>	62.6	8.95	TRIS (400)	—	0.65	See ⁱ		210
<i>Microplastic: PET ($d = 0.075-0.25$ or $0.25-0.6 \text{ mm}$); products: HET: BHET: TPA (the ratio was not indicated)</i>									
Novozym® 51032 (24)	<i>H. insolens</i>	70	7	Phosphate (200)	—	0.4–10	See ^j	No enzyme inhibition by the products TPA and HET (up to 20 mmol L^{-1}) or BHET (up to 40 mmol L^{-1}) was observed	211
<i>Microplastic: PBB ($d = 0.4$ or 0.9 mm); products: HBS: BHBS: SA (the ratio was not indicated)</i>									
Novozym® 51032 (24)	<i>H. insolens</i>	40	7	Phosphate (100)	—	40 vol. %	See ^k	No activity was present in amylase, cellulase or protease	212
<i>Microplastic: PET ($d = 5 \text{ mm}$); products: HET: BHET: TPA = 0.24 : 0.007 : 1</i>									
Novozym® 51032 (24) together with CaLipB (39)	<i>H. insolens</i> and <i>M. antarcticus</i> (CaLipB)	50	7	Phosphate (200)	CaLipB (0.4 mass %)	3.6	0.001		213
<i>Microplastic: PET ($d < 1 \text{ mm}$); products: HET: TPA = 0.27 and 1 (without CaLipB)</i>									
Novozym® 51032 (24) together with CaLipB (39)	<i>H. insolens</i> and <i>M. antarcticus</i> (CaLipB)	60	7	Phosphate (200)	CaLipB (1 mass %)	1	0.15	Out of 16 lipases, the most active one was selected (CaLipB)	214
<i>Microplastic: PET (fibre); product: TPA</i>									
Novozym® 51032 (24)	<i>H. insolens</i>	<i>First stage</i>							
		250 (4 MPa)	—	—	H ₂ O (1000 mass %)				Successive two-stage treatment
<i>Second stage</i>									
		50	7	TRIS (100)	—	20	0.36		

Table 7 (continued).

Enzyme designation (MW, kg mol ⁻¹)	source	Optimal reaction conditions					P , mg h ⁻¹ mg ⁻¹	Comments	Ref.
		T , °C	pH	medium		q (mass %)			
				buffer (mmol L ⁻¹)	other components				
		<i>Microplastic: PET (d = 0.1 mm); products: HET : BHET : TPA (the ratio was not indicated)</i>							
HiCut (20.2)	<i>H. insolens</i>	40	8	Phosphate (50)	–	0.1	0.23	168	
		<i>Microplastic: PET (d < 0.3 mm); products: HET : BHET : TPA = 5.5 : 2.5 : 1</i>							
HiCut (20.2)	<i>H. insolens</i>	50	8	Phosphate (50)	–	0.02	0.3	216	
		<i>Microplastic: PET (d = 0.05–0.5 mm); products: HET : BHET : TPA (the ratio was not indicated)</i>							
HiCut (20.2)	<i>H. insolens</i>	50	8	Phosphate (50)	–	0.01	3	Determined from the absorbance	217
		<i>Microplastic: PET (d = 0.1 mm); products: HET : BHET : TPA (the ratio was not indicated)</i>							
TfCut (32.2)	<i>T. fusca</i>	40	8	Phosphate (50)	–	0.1	0.07	168	
		<i>Microplastic: PET (d < 0.3 mm); products: HET : BHET : TPA = 11.5 : 1 : 1</i>							
TfCut (32.2)	<i>T. fusca</i>	50	8	Phosphate (50)	–	0.03	1.3	216	
		<i>Microplastic: PET (d = 0.005–0.5 mm); products: HET : BHET : TPA (the ratio was not indicated)</i>							
TfCut (32.2)	<i>T. fusca</i>	50	8	Phosphate (50)	–	0.02	2	Determined from the absorbance	217
		<i>Microplastic: PCL (d = 0.3 mm); products: HO(CH₂)₅COOH</i>							
Amano lipase PS (37.6)	<i>Burkholderia cepacia</i>	37	7.5	Phosphate (100)	–	1	–	Determined by titration. Dry lipase was mixed with PCL and then 3D printing was carried out	218
		<i>Microplastic: PET (d = 3 mm); products: HET : TPA = 0.65 (wt) and 0.24 (mutant)</i>							
lipIAF5-2 lipase with R47C/G89C/F105R/E110K/ S156P/G180A/T297P mutations (32.6)	Non-culturable bacterium	60 68 (mutant)	7	Phosphate (50)	–	0.02	0.09 (wt) 0.29 (mutant)	219	
		<i>Microplastic: PCL (d = 5 mm); product: HO(CH₂)₅COOH</i>							
AoCut- ^C His ₆ (23.1)	<i>Aspergillus oryzae</i>	40	9	Borate (20)	–	0.01	537	Determined by titration	220
		<i>Microplastic: PBBH (d = 5 mm); products: HBS : BHBS : SA and HBA : BHBA : AA (the ratio was not indicated)</i>							
AoCut- ^C His ₆ with A102D/Q105R/G106E mutations (21.7)	<i>A. oryzae</i>	50	8	TRIS (500)	Glycerol (10 mass %)	0.01	1.9 (wt) 1.5 (mutant)	Determined by titration	221

Table 7 (continued).

Enzyme		Optimal reaction conditions					P , $\text{mg h}^{-1} \text{mg}^{-1}$	Comments	Ref.
designation (MW, kg mol^{-1})	source	T , °C	pH	medium		q (mass %)			
				buffer (mmol L^{-1})	other components				
<i>Microplastic: PET (d = 5 mm); products: HET : BHET : TPA (the ratio was not indicated)</i>									
AspPETase27- ^C His ₆ (37.8)	<i>Aequorivita</i> sp.	30	8	Phosphate (100)	—	3	0.001	Triton X-100, Tween 80, SDS, PMSF and DTT inhibited, while EDTA did not inhibit the enzyme	222
<i>Microplastic: PET (d = 0.4 mm); products: HET : BHET : TPA = 1.5 : 0.07 : 1</i>									
BhrPETase (28.1)	Unidentified HR29 bacterium	70	8	HEPES (100)	CaCl ₂ (2 mmol L^{-1})	0.05	12.2		223
<i>Microplastic: PET (d = 6 mm); products: HET : TPA = 6.8 (for d = 6 mm), 4.3 (for d = 6 mm, mutant), 2.8 (micr.) and 3.6</i>									
BbPETase- ^C His ₆ (45.7)	Unidentified <i>Burkholderiales</i> bacterium	30	9	Glycine (50)	—	0.07	0.1 0.17 ¹		224
<i>Microplastic: PET (d = 6 mm); products: HET : TPA = 5</i>									
BbPETase- ^C His ₆ with H344S/F348I mutations (37.9)	Unidentified <i>Burkholderiales</i> bacterium	35	9	Glycine (50)	—	0.1	0.2		225
<i>Microplastic: PBB (d = 0.4 or 0.9 mm); products: HBS : BHBS : SA (the ratio was not indicated)</i>									
CaLipB (39)	<i>M. antarcticus</i>	40	7	Phosphate (100)	—	40 vol. %	See ^m		212
<i>Microplastic: PET (d = 6 mm); product: HET</i>									
HaEst- ^C His ₆ (33.4)	<i>Halopseudomonas aestusnigri</i>	30	7.4	Phosphate (20)	DMSO (20 vol. %)	0.05	5.2×10^{-3}		226
<i>Microplastics: PBHT, PBDT and their mixture * ecovio[®] FT, PET (d = 85 nm); products: HBT : TPA = 31 (in the case of ecovio[®] FT), 29 (in the case of PBHT), 14 (in the case of PBDT); HET : TPA = 1.1 (in the case of PET)</i>									
MbPles629- ^N His ₆ with TEE enhancer (31.3)	<i>Marinobacter</i> sp.	30	7	Phosphate (12)	NaCl (0.14 mol L^{-1})	0.05	See ⁿ	The enzyme was inhibited by the product (HBT)	227
<i>Microplastic: PET (d = 0.3 mm); products: HET : TPA = 0.07</i>									
MG8- ^C His ₆ (34.3)	Human saliva metagenome	55	9	Glycine (50)	NaCl (1–4 mol L^{-1})	0.09	0.09		228

Table 7 (continued).

Enzyme		Optimal reaction conditions				P , $\text{mg h}^{-1} \text{mg}^{-1}$	Comments	Ref.	
designation (MW, kg mol^{-1})	source	T , °C	pH	medium					q (mass %)
				buffer (mmol L^{-1})	other components				
<i>Microplastics: PET, PCL, PEB (d = 3 mm); products: the composition was not indicated</i>									
MrCut1- ^C His ₆ (24.2)	<i>Moniliophthora roreri</i>	37	7.5	Phosphate (50)	–	0.01	See ^o	Determined by titration	229
<i>Microplastic: PET; products: HET: TPA = 1.2</i>									
MtCut- ^C His ₆ (29.5)	<i>Marinactinospora thermotolerans</i>	40	8.5	TRIS (20)	NaCl (0.5 mol L ⁻¹), CaCl ₂ (10 mmol L ⁻¹), DMSO (10 vol.%)	0.5	5.7×10^{-2}	EDTA decreased the enzyme activity	230
<i>Microplastic: PET (d = 6 mm); products: HET: TPA = 2.8</i>									
PbPLip- ^C His ₆ with H216S/F220I mutations (38.2)	<i>Polyangium brachysporum</i>	40	9	Glycine (50)	–	0.1	0.19		225
<i>Microplastic: PET (d = 6 mm); products: HET: TPA = 1.46</i>									
PHL7- ^C His ₆ (29)	Compost metagenome	70	8	Phosphate (1000)	–	0.06	85		231
<i>Microplastic: PBHT (d = 0.1–0.3 mm); products: HBT: TPA = 2</i>									
PpEst- ^C His ₆ (20)	<i>Pseudomonas oleovorans</i> (former <i>Pseudomonas pseudoalcaligenes</i>)	65	7	Phosphate (100)	–	1	0.011	The enzyme is inhibited by the product (HBT)	232
<i>Microplastic: PET (d = 4 mm); products: HET: HBET: TPA = 0.34 : 0.05 : 1</i>									
PsLip or PrLip	<i>Penicillium simplicissimum</i> (PsLip); <i>Penicillium restrictum</i> (PrLip)	37	7	Phosphate (200)	–	1	1.2×10^{-5} (PsLip)	Crude enzyme	233
<i>Microplastic: PLA (d = 0.2–0.3 mm); product: MeCH(OH)COOH</i>									
PtPLA-hydrolase (58)	<i>Pseudomonas tamsuii</i>	50	10	Carbonate (50)	Plysurf A210G (0.1 g L ⁻¹)	143	5×10^{-3}	Side activity of the enzyme to fibrinogen and, to a lower extent, to casein	234
<i>Microplastic: PBHT; products: HBT: BHBT: TPA = 8.5 : 2.5 : 1 (after 72 h)</i>									
PfLip1- ^C His ₆ (44)	<i>Pelosinus fermentans</i>	50	7.5	Phosphate (100)	–	5	9.4×10^{-3}	The enzyme was inhibited by the K ⁺ , Co ²⁺ , Zn ²⁺ , Fe ³⁺ and Ni ²⁺ ions and by PMSF and EDTA. PET, PLA and PHB-co-valerate were not hydrolyzed	235

Table 7 (continued).

Enzyme		Optimal reaction conditions				P , $\text{mg h}^{-1} \text{mg}^{-1}$	Remarks	Ref.	
designation (MW, kg mol^{-1})	source	T , °C	pH	medium					q (mass %)
				buffer (mmol L^{-1})	other components				
<i>Microplastic: PET (d = 0.25 mm); products: HET : BHET : TPA (the ratio was not indicated)</i>									
RgPETase- ^C His ₆ with R281A mutations and MalE signal peptide (32.2)	<i>Rhizobacter gummiphilus</i>	30	9	Glycine (50)	—	0.01	0.18	236	
<i>Microplastic: PET (d = 5 mm); products: HET : BHET : TPA (the ratio was not indicated)</i>									
SbPETase- ^C His ₆ (29.9)	<i>Schlegelella brevitalea</i> sp. nov.	30	8	Phosphate (50)	—	0.01	0.01	237	
<i>Microplastic: PET; products: HET : BHET : TPA (the ratio was not indicated)</i>									
SsSub1- ^N . ^C His ₆ (25.3)	<i>Streptomyces scabies</i>	37	7.5	TRIS (20)	Triton X-100 (0.5%)	0.03	0.14	Determination from the absorbance 238	
<i>Microplastic: PCL (d = 5 mm); product: HO(CH₂)₅COOH</i>									
TtCut- ^C His ₆ (24.2)	<i>Thermothielavioides terrestris</i> (former <i>Thielavia terrestris</i>)	40	5	Acetate (20)	—	0.01	385	Determined by titration 220	
<i>Microplastics: PBB, PLA, PBHT; products: HBS : BHBS : SA (PBB), MeCH(OH)COOH (PLA); HBT : BHBT : TPA and HBA : BHBA : AA (PBHT) (the ratios were not indicated)</i>									
Esterases	<i>Aspergillus, Fusarium and Chrysogenum</i> fungi	65	7	Phosphate (30)	—	20000	See ^P	Crude enzyme (culture medium) 239	
<i>Microplastic: PCL, cross-linked (4-OCN-Ph)₂CH₂ and 1,4-Bu(OH)₂ (d = 5 mm); products: HOOC(CH₂)₅OC(O)-4-N⁺H₂C₆H₄CH₂C₆H₄-4-NH₂ : 4-H₃N⁺C₆H₄CH₂C₆H₄-4-NH₂ = 0.15</i>									
A mixture of amidase E4143 and esterase E3576		50	7	Phosphate (100)	—	200	2.6×10^{-5} $\text{mg h}^{-1} \text{mL}^{-1}$	— 240	

Notes. The following designations are used: wt is wild type enzyme; AoCut-^CHis₆ is hybrid cutinase containing His₆ sequence at the C-terminus of the molecule and the alpha-factor from *Saccharomyces cerevisiae* at the N-terminus; DS-TfCut2 is hybrid enzyme consisting of TfCut2 cutinase with D204C/E253C mutations and the dermaseptin O1 antimicrobial peptide (GLWSTIKQKGKEAAIAAKAAG-QAALGAL-GGGGSGGGGSGGGGS) attached *via* a spacer to the N-terminus and ^CHis₆; Dura-PETase is IsPETase-^CHis₆ with S214H/I168R/W159H/S188Q/R280A/A180I/G165A/Q119Y/L117F/T140D mutations; FAST-PETase is hybrid IsPETase containing ^CHis₆, Sppstu signal peptide at the N-terminus and S121E/D186H/R224Q/N233K/R280A mutations; IsMHETase-^CHis₆ is hybrid IsMHETase containing ^CHis₆; IsMHETase-IsPETase-^CHis₆ is hybrid enzyme consisting of IsMHETase and IsPETase connected by a glycine spacer and containing ^CHis₆; IsPETase-^N.^CHis₆ is hybrid IsPETase containing the His₆ sequence at the N- and C-termini; IsPETase-^CHis₆ is hybrid IsPETase containing ^CHis₆; IsPETase-CBM-^CHis₆ is hybrid IsPETase containing the GAGAGAGAGAG sequence at the N-terminus, S121E/D186H/R280A mutations and the cellulose-binding domain with ^CHis₆; IsPETase-Trx-^N.^CHis₆ is hybrid enzyme containing thioredoxin-A sequence (109 amino acids) at the N-terminus of IsPETase-^N.^CHis₆; LCC-ICCG is hybrid LCC with the Y127G/D238C/F243I/S283C substitution containing ^CHis₆; LCC-ICCG-ChBD is hybrid LCC-ICCG containing the chitin binding domain ChBD; LCC-WCCG is hybrid LCC with Y127G/D238C/F243W/S283C mutations containing ^CHis₆; PHL7-^CHis₆ is hybrid PHL7 containing ^CHis₆; SsSub1-^N.^CHis₆ is hybrid SsSub1 containing an additional amino acid sequence (including S-tag and His₆) at the N-terminus and ^CHis₆; TfCut2-^CHis₆ is hybrid TfCut2 containing ^CHis₆; TheCut1-^CHis₆ is hybrid TheCut1 containing ^CHis₆; TheCut1-PBM-^CHis₆ is hybrid enzyme consisting of TheCut1 cutinase and polyhydroxybutyrate-binding module (PBM) connected by a spacer composed of 25 cellobiohydrolase amino acids and containing ^CHis₆; TS-PETase is hybrid IsPETase with S121E/D186H/N233C/R280A/S282C mutations containing ^CHis₆; TtCut-^CHis₆ is hybrid TtCut cutinase containing ^CHis₆ and alpha-factor from *Saccharomyces cerevisiae* at the N-terminus of the molecule. In the case where the optimal conditions were not defined, the conditions for the catalytic reaction are indicated.

Microplastics and products: PHT is poly(hexamethylene terephthalate); MAA is methacrylic acid; DTMAC is dodecyltrimethylammonium chloride; HEF is 2-hydroxyethyl 2,5-furandicarboxylate; BHEF is bis(2-hydroxyethyl) 2,5-furandicarboxylate; PBHT is poly(1,4-butylene hexanedioate-co-terephthalate); HBT is 4-hydroxybutyl terephthalate; BHBT is bis(4-hydroxybutyl) terephthalate; AA is adipic acid; PTMT is poly(trimethylene terephthalate); PBB is poly(1,4-butylene butanedioate); PHBHP is poly(3-hydroxybutyrate-co-3-hydroxypentanoate); PBH is poly(1,4-butylene hexanedioate); HBA is 4-hydroxybutyl adipate; BHBA is bis(4-hydroxybutyl) adipate; PBDT is poly(1,4-butylene decanedioate-co-terephthalate); MCC is microcrystalline cellulose; HBS is 4-hydroxybutyl succinate; BHBS is bis(4-hydroxybutyl) succinate; SA is succinic acid; EDTA is ethylenediaminetetraacetate, TRIS is tris(hydroxymethyl) aminomethane; HEPES is 4-(2-hydroxyethyl)-1-piperazineethanesulfonic acid; Plysurf A210G is a surfactant trademark; SDS is sodium dodecyl sulfate; DTT is dithiothreitol, PMSF is phenylmethylsulfonyl fluoride. K_i is the enzyme inhibition constant for some inhibitor (in this case, reaction product).

^a P values for PET particles of different size, $\text{mg h}^{-1} \text{mg}^{-1}$: 0.21 for $d = 0.45$ mm; 12 for $d = 0.2$ mm (wt); 26 for $d = 0.2$ mm. ^b For H214S/N233C/S245R/S282C. ^c Additional Q92G/H184S/F209I/I213K mutations. ^d For PET particles with $d = 0.6$ and 3 mm, P values were 31 and 11.2 $\text{mg h}^{-1} \text{mg}^{-1}$ and the product yields were 72 and 93%, respectively. ^e P values for diols, $\text{mg h}^{-1} \text{mg}^{-1}$: 0.63 for DEG; 0.33 for 1,5- $\text{C}_5\text{H}_{10}(\text{OH})_2$; 0.25 for 1,9- $\text{C}_9\text{H}_{18}(\text{OH})_2$; 0.11 for 1,2- $\text{C}_3\text{H}_6(\text{OH})_2$; 0.05 for 1,12- $\text{C}_{12}\text{H}_{24}(\text{OH})_2$; 0.03 for 1,3- $\text{C}_3\text{H}_6(\text{OH})_2$; 0.02 for 1,6- $\text{C}_6\text{H}_{12}(\text{OH})_2$; 0.01 for 1,8- $\text{C}_8\text{H}_{16}(\text{OH})_2$. ^f P , $\text{mg h}^{-1} \text{mg}^{-1}$: 0.15 for PET+PE; 0.07 for PET+PE; 0.01 for PET ($d = 0.25-0.5$ mm); 0.014 for PET ($d = 0.1-0.25$ mm); 0.03 for PET ($d = 0.05-0.1$ mm); 0.001 for PTMT. ^g P , $\text{mg h}^{-1} \text{mg}^{-1}$: 0.77 for PET, 0.16 for PBB, 4×10^{-3} for PHBHP. ^h P , $\text{mg h}^{-1} \text{mg}^{-1}$: 0.4 for PET, 21% yield of products; 0.014 for PBAC, 1.6% yield of the product. ⁱ P values for PET particles of different size, $\text{mg h}^{-1} \text{mg}^{-1}$: 0.02 for $d < 0.21$ mm; 0.015 for $d = 0.21-0.42$ mm; 0.015 for $d = 0.42-0.85$ mm; 0.018 for $d = 0.85-1$ mm; 0.012 for $d = 1-1.18$ mm; 0.004 for $d > 1.4$ mm. ^j For PET with $d = 0.075-0.25$ mm, $K_M = 244$ g L^{-1} , $k_{\text{cat}} = 3.74$ min^{-1} , $P = 0.26$ $\text{mg h}^{-1} \text{mg}^{-1}$; for PET with $d = 0.25-0.6$ mm $K_M = 233$ g L^{-1} , $k_{\text{cat}} = 1.55$ min^{-1} . ^k For PBB with $d = 0.4$ and 0.9 mm, $P = 0.37$ and 0.85 $\text{mg h}^{-1} \text{mL}^{-1}$, respectively. ^l Truncated enzyme. ^m For PBB with $d = 0.4$ and 0.9 mm, $P = 0.37$ and 0.21 $\text{mg h}^{-1} \text{mL}^{-1}$, respectively. ⁿ P values, $\text{mg h}^{-1} \text{mg}^{-1}$: 0.76 for ecovio[®]FT, 0.19 for PBHT, 0.62 for PBDT, 0.82 for PET. ^o P values, $\text{mg h}^{-1} \text{mg}^{-1}$: 7.3 for PET, 12.4 for PCL, 8.9 for PEB. ^p P values, $\text{mg h}^{-1} \text{mL}^{-1}$: 0.7 for PBB (ChsLip), 1.25 for PLA (FoLip), 1.7 for PBHT (AwLip).

elevated temperatures, whereas the cellulose-binding domain (CBM) attached to the N-terminus of IsPETase did not give any result.¹⁷⁵

A large number of studies have been devoted to the genetic modification of enzymes with the goal to improve their catalytic activity in the microplastic transformation reactions^{158, 170, 183, 186, 205, 225, 226, 237} and/or their stability,^{166, 167, 169, 173, 174, 177, 191, 194, 195, 219, 221, 230} to increase the protein yields in the biosynthesis^{160, 161, 179, 227, 236-238} and/or to facilitate the isolation and purification of proteins for obtaining the most efficient biocatalysts. Currently, modifications facilitating the isolation and purification of the target enzymes are applied almost in all studies.

Usually, the defined goals can be achieved by genetic modification, although there are some exceptions.^{221, 237} In any case, discussion of the effect of particular mutations is beyond the scope of this review, and to get acquainted with this topic, we recommend specialized reviews (*e.g.*, Refs 243, 244).

The enhancement of stability, in particular thermal stability, of the biocatalysts is aimed at increasing the

process performance, which is easily achieved by increasing the reaction temperature, *i.e.*, enzymatic biocatalysts become comparable in temperature characteristics (Fig. 4) with the low-temperature chemical catalysts considered above (see Fig. 2). However, an advantage of enzymes, that is, moderate temperatures of biocatalysis, is thus lost.

Since a number of enzymes, for example, TfCut2, SvCut190 and LCC, were identified and isolated from thermophilic microorganisms, they have high thermal stability. The information on the structure of these proteins served as the basis for comparative analysis and introduction of necessary mutations into the structures of similar mesophilic analogues possessing no thermal stability. In addition, some enzymes, *e.g.*, SvCut190,¹⁹⁴ MtCut²³⁰ and PpEst,²³² can be additionally stabilized by the Ca^{2+} ions present in the system. However, the metal binding site is usually modified by introducing instead a disulfide bridge, which increases the thermal stability of enzymes to even a higher extent. The following important point should be mentioned: the biosynthesis of target enzymes in thermotolerant yeast is often accompanied by their glycosylation at

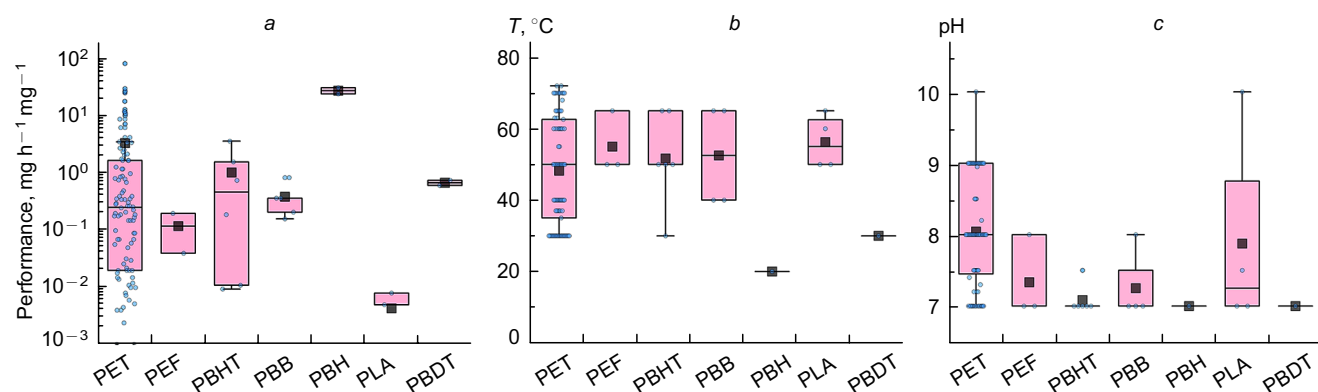


Figure 4. Statistical treatment of the results of application of various biocatalytic systems for the degradation of microplastics. (a) performance, (b) temperature, (c) pH of the reaction. The interquartile ranges (25%–75%) are enclosed by rectangles, which are divided by a line corresponding to the median value. The averages over all values and particular values are marked by square and round dots, respectively; the statistical outlier areas are indicated (Tukey's value is 1.5). The Figure was created by the authors using published data presented in Table 7.

the Asn residues. This may not only result in thermal stabilization,²²⁰ but also increase the aggregative stability and resistance to chaotropic agents;¹⁸⁸ in some cases, this markedly decreases the catalytic activity.^{202, 225}

It is often difficult to make a direct comparison of different enzymes and draw objective conclusions within one study, because enzymes are characterized by different optimal conditions of biocatalysis, and the use of some conditions is *a priori* unfavourable for some enzymes.^{158, 165, 222, 227, 231, 235, 239} Comparison of the results obtained in different works is even more difficult due to variability of conditions and, first of all, the used substrates (see Fig. 4). First, like in the case of chemical catalysts, upon a decrease in the microplastic particle size, the enzymatic activity may either increase^{190, 192, 201, 209–211, 214} or decrease.^{207, 212} Second, the substrate bioavailability starts to play an enormous role; as the crystallinity of the substrate increases, the enzyme activity decreases severalfold^{159, 176, 177, 189, 191, 193, 196, 201, 204, 208, 210, 219, 224, 236} or even several hundred-fold,^{172, 183, 214} down to complete loss of the catalytic activity.²²⁶ Apparently, in the latter case, an important role may be played by the form of the polymer material; for example, micrometre-thick films are often hydrolyzed less efficiently than separate microparticles.^{230, 235}

In this aspect, it is worth noting the study by Brizendine *et al.*,¹⁸⁹ in which, in the presence of 0.3% LCC-ICCG enzyme, the microplastic particle size did not affect the reaction rate, but the crystallinity of PET had a pronounced effect (the yield was 3–4 times lower when the degree of PET crystallinity increased from 8–11 to 33–36%). However, as the amount of the enzyme decreased 33-fold, the particle size of microplastics in a similar reaction started to be significant, so that smaller particles were hydrolyzed faster. This was accompanied by a change in the composition of products towards the formation of HET. In the study of Eugenio *et al.*,²¹¹ the Michaelis constants (K_M) for different-size PET particles were comparable, while the catalytic constant (k_{cat}) was 2.4 times higher for smaller particles.

An interesting observation was made by Chang *et al.*,¹⁹⁰ who found a direct correlation between the lag period preceding the hydrolysis of the substrate and the particle size of the microplastic. As a result, the performance was 2.8 lower in the case of larger particles. However, grinding was accompanied by a twofold increase in the crystallinity (from 6.5 to 12.6%); therefore, as previously, hydrolysis of large amorphous particles proceeded to a larger extent.

Due to the limited information on the size and crystallinity of the used microplastics reported in different studies, the contradictory data on the influence of the glass transition temperature (T_g), melting point (T_m) and the number-average (M_n) and weight-average (M_w) molecular weights of the polymer on the enzymatic activity are also difficult to interpret: in some cases, the biocatalyst activity was positively correlated with one or several parameters,¹⁹⁷ while in other cases, there was no such correlation;¹⁹⁸ in some studies, the correlation was observed only over a narrow range of parameters, but it was absent in a broad range.¹⁹⁹ The chemical structure of the polymer has a much greater effect on the enzyme activity than the variation of the physicochemical characteristics of the polymer material.^{198, 199} It is noteworthy that ageing of polymer materials under environmental conditions can also result in a considerable (1.6–2.6-fold)²⁰⁷ decrease in the efficiency of enzyme action. Apparently, this is due to structural changes in the

polymer substrate caused by its modification with functional groups that prevent normal catalysis, adsorption of compounds that inhibit the enzyme and changes in the rheological properties, including (bio)degradation of the bioavailable parts of microplastics.

A number of studies present quite successful attempts to improve the enzymatic activity of biocatalysts towards crystalline polymer substrates.^{193, 226} The number of such studies is small, since the main efforts were directed to other goals, for example, to increasing the thermal stability of enzymes. Indeed, considering the catalytic characteristics of IsPETase, the K_M value proved to be much lower (that is, better) in the case of crystalline than amorphous PET for temperatures of 30 and 40 °C.¹⁶⁶ In addition, the constant k_{cat} depended on both the temperature and crystallinity of the polymer, with the highest k_{cat} value being observed at elevated temperature with crystalline PET. The highest efficiency of enzyme action (k_{cat}/K_M) was observed under the same conditions. After two amino acid mutations, W159H/S238F, in the protein the thermal stability of the enzyme increased, but this had an adverse effect on both catalytic characteristics of the enzyme for both amorphous and crystalline PET at the two studied temperatures.

The poor applicability of optical, in particular, turbidimetric methods of product determination in the studies of biocatalytic decomposition of microplastics should be noted again. These methods give unreliable results for mixtures of products.¹⁷³ Therefore, the data obtained by high-performance liquid chromatography (HPLC)²¹⁶ and turbidimetry²¹⁷ for one and the same enzyme under the same conditions may differ by large factors, being 10–20 times overestimated for turbidimetry. Similar discrepancies are also observed when one compares the results of gravimetric analysis of the initial substrate (or determination of polymer M_n) with the product yields measured by HPLC.²¹² There are strong reasons to believe that determination by titration also gives overestimated results, since oligomeric products are formed.

An important problem is the inhibition of enzymes by inorganic and organic compounds present in the reaction medium with microplastics. Most of the enzymes that catalyze the destruction of microplastics are hydrolases containing the serine amino acid residue in the active site and are usually not inhibited by chelating agents.^{194, 222} However, these enzymes can contain additional structuring metal ions, which can be bound to chelating agents or replaced by other metals, thus leading to detectable decrease in the biocatalytic activity.^{206, 230, 236} The intermediates of PET hydrolysis (HET and BHET), which can be formed during the enzymatic reaction, are often also substrates of these enzymes; hence, they would function as competitive inhibitors, *e.g.*, for TfCut2,^{181, 182} MbPles629²²⁷ and PpEst.²³² However, some enzymes such as SvCut190 and Novozym® 51032 are quite tolerant to the presence of both intermediates over a broad range of their concentrations;^{194, 211} however, this feature may be no longer relevant at high degrees of substrate conversion.²⁰⁸ A genetic modification of these enzymes directed towards the change in their catalytic characteristics with the intermediate compounds may decrease the inhibitory activity of these compounds towards PET hydrolysis.¹⁸² An alternative method is to introduce combinations of several enzymes into the biocatalytic process^{162, 210, 213, 214, 240} and/or to perform a two-stage treatment of the polymer substrate with different enzymes.¹⁷⁰ In the former case, there is requirement that all of the enzymes function under the same reaction conditions.

In the latter case, identical conditions are not required, although finally this design would be inferior in the performance due to increase in the process duration.

Computer simulation methods are widely applied to enzyme reactions. First, the appearance and upgrading of extensive databases of nucleotide and amino acid sequences for a variety of (micro)organisms fundamentally changed the strategy of the search for new enzyme biocatalysts for the degradation of microplastics. Whereas earlier it was necessary to search for the potential destructors of microplastics and isolate them from the environmental objects, today the bioinformatic screening is performed in the automatic mode: it is sufficient to know the amino acid sequence of another enzyme with similar function (see Fig. 3). Moreover, some researchers have already prepared specialized databases on esterases that hydrolyze PET and polyurethanes.²⁴⁵ Thus, before direct biocatalytic experiments with microplastics, it is possible to select, for example, enzymes characterized by optimal operation at low temperature,²²² or, conversely, thermally stable enzymes,²²³ or those carrying a definite set of mutations.²²⁵ Therefore,

diverse sources in the form of non-culturable microorganisms, which are virtually impossible to isolate as pure cultures, do not even need to be isolated, but they remain at the level of identified metagenomes.^{219, 223, 224, 228, 231}

Second, if the amino acid sequence is available, it is possible to predict the structure and even the properties of enzymes as biocatalysts for the degradation of polymers.^{180, 182, 219, 220, 223, 224, 228, 230, 232} Third, using the predicted structure, at this stage, it is already possible to plan, for example, the introduction of point mutations to modulate the catalytic activity of enzymes^{185, 219} or, what is more important, to model the interaction with the substrate, in particular, by molecular docking techniques. Docking can be carried out using conformationally rigid^{171, 184} or flexible^{163, 165, 167} enzyme molecule; usually the procedure involves up to 4–5 monomer units of PET (or up to 7 monomers, like in the case of PLA²⁰⁵). Too short HET and BHET molecules may be considered to be inapplicable to reactions with microplastics. Docking offers more opportunities for the introduction of genetic modifications into the enzymes. Fourth, the resulting enzyme–substrate bind-

Table 8. Activation energies (E_a) of various reactions in the presence of (bio)catalysts.

Catalyst (size)	Microplastic (size)	E_a , kJ mol ⁻¹	Comments	Ref.
<i>Thermocatalytic reactions</i>				
Ga-doped HZSM-5 zeolite	PP (<0.5 mm)	100–110 (Si: Al = 30)	125–210 kJ mol ⁻¹ without catalysts	37
HZSM-12 zeolite (7.0–14.5 μm)	HDPE	100–120 (Si: Al = 25)	> 180 kJ mol ⁻¹ without catalysts. The addition of pure silica gel increased E_a . Linear dependence of E_a on the catalyst acidity	39
Y zeolite or MgCO ₃	HDPE (5 mm)	–	~ 300 kJ mol ⁻¹ without catalysts	44
[Bmim][OAc]	PBAC (3 mm)	228 (260 kPa)	E_a is higher than that for methanolysis	64
<i>Solvolytic</i>				
Zn(OAc) ₂	Low-molecular-weight PEF	105	Microwave-assisted reaction	99
Zn ²⁺ -doped PEVIA	PET (5 mm)	108		101
Zn(R ¹) ₂ , where R ¹ = 2,4-Bu ₂ ¹ -6-(MeNH(CH ₂) ₂ N=CH)C ₆ H ₄ O	PLA (5 mm)	39–65	Depending on the catalyst amount (16–4 mass %)	102
DBN:[4-MePh]	PET (74 μm)	163		107
[Me ₃ N(CH ₂) ₂ OH]CO ₂ H	PET (0.25–0.42 mm)	131		108
Zn(OAc) ₂	PET (0.25–0.4 mm)	125 (without DMSO) 75 (with DMSO)		110
Zn(OAc) ₂	PET (0.5 mm)	36.5	85 kJ mol ⁻¹ without catalysts. Microwave-assisted reaction.	111
3-Tropanol complex with c Zn(OAc) ₂ in 1 : 4 molar ratio	PET (5 mm)	89		113
Cu(OAc) ₂ : [Bmim][OAc] or Zn(OAc) ₂ : [Bmim][OAc]	PET (4 mm)	56 (Cu) 54 (Zn)		119
[Bmim][OAc]	PET (4 mm)	58.5		121
MOF ZIF-8	PET (3 mm)	138		136
[Me ₃ N(CH ₂) ₂ OH] ₃ PO ₄ together with CNTs modified by polydopamine	PET (5 mm)	81–83		138
TiO ₂ (0.1 mm) doped with 4 mass % H ₂ SO ₄	PET (4 mm)	12 (15 MPa) 15.5 (8 MPa)	Reaction in supercritical CO ₂	147

Table 8 (continued).

Catalyst (size)	Microplastic (size)	E_a , kJ mol ⁻¹	Comments	Ref.
<i>Enzymatic hydrolysis</i>				
IsMHETase-C _{His} ₆ (64 kg mol ⁻¹)	HET	58 (first barrier) ^a 83 (second barrier) ^a		162
Novozym® 51032 (24 kg mol ⁻¹)	PET (0.075–0.25 mm)	99	Enthalpy: 96 kJ mol ⁻¹ , entropy: 79 J K ⁻¹ mol ⁻¹	211
IsPETase (29 kg mol ⁻¹)	PET (2 monomer unit ^a)	84 (first barrier) ^a 63 (second barrier) ^a		246
MGS0156 (37 kg mol ⁻¹)	PCL	56	2 monomer units: 58–88 (first barrier) ^a 30.5–49 (second barrier) ^a	247
RPA1511 (33 kg mol ⁻¹)	PLA, PCL (2–4 monomer units ^a)	97 (first barrier) ^a 20 (second barrier) ^a		248

^a Computer simulation data.

ing models can be used to study the mechanism of enzyme action by molecular dynamics.^{156, 163, 171, 177, 191, 230} In exceptional cases, studies achieve the state of combined QM/MM calculations.^{162, 184} The results of determining the energy barriers for some enzymes are summarized in Table 8.

Certainly, there are much more papers on the computer simulation of enzymes capable of degrading polymers than have been mentioned, but not all of them refer directly to the decomposition of microplastics and, therefore, they are not discussed here. In any case, the efforts of many researchers produced theoretical and experimental data that served as the basis for the development of a variety of biocatalysts degrading various microplastics. The range of microplastics that can be decomposed by enzymes is still limited to polyesters and polyamides and is comparable only with the range of microplastics that are decomposed by solvolysis. Nevertheless, there are other known enzymes that catalyze, for example, redox processes involving polymers, but they have not yet been investigated in reactions with microplastics, although they have practical potential in this field. The specific features of enzymes used to decompose microplastics include the following: moderate temperatures and mild conditions of catalytic reactions (in particular, the absence of organic solvents); the lack of toxicity and biodegradability of the proper biocatalysts, and, in the absence of additional stimulating additives, the lack of toxicity of reaction media; specificity of action;

modular structure of biocatalysts (*i.e.*, different catalytically active and/or auxiliary modules can be combined in different ways or be replaced with one another in the same catalytic system).

4. Immobilized biocatalysts for decomposition of microplastics

Special discussion is required for the small group of publications addressing immobilized enzyme catalysts (Table 9). It is known²⁵⁵ that, on the one hand, immobilized enzymes are stabilized against inactivating factors and, on the other hand, they can be used in the catalytic process many times. Both these factors were successfully demonstrated in experimental works with microplastics.^{249, 251–254} Certainly immobilization of enzymes by treatment with cross-linking agents is likely to decrease the catalytic activity by a large factor.²⁵¹ However, this loss can be minimized by immobilization (Fig. 5),^{250, 252} which provides impressive binding capacity of the carriers with these enzymes (up to 0.47 g g⁻¹).

Meanwhile, immobilization opens up new prospects. For example, the use of magnetic nanoparticles as carriers allows easy separation of the biocatalyst from the reaction media or additional stimulation of the catalytic activity by using MW field and/or light.^{250, 251} A study by Li *et al.*,²⁵³ who incorporated simultaneously two enzymes into MOF is quite promising. Despite the fact that the activity of

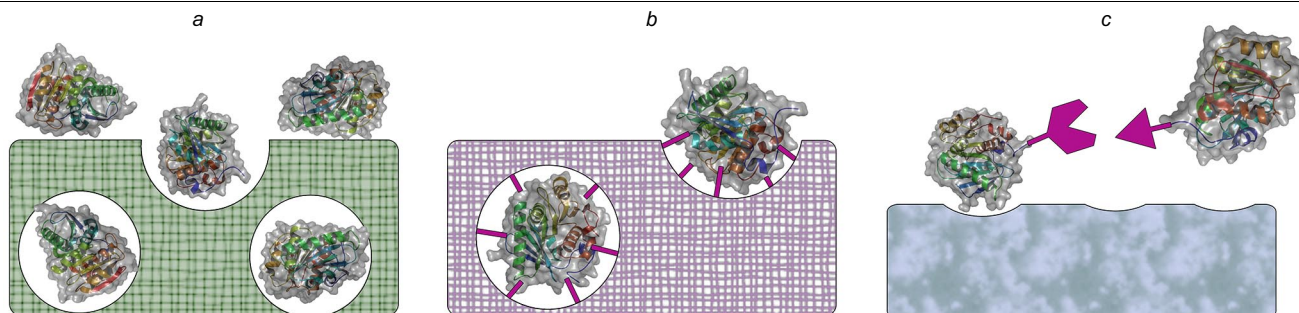


Figure 5. Basic schemes of various types of immobilization of enzymes. (a) embedding and/or absorption (adsorption) in/on a carrier; (b) covalent binding to the carrier; (c) high affinity interaction. The structure of IsPETase enzyme (PDB 6EQD) was illustrated using PyMOL (version 1.7.6, Schrödinger, LLC).

Table 9. Immobilized enzyme biocatalysts.

designation (MW, kg mol ⁻¹)	Enzyme		Optimal reaction conditions				<i>P</i> , mg h ⁻¹ mL ⁻¹	Comments	Ref.
	source	immobilization method	<i>T</i> , °C	pH	buffer (mmol L ⁻¹)	<i>q</i> (mass %)			
<i>Microplastic: PET; products: HET : BHET : TPA = 0.02 : 0.03 : 1</i>									
IsPETase- ^C His ₆ (31)	<i>I. sakaiensis</i>	Embedding into and/or adsorption on nanostructured Co ₃ (PO ₄) ₂ (<i>d</i> = 10 μm)	30	8	Phosphate (50)	2500% (v/w)	3.6 × 10 ⁻² mg h ⁻¹ mL ⁻¹ (see ^a) 20.4 × 10 ⁻² mg h ⁻¹ mL ⁻¹ (see ^b)	Crude enzyme. In the tenth cycle, the activity decreased by 30%	249
<i>Microplastic: PET (d = 0.5 mm); products: HET : BHET : TPA (the ratio was not indicated)</i>									
IsPETase- ^C His ₆ with W159H/S238F mutations (31)	<i>I. sakaiensis</i>	Adsorption on Fe ₃ O ₄ (NPs, <i>d</i> = 10 nm)	30	7.5	TRIS (50)	1.25	1.2 × 10 ⁻⁴	Determined from the absorbance	250
<i>Microplastic: PET (d = 6 mm); products: HET : BHET : TPA (the ratio was not indicated)</i>									
DuraPETase (28)	<i>I. sakaiensis</i>	Covalent immobilization via EDC/NHS on Fe ₃ O ₄ (NPs, <i>d</i> = 11 nm)	46	9	Glycine (50)	0.5	0.032	Exposure to light (0.1 W cm ⁻²). In the sixth cycle, the activity decreased by 45%	251
<i>Microplastic: PET (d = 6 mm); products: HET : TPA = 0.4^b (0.5^a)</i>									
DuraPETase-SpyT (32.9), IsMHETase-SpyC (43.5)	<i>I. sakaiensis</i>	Embedding of IsMHETase-SpyC into Ca ₃ (PO ₄) ₂ microcrystals followed by adsorption of DuraPETase-SpyT thereon	50	8.0	Phosphate (80)	27	0.14 ^a 0.21 ^b	In the presence of NaCl (40 mmol L ⁻¹)	252
<i>Microplastic: amorphous poly(glucopyranose); products: glucose</i>									
α-Amylase (51) and amyloglucosidase (97)	<i>A. oryzae</i> and <i>A. niger</i>	Embedding into MOF based on Ca ²⁺ and biphenyl-4,4'-dicarboxylic acid	45	7.4	HEPES (100)	21	10	After 8 cycles, the activity decreased by 25%; after storage for 10 days, the activity decreased by 13%	253
<i>Microplastic: crystalline poly(glucopyranose) (d = 50 μm) or poly-(carboxymethyl-glucopyranose); product: glucose</i>									
Mixture of Glu-s-ELP- ^C His ₆ (79), Eglu-s-ELP- ^C His ₆ (71), Cbh-s-ELP- ^C His ₆ (69)	<i>Coptotermes formosanus</i>	Embedding into nanostructured Cu ₃ (PO ₄) ₂ (<i>d</i> = 10–12 μm)	40	5	Acetate (100)	1.2	0.01	After 8 cycles, the activity decreased by 38%	254

Notes. The following designations are used: Cbh-s-ELP-^CHis₆ is hybrid cellobiohydrolase connected *via* a spacer (GGGGS)₃ to elastin-like domain (VPGVG)₅₀ and ^CHis₆; DuraPETase-SpyT is hybrid DuraPETase containing SpyTag and ^CHis₆; Eglu-s-ELP-^CHis₆ is hybrid endoglucanase connected *via* a spacer (GGGGS)₃ to elastin-like domain (VPGVG)₅₀ and ^CHis₆; Glu-s-ELP-^CHis₆ is hybrid β-glucanase connected *via* a spacer (GGGGS)₃ to elastin-like domain (VPGVG)₅₀ and ^CHis₆; IsMHETase-SpyC is hybrid IsMHETase containing SpyCatcher at the C-terminus and ^NHis₆; EDC is 1-ethyl-3-(3-dimethylaminopropyl)carbodiimide. ^a Soluble enzyme. ^b Immobilized enzyme.

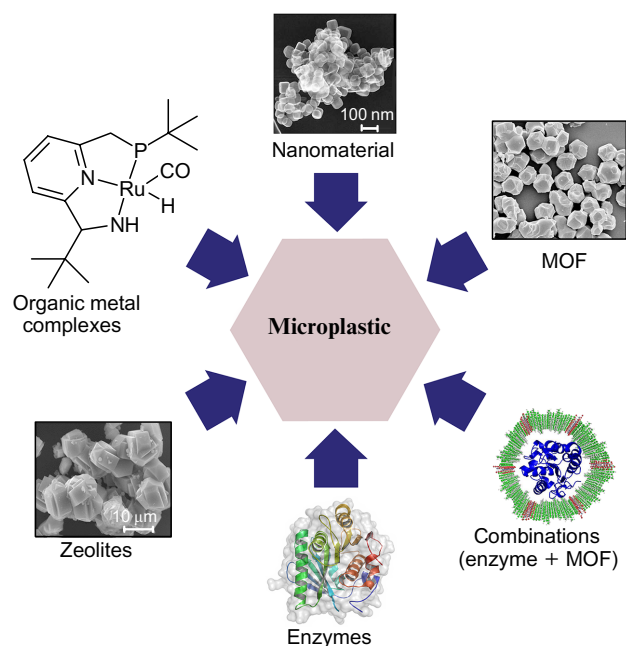


Figure 6. Some examples of (bio)catalysts for the degradation of microplastics. The images of a typical zeolite,⁵³ nanomaterial,⁷⁰ organic metal complex,⁷⁷ MOF¹³⁵ and their combination (exemplified by the enzyme and MOF)²⁵⁶ were adapted from original sources with permission from Elsevier and the American Chemical Society. The structure of the IsPETase enzyme (PDB 6EQD) was illustrated using PyMOL the (version 1.7.6, Schrödinger, LLC).

enzymes decreased 1.5–2-fold, an approach of this type could be used in the future for combining various enzymes with chemical catalysts degrading microplastics (Fig. 6). In turn, enzymes can also influence the partner introduced into the process, resulting, for example, in an increase in the size of metal nanoparticles by dozens of times.²⁵⁰ Thus, careful selection of the chemical and biocatalytic components is required, which can be greatly facilitated by using computer simulation techniques to calculate the interaction of enzymes with MOFs²⁵⁶ and with nanoparticles.²⁵⁷

A separate option is to use living cells of microorganisms that synthesize the target enzymes to degrade microplastics directly during their culturing.^{258–260} The performance of these catalyst systems is comparable to that of immobilized enzymes. In principle, several enzymes can be simultaneously expressed in a cell, thus performing multi-stage conversion of microplastics.

Returning to the issue of the energy barriers of the reactions, it should be emphasized that in some studies, the activation energies were determined experimentally and/or calculated for a number of (bio)catalysts (see Table 8). As expected, catalysts decrease the energy barriers by large factors. The energy barrier depends on not only the composition and amount of the catalyst,^{39, 102, 119} but also on additionally introduced solvents¹¹⁰ and the operating pressure.¹⁴⁷ It is quite possible that the activation energy of the reaction also decreases under MW irradiation¹¹¹ as compared to the activation energy of a similar process without it.¹¹⁰ It is noteworthy that almost in all studies, the activation energy in the presence of (bio)catalysts was determined *via* the degree of conversion of the substrate, which does not coincide with the product yield. Therefore, for correct comparison of different (bio)catalysts, it would

be reasonable to revise or even redefine the activation energies determined previously, in order to attain certain common conditions for comparison.

With rare exceptions, the energy barriers for enzyme-catalyzed reactions are usually determined by computer simulation. According to a typical mechanism of action of these catalysts, the first step is the acylation of the Ser residue (see Fig. 3), which is deacylated in the second step. This reaction pathway involves two energy barriers for both monomeric¹⁶² and dimeric substrates^{246–248} and higher-molecular-weight models. However, four or more energy barriers were identified in many studies;^{184, 261, 262} most likely, these barriers are artifacts and/or are due to the use of erroneous initial state(s) or interpretations.

Among other drawbacks, the use of truncated models for polymer substrates is noteworthy. Of course, computer modelling is too resource-demanding, but it is already evident that reduced (shortened) models give distorted results. For example, successive increase in the model length gives different values for energy barriers and different sets of amino acid residues that interact with polymers.²⁶² This set of definite amino acid residues of biocatalysts can serve for rational choice of the targets^{246–248} for their subsequent modification by rational design methods. Furthermore, the roles of the cap domain of the enzyme active site^{162, 235} and metal ions (able to induce conformational changes in the protein structure),²⁶³ which can affect the enzymatic activity, are often neglected.

5. Conclusion

As opposed to macroplastics visible by naked eye, the (bio)degradation of microplastics isolated from environmental objects is addressed in rare instances.⁵⁷ Most often, these studies use model polymer substrates or (more rarely) their mixtures. Certainly, this makes it possible to precisely control the conditions for laboratory processes, but does not appear adequate for real-life implementation.

It is also noteworthy that owing to the deficiency of studies of real samples of microplastics, the issue of how microplastics can be extracted from environmental specimens has not yet been clarified. As initial conditions, it is rational to resort to the existing practices used for analysis of microplastics in water, soil and atmosphere.^{1–4} It is evident that in the case of catalytic processes, it is likely that some procedures will be eliminated or, conversely, additional isolation stages would be required. For instance, it is known that the concentrations of microplastics in water specimens vary over a broad range: from a few to tens of thousands of particles in cubic metre of water;^{264, 265} therefore, for more efficient catalysis, it is necessary, at least, to separate the microplastics from the embedding matrix and, at most, to concentrate it to an appropriate level. For this purpose, it is expedient to use, for example, membrane technologies, which have been rather advanced to date.²⁶⁶ Here, the problem of nanoplastics deserves mention: among the publications discussed in this review, only a few papers^{89, 90, 174, 227} address model polymer nanoparticles with reliably determined size. The small number of papers allows one to hope that studies in this area, especially as applied to real samples of nanoplastics, would be intensified in the near future. This is a nontrivial and highly important task, which has a high scientific and practical potential.

Analysis of published works makes it possible to formulate several criteria that are necessary for studying the degradation of microplastics:

- identification and quantitative determination of specific decomposition products by relevant methods; semi-quantitative and qualitative determinations are acceptable only in the early and preliminary stage of investigation;

- publication of complete exhaustive procedures for conduction of the reactions; regarding the currently reported procedures, the results of many published studies cannot, in principle, be reproduced; hence, they objectively cannot be included into the list of procedures available for the review analysis;

- as full as possible characterization of the polymer substrate and the catalyst; as shown in this review, quite a number of parameters affect the process performance and the yields of products; characteristics of commercial products may vary over a wide range without notice from the manufacturer;

- determination of the toxicity of chemical catalysts and reaction products formed with these catalysts; currently this issue is ignored by authors who develop catalytic processes; however, the toxicity (gene, eco-, cyto- and immunotoxicity and other types of toxicity) should be determined, if possible, for different biological objects; this problem is especially acute when the research is switched from model to real microplastics;

- ruling out contamination of the polymer substrate by other polymers during the process; this problem is neglected in the studies discussed here, although it has been known for a long time⁵ and is discussed in the analysis of microplastics; the contaminants may be not converted to reaction products themselves, but affect the efficiency of catalysis.

The compliance with these criteria would markedly simplify both selection of the catalysts for practical application and development of new catalyst samples.

Currently, computer simulation methods are mainly used in the development of enzyme biocatalysts and are rarely used for other purposes. This obvious imbalance already affects the progress in the development of chemical catalysts; in the future, this effect would increase unless decisive measures are taken to improve the situation. One more aspect is that computer simulation is still used only to study the mechanisms of interaction of enzymes with low-molecular weight substrates. Meanwhile, these methods are suitable for much more complex systems, *e.g.*, proteins interacting with nanomaterials,^{267, 268} MOFs²⁶⁹ or polymers.²⁷⁰ The latter is especially important, because, as has been noted above, the artificial shortening of the model for the interacting substrate gives unpredictable results unrelated to the actual experiment. The use of micro- or nanoparticles composed of a definite polymer would be an ideal model.²⁷¹ In any case, irrespective of the chosen option (nanomaterial, MOF, polymer), this approach enables:

- design of (bio)catalysts of a new type, for example, those capable of targeted delivery of the (bio)catalyst towards a microplastic particle *via* its conjugation or merging with a partner that has a high affinity for the substrate;²⁷²

- fabrication of (nano)biocatalysts with enhanced stability and without an adverse influence of the carrier and/or the preparation itself on the enzymatic activity;

- combining of (bio)catalytic components with (bio)sensors and/or coagulating agents;

- combining of different type (bio)catalytic components that are allowed to react with microplastics.

In principle, this combination has already been implemented in a number of catalytic processes, and the advantages of this approach have been demonstrated. However, the combinations of catalysts are now selected by the trial and error method. Meanwhile, simulation will elevate the efficiency of such system to a new research and practice level. Indeed, using various starting enzymes, it is now possible to modify their structures and, hence, to improve the catalytic performance on the basis of a reference sample with the highest biocatalytic activity.²²⁵

A few words should be said about enzyme kinetics in heterogeneous systems. The authors of many studies actively promote the so-called inverse Michaelis–Menten kinetics for the explanation of the observed atypical decrease in the enzyme activity with increasing enzyme concentration. Moreover, some authors go even further and take the calculated values as the classical K_M and k_{cat} constants, although Scandola *et al.*,²⁷³ who were the first to propose this model, interpret the results more properly. Further studies and development of an adequate kinetic model are required to explain this unusual behaviour of enzymes. As a rule, a few variants are generated, and the one describing most closely the experimental data is chosen.²⁰⁹ That is not to say that the model and preconditions used by de Queiros Eugenio *et al.*²⁰⁹ are exhaustive (especially considering the specific adsorption and desorption processes established in other studies), but these examples demonstrate that an appropriate kinetic model for heterogeneous enzymatic reactions, including conversion of microplastics, could be developed. Adequate interpretation of the data derived from catalytic degradation of microplastics is an important part of the study of the conditions of these processes, their catalysts and products.

This review was written within the framework of the State task of the Lomonosov Moscow State University (121041500039-8) and with the support of the Interdisciplinary Scientific and Educational School of Moscow University ‘The Future of the Planet and Global Environmental Change’.

6. List of abbreviations and symbols

AA — adipic acid;
 AE — 2-aminoethanol;
 Amim — 1-allyl-3-methylimidazolium;
 BHBA — bis(4-hydroxybutyl) adipate;
 BHBS — bis(4-hydroxybutyl) succinate;
 BHBT — bis(4-hydroxybutyl) terephthalate;
 BHDET — bis(hydroxydiethylene) terephthalate;
 BHEF — bis(2-hydroxyethyl) 2,5-furandicarboxylate;
 BHET — bis(2-hydroxyethyl) terephthalate;
 Bmim — 1-butyl-3-methylimidazolium;
 [Ch]₃PO₄ — choline phosphate;
 CNTs — carbon nanotubes;
 DBN — 1,5-diazabicyclo[4.3.0]non-5-ene;
 DEG — diethylene glycol;
 DFT — density functional theory;
 DPG — dipropylene glycol;
 DTMAC — dodecyltrimethylammonium chloride;
 EDC — 1-ethyl-3-(3-dimethylaminopropyl)carbodiimide;
 EG — ethylene glycol;
 FCC — fluid cracking catalyst;
 FDA — 2,5-furandicarboxylic acid;
 HBA — 4-hydroxybutyl adipate;
 HBS — 4-hydroxybutyl succinate;

HBT — 4-hydroxybutyl terephthalate;
HDPE — high-density polyethylene;
HDPS — high-density polystyrene;
HEF — 2-hydroxyethyl 2,5-furandicarboxylate;
HET — 2-hydroxyethyl terephthalate;
Hmim — 1-hexyl-3-methylimidazolium;
LDPE — low-density polyethylene;
MAA — methacrylic acid;
MCC — microcrystalline cellulose;
Me₂TPA — dimethyl terephthalate;
MeTPA — monomethyl terephthalate
Mmim — 1-methyl-3-methylimidazolium;
[Mmim]⁺-2-COO⁻ — 1-methyl-3-methylimidazolium
2-carboxylate;
MOF — metal-organic framework;
MSA — methanesulfonic acid;
MW — molecular weight;
N-Melm — N-methylimidazole;
NP — nanoparticle;
NPG — neopentyl glycol;
P3HB — poly(3-hydroxybutyrate);
P3HP — poly(3-hydroxypropionate);
PBB — poly(1,4-butylene butanedioate);
PBBH — poly(1,4-butylene butanedioate-co-hexane-
dioate);
PBBC — poly(1,3-bis(aminomethyl)benzenecapramide);
PBBO — poly(1,3-bis(aminomethyl)benzylloxalamide);
PBBT — poly(1,3-bis(aminomethyl)benzylterephthala-
mide);
PBVI — poly(1-butyl-3-vinylimidazolium bis(trifluoro-
methane)sulfonimide);
PBH — poly(1,4-butylene hexanedioate);
PBHT — poly(1,4-butylene hexanedioate-co-terephtha-
late);
PBDT — poly(1,4-butylene decanedioate-co-terephtha-
late);
PBT — poly(1,4-butylene terephthalate);
PBAC — poly(bisphenol-A-carbonate);
PVP — polyvinylpyrrolidone;
PVC — polyvinyl chloride;
PHBHP — poly(3-hydroxybutyrate-co-3-hydroxypenta-
noate);
PHT — poly(hexamethylene terephthalate);
PHMA — poly(hexamethylene adipate);
PDHT — poly(1,6-diaminohexaneterephthalamide);
PDMAEMA — poly(dimethylaminoethyl methacry-
late);
PDO — polydioxanone;
PDCT — poly(1,4-dihydroxymethylenecyclohexane
terephthalate);
PCL — poly(ϵ -caprolactone);
PLGC — poly(lactide-co-glycolide-co- ϵ -caprolactone);
PMMA — poly(methyl methacrylate);
PMBS — poly(4,4'-methylene-bis(cyclohexanamide)suc-
cinamide);
PLA — polylactic acid;
PP — polypropylene;
PPC — poly(propylene-1,2-diol carbonate);
PS — polystyrene;
PTMT — poly(trimethylene terephthalate);
PU — polyurethane;
PPS — poly(phenylene sulfide);
PEB — poly(ethylene butanedioate);
PEVIA — poly(1-ethyl-3-vinylimidazolium acetate-co-
acrylate);
PE — polyethylene;

PEG — polyethylene glycol;
PEC — poly(ethylene carbonate);
PET — poly(ethylene terephthalate);
PEF — poly(ethylene 2,5-furandicarboxylate);
SA — succinic acid;
TBD — 1,5,7-triazabicyclo[4.4.0]dec-5-ene;
TMAD — trimethylolpropane allyl ether;
TMADC — trimethylolpropane allyl ether carbonate;
TMGase — 2-(tetramethylguanidinium)-5-R¹-benzoic
acid methyl ester, where R¹ = Cl, H or NMe₂;
TOC — total organic carbon;
TPA — terephthalic acid;
THF — tetrahydrofuran.

7. References

1. S.Palmas, A.Vacca, L.Mais. *Catalysts*, **11**, e913 (2021); <https://doi.org/10.3390/catal11080913>
2. N.P.Ivleva. *Chem. Rev.*, **121**, 11886 (2021); <https://doi.org/10.1021/acs.chemrev.1c00178>
3. C.Junhao, Z.Xining, G.Xiaodong, Z.Li, H.Qi, K.H.M.Siddique. *J. Environ. Manag.*, **294**, e112997 (2021); <https://doi.org/10.1016/j.jenvman.2021.112997>
4. G.Chen, Q.Feng, J.Wang. *Sci. Total Environ.*, **703**, e135504 (2020); <https://doi.org/10.1016/j.scitotenv.2019.135504>
5. C.S.Witzig, C.Földi, K.Wörle, P.Habermehl, M.Pittroff, Y.K.Müller, T.Lauschke, P.Fiener, G.Dierkes, K.P.Freier, N.Zumbülte. *Environ. Sci. Technol.*, **54**, 12164 (2020); <https://doi.org/10.1021/acs.est.0c03742>
6. J.C.Prata, J.P.da Costa, I.Lopes, A.C.Duarte, T.Rocha-Santos. *Sci. Total Environ.*, **702**, e134455 (2020); <https://doi.org/10.1016/j.scitotenv.2019.134455>
7. J.-S.Kim, H.-J.Lee, S.-K.Kim, H.-J.Kim. *Environ. Sci. Technol.*, **52**, 12819 (2018); <https://doi.org/10.1021/acs.est.8b04180>
8. T.Jiwarungrueangkul, J.Phaksopa, P.Sompongchaiyakul, D.Tipmanee. *Mar. Pollut. Bull.*, **168**, e112452, (2021); <https://doi.org/10.1016/j.marpolbul.2021.112452>
9. E.Hernandez, B.Nowack, D.M.Mitrano. *Environ. Sci. Technol.*, **51**, 7036 (2017); <https://doi.org/10.1021/acs.est.7b01750>
10. M.C.Zambrano, J.J.Pawlak, J.Daystar, M.Ankeny, J.J.Cheng, R.A.Venditti. *Mar. Pollut. Bull.*, **142**, 394 (2019); <https://doi.org/10.1016/j.marpolbul.2019.02.062>
11. L.G.A.Barboza, A.D.Vethaak, B.R.Lavorante, A.K.Lundebye, L.Guilhermino. *Mar. Pollut. Bull.*, **133**, 336 (2018); <https://doi.org/10.1016/j.marpolbul.2018.05.047>
12. F.M.Windsor, R.M.Tilley, C.R.Tyler, S.J.Ormerod. *Sci. Total Environ.*, **646**, 68 (2019); <https://doi.org/10.1016/j.scitotenv.2018.07.271>
13. W.Huang, B.Song, J.Liang, Q.Niu, G.Zeng, M.Shen, Y.Zhang. *J. Hazard. Mater.*, **405**, e124187 (2021); <https://doi.org/10.1016/j.jhazmat.2020.124187>
14. L.G.A.Barboza, C.Lopes, P.Oliveira, F.Bessa, F.V.Otero, B.Henriques, L.Guilhermino. *Sci. Total Environ.*, **717**, e134625 (2020); <https://doi.org/10.1016/j.scitotenv.2019.134625>
15. K.Senathirajah, S.Attwood, G.Bhagwat, M.Carbery, S.Wilson, T.Palanisami. *J. Hazard. Mater.*, **404**, e124004 (2021); <https://doi.org/10.1016/j.jhazmat.2020.124004>
16. J.C.Prata. *Environ. Pollut.*, **234**, 115 (2018); <https://doi.org/10.1016/j.envpol.2017.11.043>
17. P.Ju, Y.Zhang, Y.Zheng, F.Gao, F.Jiang, J.Li, J.C.Sun. *Sci. Total Environ.*, **734**, e139219 (2020); <https://doi.org/10.1016/j.scitotenv.2020.139219>
18. C.Campanale, C.Massarelli, I.Savino, V.Locaputo, V.F.Uricchio. *Int. J. Environ. Res. Public Health*, **17**, e1212 (2020); <https://doi.org/10.3390/ijerph17041212>
19. Z.Li, Q.Li, R.Li, Y.Zhao, J.Geng, G.Wang. *Environ. Sci. Pollut. Res.*, **27**, 30306 (2020); <https://doi.org/10.1007/s11356-020-09349-0>

20. T.T.Awet, Y.Kohl, F.Meier, S.Straskraba, A.L.Grün, T.Ruf, C.Jost, R.Drexel, E.Tunc, C.Emmerling. *Environ. Sci. Eur.*, **30**, e11 (2018); <https://doi.org/10.1186/s12302-018-0140-6>
21. O.Mbachu, G.Jenkins, P.Kaparaju, C.Pratt. *Sci. Total Environ.*, **780**, e146569 (2021); <https://doi.org/10.1016/j.scitotenv.2021.146569>
22. T.Roy, T.K.Dey, M.Jamal. *Environ. Monit. Assess.*, **195**, e27 (2023); <https://doi.org/10.1007/s10661-022-10654-z>
23. A.Kumari, V.D.Rajput, S.S.Mandzhieva, S.Rajput, T.Minkina, R.Kaur, S.Sushkova, P.Kumari, A.Ranjan, V.P.Kalinitchenko, A.P. Glinushkin. *Plants*, **11**, e340 (2022); <https://doi.org/10.3390/plants11030340>
24. Y.Wan, C.Wu, Q.Xue, X.Hui. *Sci. Total Environ.*, **654**, 576 (2019); <https://doi.org/10.1016/j.scitotenv.2018.11.123>
25. N.Khalid, M.Aqeel, A.Noman. *Environ. Pollut.*, **267**, e115653 (2020); <https://doi.org/10.1016/j.envpol.2020.115653>
26. W.Yang, P.Cheng, C.A.Adams, S.Zhang, Y.Sun, H.Yu, F.Wang. *Soil Biol. Biochem.*, **155**, e108179 (2021); <https://doi.org/10.1016/j.soilbio.2021.108179>
27. L.Hou, D.Kumar, C.G.Yoo, I.Gitsov, E.L.W.Majumder. *Chem. Eng. J.*, **406**, e126715 (2021); <https://doi.org/10.1016/j.cej.2020.126715>
28. M.Lv, B.Jiang, Y.Xing, H.Ya, T.Zhang, X.Wang. *Environ. Sci. Pollut. Res.*, **29**, 65887 (2022); <https://doi.org/10.1007/s11356-022-22004-0>
29. I.Ali, T.Ding, C.Peng, I.Naz, H.Sun, J.Li, J.Liu. *Chem. Eng. J.*, **423**, e130205 (2021); <https://doi.org/10.1016/j.cej.2021.130205>
30. K.H.D.Tang, S.S.M.Lock, P.-S.Yap, K.W.Cheah, Y.H.Chan, C.L.Yiin., A.Z.E.Ku, A.C.M.Loy, B.L.F.Chin, Y.H.Chai. *Sci. Total Environ.*, **832**, e154868 (2022); <https://doi.org/10.1016/j.scitotenv.2022.154868>
31. A.J.Martin, C.Mondelli, S.D.Jaydev, J.Pérez-Ramírez. *Chem.*, **7**, 1487 (2021); <https://doi.org/10.1016/j.chempr.2020.12.006>
32. L.O.Mark, M.C.Cendejas, I.Hermans. *ChemSusChem*, **13**, 5808 (2020); <https://doi.org/10.1002/cssc.202001905>
33. Y.M.Kim, J.Jae, B.S.Kim, Y.Hong, S.C.Jung, Y.K.Park. *Energy Convers. Manag.*, **149**, 966 (2017); <https://doi.org/10.1016/j.enconman.2017.04.033>
34. B.Muneer, M.Zeeshan, S.Qaisar, M.Razzaq, H.Iftikhar. *J. Clean. Prod.*, **237**, e117762 (2019); <https://doi.org/10.1016/j.jclepro.2019.117762>
35. S.Xu, B.Cao, B.B.Uzoejinwa, E.A.Odey, S.Wang, H.Shang, H.C.Li, Y.Hu, Q.Wang, J.N.Nwakaire. *Process Saf. Environ. Prot.*, **137**, 34 (2020); <https://doi.org/10.1016/j.psep.2020.02.001>
36. B.Fekhar, L.Gombor, N.Miskolczi. *J. Energy Inst.*, **92**, 1270 (2019); <https://doi.org/10.1016/j.joei.2018.10.007>
37. S.Pyo, Y.-M.Kim, Y.Park, S.B.Lee, K.-S.Yoo, M.A.Khan, B.-H.Jeon, Y.Jun Choi, G.Hoon Rhee, Y.-K.Park. *J. Ind. Eng. Chem.*, **103**, 136 (2021); <https://doi.org/10.1016/j.jiec.2021.07.027>
38. C.Kassargy, S.Awad, G.Burnens, K.Kahine, M.Tazerout. *J. Anal. Appl. Pyrolysis*, **127**, 31 (2017); <https://doi.org/10.1016/j.jaap.2017.09.005>
39. A.O.S.Silva, M.J.B.Souza, A.M.G.Pedrosa, A.C.F.Coriolano, V.J.Fernandes, A.S.Araujo. *Microporous Mesoporous Mater.*, **244**, 1 (2017); <https://doi.org/10.1016/j.micromeso.2017.02.049>
40. C.Ma, J.Yu, B.Wang, Z.Song, J.Xiang, S.Hu, S.Su, L.Sun. *Fuel Process. Technol.*, **155**, 32 (2017); <https://doi.org/10.1016/j.fuproc.2016.01.018>
41. K.Li, S.Lee, G.Yuan, J.Lei, S.Lin, P.Weerachanchai, Y.Yang, J.-Y.Wang. *Energies*, **9**, e431 (2016); <https://doi.org/10.3390/en9060431>
42. K.Saeung, N.Phusunti, W.Phetwarotai, S.Assabumrungrat, B.Cheirsilp. *Waste Manag.*, **127**, 101 (2021); <https://doi.org/10.1016/j.wasman.2021.04.024>
43. K.P.Kumar, S.Srinivas. *Energy Fuels*, **34**, 460 (2020); <https://doi.org/10.1021/acs.energyfuels.9b03135>
44. B.Kunwar., B.R.Moser, S.R.Chandrasekaran, N.Rajagopalan, B.K.Sharma. *Energy*, **111**, 884 (2016); <https://doi.org/10.1016/j.energy.2016.06.024>
45. I.Vollmer, M.J.Jenks, R.Mayorga González, F.Meirer, B.M.Weckhuysen. *Angew. Chem., Int. Ed. Engl.*, **60**, 16101 (2021); <https://doi.org/10.1002/anie.202104110>
46. J.G.Faillace, C.F.de Melo, S.P.L.de Souza, M.R.da Costa Marques. *J. Anal. Appl. Pyrolysis*, **126**, 70 (2017); <https://doi.org/10.1016/j.jaap.2017.06.023>
47. W.U.Eze, I.C.Madufor, G.N.Onyeagoro, H.C.Obasi, M.I.Ugbaja. *Polym. Bull.*, **78**, 377 (2021); <https://doi.org/10.1007/s00289-020-03116-4>
48. S.Attique, M.Batool, M.Yaqub, O.Görke, D.Gregory, A.Shah. *Waste Manag. Res.*, **38**, 689 (2020); <https://doi.org/10.1177/0734242X19899718>
49. A.K.Panda, A.Alotaibi, I.V.Kozhevnikov, N.R.Shiju. *Waste Biomass Valorization*, **11**, 6337 (2020); <https://doi.org/10.1007/s12649-019-00841-4>
50. M.N.Almustapha, M.Farooq, M.L.Mohammed, M.Farhan, M.Imran, J.M.Andresen. *Environ. Sci. Pollut. Res.*, **27**, 55 (2020); <https://doi.org/10.1007/s11356-019-04878-9>
51. J.Su, C.Fang, M.Yang, C.You, Q.Lin, X.Zhou, H.Li. *J. Anal. Appl. Pyrolysis*, **139**, 274 (2019); <https://doi.org/10.1016/j.jaap.2019.02.015>
52. J.Shah, M.R.Jan. *J. Anal. Appl. Pyrolysis*, **109**, 196 (2014); <https://doi.org/10.1016/j.jaap.2014.06.013>
53. A.L.Figueiredo, A.S.Araujo, M.Linares, A.Peral, R.A.García, D.P.Serrano, V.J.Fernandes Jr. *J. Anal. Appl. Pyrolysis*, **117**, 132 (2016); <https://doi.org/10.1016/j.jaap.2015.12.005>
54. B.Whajah, N.da Silva Moura, J.Blanchard, S.Wicker, K.Gandar, J.A.Dorman, K.M.Dooley. *Ind. Eng. Chem. Res.*, **60**, 15141 (2021); <https://doi.org/10.1021/acs.iecr.1c02674>
55. F.Zhang, M.Zeng, R.D.Yappert, J.Sun, Y.H.Lee, A.M.LaPointe, B.Peters, M.M.Abu-Omar, S.L.Scott. *Science*, **370**, 437 (2020); <https://doi.org/10.1126/science.abc5441>
56. C.Park, S.Kim, Y.Kwon, C.Jeong, Y.Cho, C.G.Lee, S.Jung, K.-Y.Choi, J.Lee. *Catalysts*, **10**, e496 (2020); <https://doi.org/10.3390/catal10060655>
57. J.M.Jung, S.H.Cho, S.Jung, K.Y.A.Lin, W.H.Chen, Y.F.Tsang, E.E.Kwon. *J. Hazard. Mater.*, **430**, e128454 (2022); <https://doi.org/10.1016/j.jhazmat.2022.128454>
58. R.-X.Yang, S.-L.Wu, S.-L., K.-H.Chuang, M.-Y.Wey. *Renew. Energy*, **159**, 10 (2020); <https://doi.org/10.1016/j.renene.2020.05.141>
59. X.Jie, W.Li, D.Slocombe, Y.Gao, I.Banerjee, S.Gonzalez-Cortes, B.Yao, H.AIMegren, S.Alshihri, J.Dilworth, J.Thomas, T.Xiao, P.Edwards. *Nat. Catal.*, **3**, 902 (2020); <https://doi.org/10.1038/s41929-020-00518-5>
60. H.Jiang, W.Liu, X.Zhang, J.Qiao. *Glob. Chall.*, **4**, e1900074 (2020); <https://doi.org/10.1002/gch2.201900074>
61. C.Alberti, S.Enthaler. *Waste Biomass Valorization*, **11**, 4621 (2020); <https://doi.org/10.1007/s12649-019-00794-8>
62. N.Cai, H.Yang, X.Zhang, S.Xia, D.Yao, P.Bartocci, F.Fantozzi, Y.Chen, H.Chen, P.T.Williams. *Waste Manag.*, **109**, 119 (2020); <https://doi.org/10.1016/j.wasman.2020.05.003>
63. G.Grause, R.Ka'rrbrant, T.Kameda, T.Yoshioka. *Ind. Eng. Chem. Res.*, **53**, 4215 (2014); <https://doi.org/10.1021/ie404263a>
64. X.Song, F.Liu, L.Li, X.Yang, S.Yu, X.Ge. *J. Hazard. Mater.*, **244**, 204 (2013); <https://doi.org/10.1016/j.jhazmat.2012.11.044>
65. W.Nabgan, B.Nabgan, T.A.T.Abdullah, M.Ikram, A.H.Jadhav, A.A.Jalil, M.W.Ali. *ACS Omega*, **7**, 3324 (2022); <https://doi.org/10.1021/acsomega.1c05488>
66. W.Nabgan, B.Nabgan, T.A.T.Abdullah, M.Ikram, A.H.Jadhav, M.W.Ali, A.A.Jalil. *Catal. Today*, **400**, 35 (2022); <https://doi.org/10.1016/j.cattod.2021.11.026>
67. W.Chen, J.Lu, C.Zhang, Y.Xie, Y.Wang, J.Wang, R.Zhang. *J. Anal. Appl. Pyrolysis*, **147**, e104800 (2020); <https://doi.org/10.1016/j.jaap.2020.104800>

68. A. Bin Jumah, V. Anbumuthu, A. A. Tedstone, A. A. Garforth. *Ind. Eng. Chem. Res.*, **58**, 20601 (2019); <https://doi.org/10.1021/acs.iecr.9b04263>
69. W.-T. Lee, F. D. Bobbink, A. P. van Muyden, K.-H. Lin, C. Corminboeuf, R. R. Zamani, P. J. Dyson. *Cell Rep. Phys. Sci.*, **2**, e100332 (2021); <https://doi.org/10.1016/j.xcrp.2021.100332>
70. G. R. M. Celik, R. A. Kennedy, M. Hackler, A. Ferrandon, S. Tennakoon, A. M. Patnaik, S. C. Lapointe, A. Ammal, F. A. Heyden, F. A. Perras, M. Pruski, S. L. Scott, K. R. Poepelmeier, A. D. Sadow, M. Delferro. *ACS Cent. Sci.*, **5**, 1795 (2019); <https://doi.org/10.1021/acscentsci.9b00722>
71. J. E. Rorrer, G. T. Beckham, Y. Román-Leshkov. *JACS Au*, **1**, 8 (2021); <https://doi.org/10.1021/jacsau.0c00041>
72. C. Jia, S. Xie, W. Zhang, N. N. Intan, J. Sampath, J. Pfaendtner, H. Lin. *Chem. Catal.*, **1**, 437 (2021); <https://doi.org/10.1016/j.checat.2021.04.002>
73. J. E. Rorrer, C. Troyano-Valls, G. T. Beckham, Y. Román-Leshkov. *ACS Sustain. Chem. Eng.*, **9**, 11661 (2021); <https://doi.org/10.1021/acssuschemeng.1c03786>
74. Y. Nakaji, M. Tamura, S. Miyaoka, S. Kumagai, M. Tanji, Y. Nakagawa, K. Tomishige. *Appl. Catal. B Environ.*, **285**, e119805 (2020); <https://doi.org/10.1016/j.apcatb.2020.119805>
75. L. Gausas, S. K. Kristensen, H. Sun, A. Ahrens, B. S. Donslund, A. T. Lindhardt, T. Skrydstrup. *JACS Au*, **1**, 517 (2021); <https://doi.org/10.1021/jacsau.1c00050>
76. E. M. Krall, T. W. Klein, R. J. Andersen, A. J. Nett, R. W. Glasgow, D. S. Reader, B. C. Dauphinais, S. P. Mc Ilrath, A. A. Fischer, M. J. Carney, D. J. Hudson, N. J. Robertson. *Chem. Commun. (Camb.)*, **50**, 4884 (2014); <https://doi.org/10.1039/c4cc00541d>
77. A. Kumar, N. von Wolff, M. Rauch, Y.-Q. Zou, G. Shmul, Y. Ben-David, G. Leitus, L. Avram, D. Milstein. *J. Am. Chem. Soc.*, **142**, 14267 (2020); <https://doi.org/10.1021/jacs.0c05675>
78. S. Westhues, J. Idel, J. Klankermayer. *Sci. Adv.*, **4**, eaat9669 (2018); <https://doi.org/10.1126/sciadv.aat9669>
79. Y. Li, M. Wang, X. Liu, C. Hu, D. Xiao, D. Ma. *Angew. Chem., Int. Ed. Engl.*, **61**, e202117205 (2022); <https://doi.org/10.1002/anie.202117205>
80. Y. Kratish, J. Li, S. Liu, Y. Gao, T. J. Marks. *Angew. Chem., Int. Ed. Engl.*, **59**, 19857 (2020); <https://doi.org/10.1002/anie.202007423>
81. Y. Wu, X. Wang, K. O. Kirlikovali, X. Gong, A. Atilgan, K. Ma, N. M. Schweitzer, N. C. Gianneschi, Z. Li, X. Zhang, O. K. Farha. *Angew. Chem., Int. Ed. Engl.*, **61**, e202117528 (2022); <https://doi.org/10.1002/anie.202117528>
82. L. Monsigny, J.-C. Berthet, T. Cantat. *ACS Sustain. Chem. Eng.*, **6**, e10481 (2018); <https://doi.org/10.1021/acssuschemeng.8b01842>
83. A. C. Fernandes. *ChemSusChem*, **14**, 4228 (2021); <https://doi.org/10.1002/cssc.202100130>
84. E. Feghali, T. Cantat. *ChemSusChem*, **8**, 980 (2015); <https://doi.org/10.1002/cssc.201500054>
85. F. Miao, Y. Liu, M. Gao, X. Yu, P. Xiao, M. Wang, S. Wang, X. Wang. *J. Hazard. Mater.*, **399**, e123023 (2020); <https://doi.org/10.1016/j.jhazmat.2020.123023>
86. Y. Li, S. Wan, C. Lin, Y. Gao, Y. Lu, L. Wang, K. Zhang. *Sol. RRL*, **5**, e2000427 (2021); <https://doi.org/10.1002/solr.202000427>
87. J. Xu, X. Jiao, K. Zheng, W. Shao, S. Zhu, X. Li, J. Zhu, Y. Pan, Y. Sun, Y. Xie. *Natl. Sci. Rev.*, **9**, nwac011 (2022); <https://doi.org/10.1093/nsr/nwac011>
88. X. Jiao, K. Zheng, Q. Chen, X. Li, Y. Li, W. Shao, J. Xu, J. Zhu, Y. Pan, Y. Sun, Y. Xie. *Angew. Chem., Int. Ed. Engl.*, **59**, 15497 (2020); <https://doi.org/10.1002/anie.201915766>
89. L. P. Domínguez-Jaimes, E. I. Cedillo-González, E. Luévano-Hipólito, J. D. Acuña-Bedoya, J. M. Hernández-López. *J. Hazard. Mater.*, **413**, e125452 (2021); <https://doi.org/10.1016/j.jhazmat.2021.125452>
90. P. H. Allé, P. Garcia-Muñoz, K. Adouby, N. Keller, D. Robert. *Environ. Chem. Lett.*, **19**, 1803 (2021); <https://doi.org/10.1007/s10311-020-01099-2>
91. Z. Huang, M. Shanmugam, Z. Liu, A. Brookfield, E. L. Bennett, R. Guan, D. E. Vega Herrera, J. A. Lopez-Sanchez, A. G. Slater, E. G. L. McInnes, X. Qi, J. Xiao. *J. Am. Chem. Soc.*, **144**, 6532 (2022); <https://doi.org/10.1021/jacs.2c08951>
92. C. F. Chow, W. L. Wong, K. Y. Ho, C. S. Chan, C. B. Gong. *Chem. – Eur. J.*, **22**, 9513 (2016); <https://doi.org/10.1002/chem.201600856>
93. C. F. Chow, W. L. Wong, C. W. Chan, C. S. Chan. *Waste Manage.*, **75**, 174 (2018); <https://doi.org/10.1016/j.wasman.2018.01.034>
94. K. Hu, P. Zhou, Y. Yang, T. Hall, G. Nie, Y. Yao, X. Duan, S. Wang. *ACS EST Eng.*, **2**, 110 (2021); <https://doi.org/10.1021/acsestengg.1c00323>
95. Y. Lai, X. Sheng, L. Dong, P. Li, Q. Li, S. Yu, Q. Zhou, J. Liu. *Anal. Chem.*, **93**, 11184 (2021); <https://doi.org/10.1021/acs.analchem.1c01727>
96. Z. Ouyang, S. Li, M. Zhao, Q. Wangmu, R. Ding, C. Xiao, X. Guo. *J. Hazard. Mater.*, **424**, e127461 (2022); <https://doi.org/10.1016/j.jhazmat.2021.127461>
97. E. Backstrom, K. Odellius, M. Hakkarainen. *Ind. Eng. Chem. Res.*, **56**, 14814 (2017); <https://doi.org/10.1021/acs.iecr.7b04091>
98. C. Jehanno, J. Demarteau, D. Mantione, M. C. Arno, F. Ruiperez, J. L. Hedrick, A. P. Dove, H. Sardon. *Angew. Chem., Int. Ed. Engl.*, **60**, 6710 (2021); <https://doi.org/10.1002/anie.202014860>
99. C. Alberti, K. Matthiesen, M. Wehrmeister, S. Bycinskij, S. Enthaler. *ChemistrySelect*, **6**, 7972 (2021); <https://doi.org/10.1002/slct.202102427>
100. X. Qu, G. Zhou, R. Wang, B. Yuan, M. Jiang, J. Tang. *Green Chem.*, **23**, 1871 (2021); <https://doi.org/10.1039/D0GC04019C>
101. Z. Jiang, D. Yan, J. Xin, F. Li, M. Guo, Q. Zhou, J. Xu, Y. Hu, X. Lu. *Polym. Degrad. Stab.*, **199**, e109905 (2022); <https://doi.org/10.1016/j.polymdegradstab.2022.109905>
102. L. A. Román-Ramírez, P. Mckeown, M. D. Jones, J. Wood. *ACS Catal.*, **9**, 409 (2018); <https://doi.org/10.1021/acscatal.8b04863>
103. P. McKeown, L. A. Román-Ramírez, S. Bates, J. Wood, M. D. Jones. *ChemSusChem*, **12**, 5233 (2019); <https://doi.org/10.1002/cssc.201902755>
104. M. Fuchs, M. Walbeck, E. Jagla, A. Hoffmann, S. Herres-Pawlis. *ChemPlusChem*, **87**, e202200029 (2022); <https://doi.org/10.1002/cplu.202200029>
105. J. R. Fernandes, L. P. Amaro, E. C. Muniz, S. L. Favaro, E. Radovanovic. *J. Supercrit. Fluids*, **158**, e104715 (2020); <https://doi.org/10.1016/j.supflu.2019.104715>
106. C. Jehanno, I. Flores, A. P. Dove, A. J. Muller, F. Ruiperez, H. Sardon. *Green Chem.*, **20**, 1205 (2018); <https://doi.org/10.1039/C7GC03396F>
107. T. Wang, C. Shen, G. Yu, X. Chen. *Polym. Degrad. Stab.*, **203**, e110050 (2022); <https://doi.org/10.1016/j.polymdegradstab.2022.110050>
108. Y. Liu, X. Yao, H. Yao, Q. Zhou, J. Xin, X. Lu, S. Zhang. *Green Chem.*, **22**, 3122 (2020); <https://doi.org/10.1039/D0GC00327A>
109. L. N. T. Ho, D. M. Ngo, J. Cho, H. M. Jung. *Polym. Degrad. Stab.*, **155**, 15 (2018); <https://doi.org/10.1016/j.polymdegradstab.2018.07.003>
110. B. Liu, X. Lu, Z. Ju, P. Sun, J. Xin, X. Yao, Q. Zhou, S. Zhang. *Ind. Eng. Chem. Res.*, **57**, 16239 (2018); <https://doi.org/10.1021/acs.iecr.8b03854>
111. F. Chen, G. Wang, C. Shi, Y. Zhang, L. Zhang, W. Li, F. Yang. *J. Appl. Polym. Sci.*, **127**, 2809 (2013); <https://doi.org/10.1002/app.37608>
112. S. Chaudhary, P. Surekha, D. Kumar, C. Rajagopal, P. K. Roy. *Appl. Polym. Sci.*, **129**, 2779 (2013); <https://doi.org/10.1002/app.38970>
113. L. Deng, R. Li, Y. Chen, J. Wang, H. Song. *J. Mol. Liq.*, **334**, e116419 (2021); <https://doi.org/10.1016/j.molliq.2021.116419>

114. M.Zhu, S.Li, Z.Li, X.Lu, S.Zhang. *Chem. Eng. J.*, **185**–**186**, 168 (2012); <https://doi.org/10.1016/j.cej.2012.01.068>
115. Q.F.Yue, L.F.Xiao, M.L.Zhang, X.F.Bai. *Polymers*, **5**, 1258 (2013); <https://doi.org/10.3390/polym5041258>
116. Q.Wang, X.Lu, X.Zhou, M.Zhu, H.He, X.Zhang. *J. Appl. Polym. Sci.*, **129**, 3574 (2013); <https://doi.org/10.1002/app.38706>
117. Q.Wang, Y.Geng, X.Lu, S.Zhang. *ACS Sustain. Chem. Eng.*, **3**, 340 (2015); <https://doi.org/10.1021/sc5007522>
118. C.Shuangjun, S.Weih, C.Haidong, Z.Hao, Z.Zhenwei, F.Chaonan. *J. Therm. Anal. Calorim.*, **143**, 3489 (2021); <https://doi.org/10.1007/s10973-020-10331-8>
119. A.M.Al-Sabagh, F.Z.Yehia, A.M.F.Eissa, M.E.Moustafa, G.Eshaq, A.M.Rabie, A.E.Elmetwally. *Polym. Degrad. Stab.*, **110**, 364 (2014); <https://doi.org/10.1016/j.polymdegradstab.2014.10.005>
120. L.Wang, G.A.Nelson, J.Toland, J.D.Holbrey. *ACS Sustain. Chem. Eng.*, **8**, 13362 (2020); <https://doi.org/10.1021/acssuschemeng.0c04108>
121. A.M.Al-Sabagh, F.Z.Yehia, A.-M.M.F.Eissa, M.E.Moustafa, G.Eshaq, A.R.M.Rabie, A.E.Elmetwally. *Ind. Eng. Chem. Res.*, **53**, 18443 (2014); <https://doi.org/10.1021/ie503677w>
122. T.L.Wang, C.C.Shen, G.R.Yu, X.C.Chen. *Polym. Degrad. Stab.*, **194**, e109751 (2021); <https://doi.org/10.1016/j.polymdegradstab.2021.109751>
123. M.Imran, W.A.Al-Masry, A.Mahmood, A.Hassan, S.Haider, S.M.Ramay. *Polym. Degrad. Stab.*, **98**, 904 (2013); <https://doi.org/10.1016/j.polymdegradstab.2013.01.007>
124. G.H.Eshaq, A.E.Elmetwally. *J. Mol. Liq.*, **214**, 1 (2016); <https://doi.org/10.1016/j.molliq.2015.11.049>
125. A.Bahramian. *Polym. Degrad. Stab.*, **179**, e109243 (2020); <https://doi.org/10.1016/j.polymdegradstab.2020.109243>
126. F.F.Chen, G.H.Wang, W.Li, F.Yang. *Ind. Eng. Chem. Res.*, **52**, 565 (2013); <https://doi.org/10.1021/ie302091j>
127. Y.Geng, T.Dong, P.Fang, Q.Zhou, X.Lu, S.Zhang. *Polym. Degrad. Stab.*, **117**, 30 (2015); <https://doi.org/10.1016/j.polymdegradstab.2015.03.019>
128. L.X.Yun, H.Wu, Z.G.Shen, J.W.Fu, J.X.Wang. *ACS Sustain. Chem. Eng.*, **10**, 5278 (2022); <https://doi.org/10.1021/acssuschemeng.2c00480>
129. L.Bartolome, M.Imran, K.G.Lee, A.Sangalang, J.K.Ahn. *Green Chem.*, **16**, 279 (2014); <https://doi.org/10.1039/C3GC41834K>
130. A.M.Al-Sabagh, F.Z.Yehia, D.R.K.Harding, G.Eshaq, A.E.Elmetwally. *Green Chem.*, **18**, 3997 (2016); <https://doi.org/10.1039/C6GC00534A>
131. G.R.Lima, W.F.Monteiro, B.O.Toledo, R.A.Ligabue, R.M.C.Santana. *Macromol. Symp.*, **383**, e1800008 (2019); <https://doi.org/10.1002/masy.201800008>
132. F.R.Veregue, C.T.P.da Silva, M.P.Moisés, J.G.Meneguin, M.R.Guilherme, P.A.Arroyo, S.L.Favaro, E.Radovanovic, E.M.Girotto, A.W.Rinaldi. *ACS Sustain. Chem. Eng.*, **6**, 12017 (2018); <https://doi.org/10.1021/acssuschemeng.8b02294>
133. G.Park, L.Bartolome, K.G.Lee, S.J.Lee, D.H.Kim, T.J.Park. *Nanoscale*, **4**, 3879 (2012); <https://doi.org/10.1039/c2nr30168g>
134. I.Cano, C.Martin, J.A.Fernandes, R.W.Lodge, J.Dupont, F.A.Casado-Carmona, R.Lucena, S.Cardenas, V.Sans, I.de Pedro. *Appl. Catal. B: Environ.*, **260**, e118110 (2020); <https://doi.org/10.1016/j.apcatb.2019.118110>
135. T.Wang, C.Shen, G.Yu, X.Chen. *Fuel*, **304**, e121397 (2021); <https://doi.org/10.1016/j.fuel.2021.121397>
136. Q.Suo, J.Zi, Z.Bai, S.Qi. *Catal. Lett.*, **147**, 240 (2017); <https://doi.org/10.1007/s10562-016-1897-0>
137. R.X.Yang, Y.T.Bieh, C.H.Chen, C.-Y.Hsu, Y.Kato, H.Yamamoto, C.-K.Tsung, K.C.W.Wu. *ACS Sustain. Chem. Eng.*, **9**, 6541 (2021); <https://doi.org/10.1021/acssuschemeng.0c08012>
138. Y.Liu, Q.Zhong, P.Xu, H.Huang, F.Yang, M.Cao, L.He, Q.Zhang, J.Chen. *Matter*, **5**, 1305 (2022); <https://doi.org/10.1016/j.matt.2022.02.002>
139. N.George, T.Kurian. *Prog. Rubber Plast. Recycl. Technol.*, **32**, 153 (2016); <https://doi.org/10.1177/147776061603200304>
140. K.Fukushima, J.M.Lecuyer, D.S.Wei, H.W.Horn, G.O.Jones, H.A.Al-Megren, A.M.Alabulrahman, F.D.Alsewailam, M.A.McNeil, J.E.Rice, J.L.Hedrick. *Polym. Chem.*, **4**, 1610 (2013); <https://doi.org/10.1039/C2PY20793A>
141. K.Fukushima, G.O.Jones, H.W.Horn, J.E.Rice, T.Kato, J.L.Hedrick. *Polym. Chem.*, **11**, 4904 (2020); <https://doi.org/10.1039/D0PY00436G>
142. V.Vinitha, M.Preeyanghaa, M.Anbarasu, G.Jeya, B.Neppolian, V.Sivamurugan. *J. Polym. Environ.*, **30**, 3566 (2022); <https://doi.org/10.1007/s10924-022-02455-9>
143. H.I.Khalaf, O.A.Hasan. *Chem. Eng. J.*, **192**, 45 (2012); <https://doi.org/10.1016/j.cej.2012.03.081>
144. N.R.Paliwal, A.K.Mungray. *Polym. Degrad. Stab.*, **98**, 2094 (2013); <https://doi.org/10.1016/j.polymdegradstab.2013.06.030>
145. H.Zhou, Y.Ren, Z.Li, M.Xu, Y.Wang, R.Ge, X.Kong, L.Zheng, H.Duan. *Nat. Commun.*, **12**, e4679 (2021); <https://doi.org/10.1038/s41467-021-23548-4>
146. T.Uekert, H.Kasap, E.Reisner. *J. Am. Chem. Soc.*, **141**, 15201 (2019); <https://doi.org/10.1021/jacs.9b06872>
147. X.K.Li, H.Lu, W.Z.Guo, G.P.Cao, H.L.Liu, Y.H.Shi. *AIChE J.*, **61**, 200 (2015); <https://doi.org/10.1002/aic.14632>
148. G.N.Ricarte, M.L.Dias, L.Sirelli, M.A.P.Langone, A.M.de Castro, M.A.Z.Coelho, B.D.Ribeiro. *J. Chem. Technol. Biotechnol.*, **96**, 3237 (2021); <https://doi.org/10.1002/jctb.6882>
149. H.T.Kim, M.H.Ryu, Y.J.Jung, S.Lim, H.M.Song, J.Park, S.Y.Hwang, H.-S.Lee, Y.J.Yeon, B.H.Sung, U.T.Bornscheuer, S.J.Park, J.C.Joo, D.X.Oh. *ChemSusChem*, **14**, 4251 (2021); <https://doi.org/10.1002/cssc.202100909>
150. A.G.Okunev, E.V.Parkhomchuk, A.I.Lysikov, P.D.Parunin, V.S.Semeykina, V.N.Parmon. *Russ. Chem. Rev.*, **84**, 981 (2015) [*YcØexù xüüü*, **84**, 981 (2015)]; <https://doi.org/10.1070/RCR4486>
151. F.Radford, L.M.Zapata-Restrepo, A.A.Horton, M.D.Hudson, P.J.Shaw, I.D.Williams. *Anal. Methods*, **13**, 1695 (2021); <https://doi.org/10.1039/D0AY02086A>
152. I.V.Sedov, P.E.Matkovskiy. *Russ. Chem. Rev.*, **81**, 239 (2012); <https://doi.org/10.1070/RC2012v081n03ABEH004226>
153. V.V.Butova, M.A.Soldatov, A.A.Guda, K.A.Lomachenko, C.Lamberti. *Russ. Chem. Rev.*, **85**, 280 (2016); <https://doi.org/10.1070/RCR4554>
154. N.Mohanan, Z.Montazer, P.K.Sharma, D.B.Levin. *Front. Microbiol.*, **11**, e580709 (2020); <https://doi.org/10.3389/fmicb.2020.580709>
155. R.Wie, W.Zimmermann. *Microb. Biotechnol.*, **10**, 1308 (2017); <https://doi.org/10.1111/1751-7915.12710>
156. P.Wagner-Egea, V.Tosi, P.Wang, C.Grey, B.Zhang, J.A.Linares-Pastén. *Appl. Sci.*, **11**, e8315 (2021); <https://doi.org/10.3390/app11188315>
157. S.Yoshida, K.Hiraga, I.Taniguchi, K.Oda. *Methods Enzymol.*, **648**, 187 (2021); <https://doi.org/10.1016/bs.mie.2020.12.007>
158. M.Furukawa, N.Kawakami, K.Oda, K.Miyamoto. *ChemSusChem*, **11**, 4018 (2018); <https://doi.org/10.1002/cssc.201802096>
159. S.Yoshida, K.Hiraga, T.Takehana, I.Taniguchi, H.Yamaji, Y.Maeda, K.Toyohara, K.Miyamoto, Y.Kimura, K.Oda. *Science*, **351**, 1196 (2016); <https://doi.org/10.1126/science.aad6359>
160. L.Shi, H.Liu, S.Gao, Y.Weng, L.Zhu. *J. Agric. Food Chem.*, **69**, 2245 (2021); <https://doi.org/10.1021/acs.jafc.0c07469>
161. H.Seo, S.Kim, H.F.Son, H.Y.Sagong, S.Joo, K.J.Kim. *Biochem. Biophys. Res. Commun.*, **508**, 250 (2019); <https://doi.org/10.1016/j.bbrc.2018.11.087>

162. B.C.Knott, E.Erickson, M.D.Allen, J.E.Gado, R.Graham, F.L.Kearns, I.Pardo, E.Topuzlu, J.J.Anderson, H.P.Austin, G.Dominick, C.W.Johnson, N.A.Rorrer, C.J.Szostkiewicz, V.Copie, C.M.Payne, H.L.Woodcock, B.S.Donohoe, G.T.Beckham, J.E.McGeehan. *Proc. Natl. Acad. Sci. USA*, **117**, 25476 (2020); <https://doi.org/10.1073/pnas.2006753117>
163. B.Guo, S.R.Vanga, X.Lopez-Lorenzo, P.Saenz-Mendez, S.R.Ericsson, Y.Fang, X.Ye, K.Schriever, E.Backstrom, A.Biundo, R.A.Zubarev, I.Furo, M.Hakkarainen, P.O.Syrén. *ACS Catal.*, **12**, 3397 (2022); <https://doi.org/10.1021/acscatal.1c05548>
164. B.Liu, L.He, L.Wang, T.Li, C.Li, H.Liu, Y.Luo, R.Bao. *ChemBioChem*, **19**, 1471 (2018); <https://doi.org/10.1002/cbic.201800097>
165. S.Joo, I.J.Cho, H.Seo, H.F.Son, H.-Y.Sagong, T.J.Shin, S.Y.Choi, S.Y.Lee, K.-J.Kim. *Nat. Commun.*, **9**, e382 (2018); <https://doi.org/10.1038/s41467-018-02881-1>
166. E.Erickson, T.J.Shakespeare, F.Bratti, B.L.Buss, R.Graham, M.A.Hawkins, G.Konig, W.E.Michener, J.Miscall, K.J.Ramirez, N.A.Rorrer, M.Zahn, A.R.Pickford, J.E.McGeehan, G.T.Beckham. *ChemSusChem*, **15**, e202101932 (2022); <https://doi.org/10.1002/cssc.202101932>
167. F.Son, S.Joo, H.Seo, H.Y.Sagong, S.H.Lee, H.Hong, K.-J.Kim. *Enzyme Microb. Technol.*, **141**, e109656 (2020); <https://doi.org/10.1016/j.enzmictec.2020.109656>
168. S.F.Badino, J.A.Bååth, K.Borch, K.Jensen, P.Westh. *Enzyme Microb. Technol.*, **152**, e109937 (2021); <https://doi.org/10.1016/j.enzmictec.2021.109937>
169. H.F.Son, I.J.Cho, S.Joo, H.Seo, H.Y.Sagong, S.Y.Choi, S.Y.Lee, K.-J.Kim. *ACS Catal.*, **9**, 3519 (2019); <https://doi.org/10.1021/acscatal.9b00568>
170. H.Y.Sagong, H.Seo, T.Kim, H.F.Son, S.Joo, S.H.Lee, J.-S.Woo, S.Y.Hwang, K.-J.Kim. *ACS Catal.*, **10**, 4805 (2020); <https://doi.org/10.1021/acscatal.9b05604>
171. Y.Liu, Z.Liu, Z.Guo, T.Yan, C.Jin, J.Wu. *Sci. Total Environ.*, **834**, e154947 (2022); <https://doi.org/10.1016/j.scitotenv.2022.154947>
172. H.Lu, D.J.Diaz, N.J.Czarnecki, C.Zhu, W.Kim, R.Shroff, D.J.Acosta, B.R.Alexander, H.O.Cole, Y.Zhang, N.A.Lynd, A.D.Ellington, H.S.Alper. *Nature (London)*, **604**, 662 (2022); <https://doi.org/10.1038/s41586-022-04599-z>
173. E.Z.L.Zhong-Johnson, C.A.Voigt, A.J.Sinskey. *Sci. Rep.*, **11**, e928 (2021); <https://doi.org/10.1038/s41598-020-79031-5>
174. S.Brott, L.Pfaff, J.Schuricht, J.-N.Schwarz, D.Böttcher, C.P.S.Badenhorst, R.Wei, U.T.Bornscheuer. *Eng. Life Sci.*, **22**, 192 (2022); <https://doi.org/10.1002/elsc.202100105>
175. L.Dai, Y.Qu, J.-W.Huang, Y.Hu, H.Hu, S.Li, C.-C.Chen, R.-T.Guo. *J. Biotechnol.*, **334**, 47 (2021); <https://doi.org/10.1016/j.jbiotec.2021.05.006>
176. K.Chen, M.Quan, X.Dong, Q.Shi, Y.Sun. *Biochem. Eng. J.*, **175**, e108151 (2021); <https://doi.org/10.1038/s41928-021-00560-6>
177. K.Chen, Y.Hu, X.Dong, Y.Sun. *ACS Catal.*, **11**, 7358 (2021); <https://doi.org/10.1021/acscatal.1c01062>
178. N.Puspitasari, S.-L.Tsai, C.-K.Lee. *Int. J. Biol. Macromol.*, **176**, 157 (2021); <https://doi.org/10.1016/j.jbiomac.2021.02.026>
179. L.Cui, Y.Qiu, Y.Liang, C.Du, W.Dong, C.Cheng, B.He. *Int. J. Biol. Macromol.*, **188**, 568 (2021); <https://doi.org/10.1016/j.jbiomac.2021.08.012>
180. L.Dai, Y.Qu, Y.Hu, J.Min, X.Yu, C.-C.Chen, J.-W.Huang, R.-T.Guo. *Int. J. Biol. Macromol.*, **190**, 456 (2021); <https://doi.org/10.1016/j.jbiomac.2021.09.005>
181. M.Barth, T.Oeser, R.Wei, J.Then, J.Schmidt, W.Zimmermann. *Biochem. Eng. J.*, **93**, 222 (2015); <https://doi.org/10.1016/j.bej.2014.10.012>
182. R.Wei, T.Oeser, J.Schmidt, R.Meier, M.Barth, J.Then, W.Zimmermann. *Biotechnol. Bioeng.*, **113**, 1658 (2016); <https://doi.org/10.1002/bit.25941>
183. M.Furukawa, N.Kawakami, A.Tomizawa, K.Miyamoto. *Sci. Rep.*, **9**, e16038 (2019); <https://doi.org/10.1038/s41598-019-52379-z>
184. X.-Q.Chen, Z.-Y.Guo, L.Wang, Z.-F.Yan, C.-X.Jin, Q.-S.Huang, D.-M.Kong, D.-M.Rao, J.Wu. *J. Hazard. Mater.*, **433**, e128816 (2022); <https://doi.org/10.1016/j.jhazmat.2022.128816>
185. Q.Li, Y.Zheng, T.Su, Q.Wang, Q.Liang, Z.Zhang, Q.Qi, J.Tian. *Comput. Struct. Biotechnol. J.*, **20**, 459 (2022); <https://doi.org/10.1016/j.csbj.2021.12.042>
186. Z.Liu, Y.Zhang, J.Wu. *Enzyme Microb. Technol.*, **156**, e110004 (2022); <https://doi.org/10.1016/j.enzmictec.2022.110004>
187. J.A.Bååth, K.Jensen, K.Borch, P.Westh, J.Kari. *JACS Au*, **2**, 1223 (2022); <https://doi.org/10.1021/jacsau.2c00204>
188. A.N.Shirke, C.White, J.A.Englaender, A.Zwarycz, G.L.Butterfoss, R.J.Linhardt, R.A.Gross. *Biochemistry*, **57**, 1190 (2018); <https://doi.org/10.1021/acs.biochem.7b01189>
189. R.K.Brizendine, E.Erickson, S.J.Haugen, K.J.Ramirez, J.Miscall, D.Salvachúa, A.R.Pickford, M.J.Sobkowicz, J.E.McGeehan, G.T.Beckham. *ACS Sustain. Chem. Eng.*, **10**, 9131 (2022); <https://doi.org/10.1021/acssuschemeng.2c01961>
190. A.C.Chang, A.Patel, S.Perry, Y.V.Soong, C.Ayafar, H.W.Wong, D.Xie, M.J.Sobkowicz. *Macromol. Rapid Commun.*, **43**, e2100929 (2022); <https://doi.org/10.1002/marc.202270069>
191. V.Tournier, C.M.Topham, A.Gilles, B.David, C.Folgoas, E.Moya-Leclair, E.Kamionka, M.-L.Desrousseaux, H.Texier, S.Gavalda, M.Cot, E.Guémard, M.Dalibey, J.Nomme, G.Cioci, S.Barbe, M.Chateau, I.André, S.Duquesne, A.Marty. *Nature (London)*, **580**, 216 (2020); <https://doi.org/10.1038/s41586-020-2149-4>
192. J.C.Sadler, S.Wallace. *Green Chem.*, **23**, 4665 (2021); <https://doi.org/10.1039/D1GC00931A>
193. R.Xue, Y.Chen, H.Rong, R.Wei, Z.Cui, J.Zhou, W.Dong, M.Jiang. *Front. Bioeng. Biotechnol.*, **9**, e762854 (2021); <https://doi.org/10.3389/fbioe.2021.762854>
194. F.Kawai, M.Oda, T.Tamashiro, T.Waku, N.Tanaka, M.Yamamoto, H.Mizushima, T.Miyakawa, M.Tanokura. *Appl. Microbiol. Biotechnol.*, **98**, 10053 (2014); <https://doi.org/10.1007/s00253-014-5860-y>
195. M.Oda, Y.Yamagami, S.Inaba, I.Oida, M.Yamamoto, S.Kitajima, F.Kawai. *Appl. Microbiol. Biotechnol.*, **102**, 10067 (2018); <https://doi.org/10.1007/s00253-018-9374-x>
196. S.Weinberger, J.Canadell, F.Quartinello, B.Yeniad, A.Arias, A.Pellis, G.M.Guebitz. *Catalysts*, **7**, e318 (2017); <https://doi.org/10.3390/catal7110318>
197. A.Pellis, K.Haernvall, C.M.Pichler, G.Ghazaryan, R.Breinbauer, G.M.Guebitz. *J. Biotechnol.*, **235**, 47 (2016); <https://doi.org/10.1016/j.jbiotec.2016.02.006>
198. K.Haernvall, S.Zitzenbacher, H.Amer, M.T.Zumstein, M.Sander, K.McNeill, M.Yamamoto, M.B.Schick, D.Ribitsch, G.M.Guebitz. *Biotechnol. J.*, **12**, e1600741 (2017); <https://doi.org/10.1002/biot.201600741>
199. V.Perz, K.Bleymaier, C.Sinkel, U.Kueper, M.Bonnekessel, D.Ribitsch, G.M.Guebitz. *New Biotechnol.*, **33**, 295 (2016); <https://doi.org/10.1016/j.nbt.2015.11.004>
200. J.A.Bååth, V.Novy, L.V.Carneiro, G.M.Guebitz, L.Olsson, P.Westh, D.Ribitsch. *Biotechnol. Bioeng.*, **119**, 470 (2016); <https://doi.org/10.1002/bit.27984>
201. C.Gamerith, B.Zartl, A.Pellis, F.Guillamot, A.Marty, E.H.Acero, G.M.Guebitz. *Process Biochem.*, **59**, 58 (2017); <https://doi.org/10.1016/j.procbio.2017.01.004>
202. C.Gamerith, M.Vastano, S.M.Ghorbanpour, S.Zitzenbacher, D.Ribitsch, M.T.Zumstein, M.Sander, E.H.Acero, A.Pellis, G.M.Guebitz. *Front. Microbiol.*, **8**, e938 (2017); <https://doi.org/10.3389/fmicb.2017.00938>
203. V.Perz, M.T.Zumstein, M.Sander, S.Zitzenbacher, D.Ribitsch, G.M.Guebitz. *Biomacromolecules*, **16**, 3889 (2015); <https://doi.org/10.1021/acs.biomac.5b01219>
204. A.Pellis, C.Gamerith, G.Ghazaryan, A.Ortner, E.H.Acero, G.M.Guebitz. *Bioresour. Technol.*, **218**, 1298 (2016); <https://doi.org/10.1016/j.biortech.2016.07.106>

205. D.Ribitsch, A.Hromic, S.Zitzenbacher, B.Zartl, C.Gamerith, A.Pellis, A.Jangbauer, A.Lyskowski, G.Steinkellner, K.Gruber, R.Tscheliessnig, E.H.Acero, G.M.Guebitz. *Biotechnol. Bioeng.*, **114**, 2481 (2017); <https://doi.org/10.1002/bit.26372>
206. A.Carniel, A.D.C.Gomes, M.A.Z.Coelho, A.M.de Castro. *Bioprocess Biosyst. Eng.*, **44**, 507 (2021); <https://doi.org/10.1007/s00449-020-02461-y>
207. A.M.de Castro, A.Carniel, S.M.Menezes, L.S.C.Júnior, H.de Honorato, A.P.Lima, E.G.Chaves. *J. Chem. Technol. Biotechnol.*, **97**, 709 (2022); <https://doi.org/10.1002/jctb.6955>
208. S.Kaabel, J.P.D.Therien, C.E.Deschênes, D.Duncan, T.Frišćić, K.Auclair. *Proc. Nat. Acad. Sci. USA*, **118**, e2026452118 (2021); <https://doi.org/10.1073/pnas.2026452118>
209. E.de Queiros Eugenio, I.S.P.Campisano, A.M.de Castro, M.A.Z.Coelho, M.A.P.Langone. *J. Biotechnol.*, **341**, 76 (2021); <https://doi.org/10.1016/j.jbiotec.2021.09.007>
210. A.M.de Castro, A.Carniel, D.Stahelin, L.S.C.Júnior, H.de Honorato, S.M.C.de Menezes. *Proc. Biochem.*, **81**, 85 (2019); <https://doi.org/10.1016/j.procbio.2019.03.006>
211. E.Q.Eugenio, I.S.P.Campisano, A.M.de Castro, M.A.Z.Coelho, M.A.P.Langone. *J. Polym. Environ.*, **30**, 1627 (2022); <https://doi.org/10.1007/s10924-021-02301-4>
212. L.Dutra, M.C.C.Pinto, R.C.Lima, M.Franco, M.Viana, E.P.Cipolatti, E.A.Manoel, D.M.G.Freire, J.C.Pinto. *J. Polym. Environ.*, **30**, 1893 (2022); <https://doi.org/10.1007/s10924-021-02313-0>
213. A.Carniel, E.Valoni, J.N.Júnior, A.G.da Conceição, A.M.de Castro. *Proc. Biochem.*, **59**, 84 (2017); <https://doi.org/10.1016/j.procbio.2016.07.023>
214. A.M.de Castro, A.Carniel, J.N.Júnior, A.G.da Conceição, E.Valoni. *J. Ind. Microbiol. Biotechnol.*, **44**, 835 (2017); <https://doi.org/10.1007/s10295-017-1942-z>
215. F.Quartinello, S.Vajnhandl, J.V.Valh, T.J.Farmer, B.Vončina, A.Lobnik, E.H.Acero, A.Pellis, G.M.Guebitz. *J. Microbiol. Biotechnol.*, **10**, 1376 (2017); <https://doi.org/10.1111/1751-7915.12734>
216. J.A.Bååth, K.Borch, P.Westh. *Anal. Biochem.*, **607**, e113873 (2020); <https://doi.org/10.1016/j.ab.2020.113873>
217. J.A.Bååth, K.Borch, K.Jensen, J.Brask, P.Westh. *ChemBioChem*, **22**, 1627 (2021); <https://doi.org/10.1002/cbic.202000793>
218. A.F.Greene, A.Vaid, C.Collet, K.R.Wade, M.Patel, M.Gaugler, M.West, M.Petcu, K.Parker. *Biomacromolecules*, **22**, 1999 (2021); <https://doi.org/10.1021/acs.biomac.1c00105>
219. A.Nakamura, N.Kobayashi, N.Koga, R.Iino. *ACS Catal.*, **11**, 8550 (2021); <https://doi.org/10.1021/acscatal.1c01204>
220. A.N.Shirke, D.Basore, S.Holton, A.Su, E.Baugh, G.L.Butterfoss, G.Makhatadze, C.Bystroff, R.A.Gross. *Appl. Microbiol. Biotechnol.*, **100**, 4435 (2016); <https://doi.org/10.1007/s00253-015-7254-1>
221. A.N.Shirke, D.Basore, G.L.Butterfoss, R.Bonneau, C.Bystroff, R.A.Gross. *Proteins Struct. Funct. Genet.*, **84**, 60 (2016); <https://doi.org/10.1002/prot.24955>
222. H.Zhang, P.Perez-Garcia, R.F.Dierkes, V.Applegate, J.Schumacher, C.M.Chibani, S.Sternagel, L.Preuss, S.Weigert, C.Schmeisser, D.Danso, J.Pleiss, A.Almeida, B.Höcker, S.J.Hallam, R.A.Schmitz, S.H.J.Smits, J.Chow, W.R.Streit. *Front. Microbiol.*, **12**, e803896 (2021); <https://doi.org/10.3389/fmicb.2021.801257>
223. X.Xi, K.Ni, H.Hao, Y.Shang, B.Zhao, Z.Qian. *Enzym. Microb. Technol.*, **143**, e109715 (2021); <https://doi.org/10.1016/j.enzmictec.2020.109715>
224. H.-Y.Sagong, S.Kim, D.Lee, H.Hong, S.H.Lee, H.Seo, K.-J.Kim. *J. Hazard. Mater.*, **429**, e128267 (2022); <https://doi.org/10.1016/j.jhazmat.2022.128267>
225. C.-C.Chen, X.Han, X.Li, P.Jiang, D.Niu, L.Ma, W.Liu, S.Li, Y.Qu, H.Hu, J.Min, Y.Yang, L.Zhang, W.Zeng, J.-W.Huang, L.Dai, R.-T.Guo. *Nat. Catal.*, **4**, 425 (2021); <https://doi.org/10.1038/s41929-021-00616-y>
226. A.Bollinger, S.Thies, E.Knieps-Grünhagen, C.Gertzen, S.Kobus, A.Hoppner, M.Ferrer, H.Gohlke, S.H.Smits, K.-E.Jaeger. *Front. Microbiol.*, **11**, e114 (2020); <https://doi.org/10.3389/fmicb.2020.00114>
227. I.E.M.Cifuentes, P.Wu, Y.Zhao, W.Liu, M.N.Schaal, L.Pfaff, J.Barys, Z.Li, J.Gao, X.Han, U.T.Bornscheuer, R.Wei, B.Ozturk. *Front. Bioeng. Biotechnol.*, **10**, e930140 (2022); <https://doi.org/10.3389/fbioe.2022.930140>
228. B.Eiamthong, P.Meesawat, T.Wongsatit, J.Jitdee, R.Sangsri, M.Patchesung, K.Aphicho, S.Suraritdechachai, N.H.Dezot, S.Tang, W.Suginta, B.Paosawatyanong, M.M.Babu, J.W.Chin, D.Pakotiprapha, W.Bhanthumnavin, C.Uttamapinan. *Angew. Chem., Int. Ed.*, **61**, e202203061 (2022); <https://doi.org/10.1002/anie.202203061>
229. L.V.Alcántara, R.M.O.Ros, A.G.Bórquez, C.P.Montes. *Microbiol. Spectr.*, **9**, e0097621 (2021); <https://doi.org/10.1128/spectrum.00976-21>
230. Y.Liu, C.Liu, H.Liu, Q.Zeng, X.Tian, L.Long, J.Yang. *Front. Bioeng. Biotechnol.*, **10**, e865787 (2022); <https://doi.org/10.3389/fbioe.2022.963008>
231. C.Sonnendecker, J.Oeser, P.K.Richter, P.Hille, Z.Zhao, C.Fischer, H.Lippold, P.B.Sánchez, F.Engelberger, C.A.R.Sarmiento, T.Oeser, Y.Lihanova, R.Frank, H.-G.Jahnke, S.Billig, B.Abel, N.Sträter, J.Matysik, W.Zimmermann. *ChemSusChem*, **15**, e202101062 (2022); <https://doi.org/10.1002/cssc.202101062>
232. P.W.Wallace, K.Haernvall, D.Ribitsch, S.Zitzenbacher, M.Schittmayer, G.Steinkellner, K.Gruber, G.M.Guebitz, R.B.Gruenberger. *Appl. Microbiol. Biotechnol.*, **101**, 2291 (2017); <https://doi.org/10.1007/s00253-016-7992-8>
233. D.N.Moyses, D.A.Teixeira, V.A.Waldow, D.M.G.Freire, A.M.Castro. *3 Biotech*, **11**, e435 (2021); <https://doi.org/10.1007/s13205-021-02988-1>
234. T.-W.Liang, S.-N.Jen, A.D.Nguyen, S.-L.Wang. *Polymers*, **8**, e98 (2016); <https://doi.org/10.3390/polym8030098>
235. A.Biundo, A.Hromic, T.P.Keller, K.Gruber, F.Quartinello, K.Haernvall, V.Perz, M.S.Arrell, M.Zinn, D.Ribitsch, G.M.Guebitz. *Appl. Microbiol. Biotechnol.*, **100**, 1753 (2016); <https://doi.org/10.1007/s00253-015-7031-1>
236. H.-Y.Sagong, H.F.Son, H.Seo, H.Hong, D.Lee, K.-J.Kim. *J. Hazard. Mater.*, **416**, e126075 (2021); <https://doi.org/10.1016/j.jhazmat.2021.126075>
237. X.Wang, C.Song, Q.Qi, Y.Zhang, R.Li, L.Huo. *Eng. Microbiol.*, **2**, e100020 (2022); <https://doi.org/10.1016/j.engmic.2022.100020>
238. R.Jabloune, M.Khalil, I.E.B.Moussa, A.-M.S.Beaunoir, S.Lerat, R.Brzezinski, C.Beaulieu. *Microbes Environ.*, **35**, ME19086 (2020); <https://doi.org/10.1264/jmsme2.ME19086>
239. S.Weinberger, R.Beyer, C.Schüller, J.Strauss, A.Pellis, D.Ribitsch, G.M.Guebitz. *Front. Microbiol.*, **11**, e554 (2020); <https://doi.org/10.3389/fmicb.2020.00554>
240. A.Magnin, E.Pollet, R.Perrin, C.Ullmann, C.Persillon, V.Phalip, L.Averous. *Waste Manag.*, **85**, 141 (2019); <https://doi.org/10.1016/j.wasman.2018.12.024>
241. A.R.Bagheri, C.Laforsch, A.Greiner, S.Agarwal. *Glob. Chall.*, **1**, e1700048 (2017); <https://doi.org/10.1002/gch2.201700048>
242. M.Lykaki, Y.-Q.Zhang, M.Markiewicz, S.Brandt, S.Kolbe, J.Schrick, M.Rabeb, S.Stolte. *Green Chem.*, **23**, 5212 (2021); <https://doi.org/10.1039/D1GC00883H>
243. R.P.Magalhães, J.M.Cunha, S.F.Sousa. *Int. J. Mol. Sci.*, **22**, e11257 (2021); <https://doi.org/10.3390/ijms222011257>
244. A.Berselli, M.J.Ramos, M.C.Menziani. *ChemBioChem*, **22**, 2032 (2021); <https://doi.org/10.1002/cbic.202000841>
245. P.C.F.Buchholz, G.Feuerriegel, H.Zhang, P.P.Garcia, L.-L.Nover, J.Chow, W.R.Streit, J.Pleiss. *Proteins*, **90**, 1443 (2022); <https://doi.org/10.1002/prot.26325>
246. C.Jerves, R.P.P.Neves, M.J.Ramos, S.da Silva, P.A.Fernandes. *ACS Catal.*, **11**, 11626 (2021); <https://doi.org/10.1021/acscatal.1c03700>

247. S.Feng, Y.Yue, J.Chen, J.Zhou, Y.Li, Q.Zhang. *Environ. Sci. Processes Impacts*, **22**, 2332 (2020); <https://doi.org/10.1039/D0EM00340A>
248. X.Wang, J.Chen, X.Tang, J.Wang, L.Zhu, W.Zhang, H.Wang, Y.Li, Q.Zhang. *Chemosphere*, **231**, 126 (2019); <https://doi.org/10.1016/j.chemosphere.2019.05.112>
249. Y.Jia, N.A.Samak, X.Hao, Z.Chen, G.Yang, X.Zhao, T.Mu, M.Yang, J.Xing. *Biochem. Eng. J.*, **176**, e108205 (2021); <https://doi.org/10.1016/j.bej.2021.108205>
250. S.P.Schwaminger, S.Fehn, S.Rauwolf, T.Steegmüller, H.Löwe, K.Pflüger-Grau, S.Berensmeier. *Nanoscale Adv.*, **4**, 4395 (2021); <https://doi.org/10.1039/D1NA00243K>
251. Z.Li, K.Chen, L.Yu, Q.Shi, Y.Sun. *Biochem. Eng. J.*, **180**, e108344 (2022); <https://doi.org/10.1016/j.bej.2022.108344>
252. K.Chen, X.Dong, Y.Sun. *J. Hazard. Mater.*, **438**, e129517 (2022); <https://doi.org/10.1016/j.jhazmat.2022.129517>
253. Q.Li, Y.Pan, H.Li, M.Lenertz, K.Reed, D.Jordahl, T.Bjerke, A.Ugrinov, B.Chen, Z.Yang. *ACS Appl. Mater. Interfaces*, **13**, 43085 (2021); <https://doi.org/10.1021/acsami.1c12209>
254. J.Han, H.Feng, J.Wu, Y.Li, Y.Zhou, L.Wang, P.Luo, Y.Wang. *J. Agric. Food Chem.*, **69**, 7910 (2021); <https://doi.org/10.1021/acs.jafc.1c02056>
255. I.V.Lyagin, E.N.Efremenko, S.D.Varfolomeev. *Russ. Chem. Rev.*, **86**, 339 (2017); <https://doi.org/10.1070/RCR4678>
256. T.N.A.Tuan Kob, M.F.Ismail, M.B.Abdul Rahman, K.E.Cordova, M.A.Mohammad Latif. *J. Phys. Chem. B*, **124**, 3678 (2020); <https://doi.org/10.1021/acs.jpcc.0c02145>
257. F.Tavanti, A.Pedone, M.C.Menziani. *J. Phys. Chem. C*, **119**, 22172 (2015); <https://doi.org/10.1021/acs.jpcc.5b05796>
258. K.E.Kosiorowska, A.D.Moreno, R.Iglesias, K.Leluk, A.M.Mirończuk. *Sci. Total Environ.*, **846**, e157358 (2022); <https://doi.org/10.1039/D1NA00243K>
259. P.Liu, T.Zhang, Y.Zheng, Q.Li, T.Su, Q.Qi. *Eng. Microbiol.*, **1**, e100003 (2021); <https://doi.org/10.1016/j.engmic.2021.100003>
260. K.E.Kosiorowska, P.Biniarz, A.Dobrowolski, K.Leluk, A.M.Mirończuk. *Sci. Total Environ.*, **831**, e154841 (2022); <https://doi.org/10.1016/j.scitotenv.2022.154841>
261. M.Zheng, Y.Li, W.Dong, W.Zhang, S.Feng, Q.Zhang, W.Wang. *ACS Sustain. Chem. Eng.*, **10**, 7341 (2022); <https://doi.org/10.1021/acssuschemeng.2c01093>
262. S.Boneta, K.Arafet, V.Moliner. *J. Chem. Inf. Model.*, **61**, 3041 (2021); <https://doi.org/10.1021/acs.jcim.1c00394>
263. N.Numoto, N.Kamiya, G.-J.Bekker, Y.Yamagami, S.Inaba, K.Ishii, S.Uchiyama, F.Kawai, N.Ito, M.Oda. *Biochemistry*, **57**, 5289 (2018); <https://doi.org/10.1021/acs.biochem.8b00624>
264. T.J.Park, S.H.Lee, M.S.Lee, J.K.Lee, J.H.Park, K.D.Zoh. *Water*, **12**, e3333 (2020); <https://doi.org/10.3390/w12123333>
265. G.Zhou, Q.Wang, J.Zhang, Q.Li, Y.Wang, M.Wang, X.Huang. *Environ. Res.*, **189**, e109893 (2020); <https://doi.org/10.1016/j.envres.2020.109893>
266. N.Poerio, E.Piacentini, R.Mazzei. *Molecules*, **24**, e4148 (2019); <https://doi.org/10.3390/molecules24224148>
267. F.Tavanti, A.Pedone, M.C.Menziani. *Int. J. Mol. Sci.*, **20**, e3539 (2019); <https://doi.org/10.3390/ijms20143539>
268. A.A.Sousa, P.Schuck, S.A.Hassan. *Nanoscale Adv.*, **3**, 2995 (2021); <https://doi.org/10.1039/D1NA00086A>
269. W.Liang, P.Wied, F.Carraro, C.J.Sumby, B.Nidetzky, C.-K.Tsung, P.Falcaro, C.J.Doonan. *Chem. Rev.*, **121**, 1077 (2021); <https://doi.org/10.1021/acs.chemrev.0c01029>
270. I.V.Lyagin, E.N.Efremenko. *Biochimie*, **144**, 115 (2018); <https://doi.org/10.1016/j.biochi.2017.10.023>
271. J.P.P.Ramalho, A.V.Dordio, A.J.P.Carvalho. *J. Mol. Struct.*, **1249**, e131520 (2022); <https://doi.org/10.1016/j.molstruc.2021.131520>
272. J.N.Vranish, M.G.Ancona, S.A.Walper, I.L.Medintz. *Langmuir*, **34**, 2901 (2018); <https://doi.org/10.1021/acs.langmuir.7b02588>
273. M.Scandola, M.L.Focarete, G.Frisoni. *Macromolecules*, **31**, 3846 (1998); <https://doi.org/10.1021/ma980137y>